הטכניון
מכון טכנולוגי לישראל
TECHNION
Israel Institute of Technology

ספריות הטכניון
The Technion Libraries

בית הספר ללימודי מוסמכים ע"ש ארווין וג'ואן ג'ייקובס
Irwin and Joan Jacobs Graduate School

Graph-Based Model Reduction Methods for Multi-Agent Systems

Research Thesis
In Partial Fulfillment of the Requirements for the
Degree of Doctor of Philosophy

Noam Leiter

Submitted to the Senate of the Technion - Israel Institute of Technology
Iyyar 5782, Haifa, May 2022

The Research Thesis Was Done Under The Supervision of Prof. Daniel Zelazo in the Faculty of Aerospace Engineering

The Generous Financial Help Of The Israel Science Foundation and The United States-Israel Binational Science Foundation (BSF) is Gratefully Acknowledged

To my children, Yuval and Alon

Contents

List of Figures

List of Tables

Acknowledgements

Throughout the years of my PhD, I have found support and got assistance from faculty, colleagues, friends, and family. I wish to acknowledge those people that were significant in my journey.

First and foremost, I wish to express my very great appreciation to my PhD advisor Prof. Daniel Zelazo for his efforts throughout my doctoral studies, and for bringing me to achieve higher levels of research. I also thank him for introducing me to graph theory, and for teaching me how to see control systems from a networked perspective. My greatest appreciation to Prof. David Geller from Utah State University who motivated me to pursue a PhD and introduced me to model reduction. I highly appreciate the advice and motivation given by Prof. Pini Gurfil, my former master's degree advisor. I would also like to thank the members of my doctoral examination committee Prof. Yoram Halevi, Prof. Izchak Lewkowicz (Ben Gurion University), and Prof. Yaakov Oshman for their review of my thesis. In particular, I sincerely thank Prof. Lewkowicz for his insightful comments and positive assessment of my work, and to offer my special thanks to Prof. Oshman who has inspired me to pursue research in estimation and control theory.

I am particularly grateful for the assistance and guidance that were given throughout my studies by Ms. Judith Greenberg from the Faculty of Aerospace Engineering Graduate Studies Office. I wish to thank my friends and colleagues at the Philadelphia Flight Control Laboratory, of which special thanks are reserved for Ori Rappel, Dr. Roni Tsalik, and Dr. Nir Emuna with whom I have shared researched ideas and had fruitful conversations and Mr. Daniel Weinfeld which created a professional and pleasant research atmosphere and was always helpful.

To Noga, Dorit and Igal, I thank you for always being helpful and available, and for prioritizing my studies during the most stressful times. My special thanks are extended to my partner Gome, for her patience and support and for encouraging me to complete my research. Finally, I would like to thank my loving parents Ilana and Yehiel, you have embedded in me the curiosity and chutzpah to ask questions and the persistence to look for answers.

Abstract

Model reduction is an active branch of linear system theory with increasing importance, as modern applications may be extremely large-scale. Reduced-order models are required whenever it is computationally infeasible to implement, analyze or simulate the full order system, of which orthogonal projection-based reduced order models (PROM) are the most widely-used.

Graphs are mathematical objects composed of a set of vertices and a set of interconnecting edges. As simple as they are constructed, the study of graphs has developed into a formal branch of mathematics, with numerous applications in computer science, biology and social science, to mention a few. Graphs characterize the structure of multi-agent systems, where each node is an agent with a low-order dynamical system, and edges represent the local interaction between adjacent agents. As the number of agents increases, multi-agent systems may be extremely large-scale and require model-reduction. Graph contractions over vertex partitions have been extensively studied in the context of model reductions of multi-agent systems. We define such model reduction methods that preserve the networked structure of the system, as a new kind of model reduction, named "graph-based model reduction".

In the first part of the study, we investigate classes of graph contractions where the edges of the graph are the basis for the contraction operation. The combinatorial operation of these edge-based contractions is derived, and we construct, for the first time, the algebraic representations of graph contractions, such as incidence and Laplacian matrices. A spectral interlacing theorem is then proven for two types of edge-matching contractions, and two efficient algorithms are provided for finding Laplacian-type interlacing contractions.

In the second part of the thesis, we reexamine the well known orthogonal PROMs and their realizations. A novel product form is derived for the reduction error system of these reduced models, and investigating the error system product form, we then define interface-invariant PROMs, model order reductions with projection-invariant input and output matrices. It is shown that for such PROMs the error product systems are strictly proper. Furthermore, exploiting this structure, an analytic $\mathcal{H}_\infty$ reduction error bound is obtained and an $\mathcal{H}_\infty$ bound optimization problem is defined. We then present a sub-optimal greedy-edge efficient algorithm for $\mathcal{H}_\infty$ graph-based model reduction of multi-agent systems utilizing the derived edge-matching graph contractions and the analytic $\mathcal{H}_\infty$ reduction error bound.

Table of Notation

In this dissertation, we will also use the following notation:

Notation	Meaning
$\|A\|$	The cardinality (size) of the set A.
$\mathbb{R}$	The set of real numbers.
$\mathbb{R}_+$	The set of non-negative real numbers.
$\mathbb{C}$	The set of complex numbers.
$\mathbb{Q}$	The set of rational numbers.
$\mathbb{Z}$	The set of integers.
x_i,$[x]_i$	The i'th variable of vector x.
A_{ij},$[A]_{ij}$	The i-j entry of a matrix A.
0_d, $0_{d\times d}$	The all-zero vector of length d, all-zero matrix of size $d \times d$.
$\mathbb{1}_d$	The all-one vector of length d.
$\hat{\mathrm{e}}_i^{(d)}$	The i-th standard basis vector in $\mathbb{R}^d$.
$I_{d\times d}$	The identity matrix of size $d \times d$.
$\ker(A)$	The kernel of the linear transformation A.
$U^\perp$	The orthogonal complement of the linear subspace U.
$\mathrm{Diag}\,(A, B)$	The block diagonal of matrices A and B.
$A \otimes B$	The Kronecker product of the matrices A and B.
$\|x\|$	The Euclidean norm of the vector x.
$\|A\|_F$	The Frobenius norm of a matrix A.
$A^\dagger$	The left pseudo-inverse of a square matrix A
$A \succeq B$	The matrix $A - B$ is positive semi-definite.
$A \succ B$	The matrix $A - B$ is positive-definite.
$\sigma_{\min}(A)$	The minimal singular value of A
$\sigma_{\max}(A)$	The maximal singular value of A
$\lambda_{\min}(A)$	The minimal eigenvalue of A
$\lambda_{\max}(A)$	The maximal eigenvalue of A
$\lambda(A)$	The spectrum of A
$\delta(A)$	The diagonal of A
$\Lambda(A)$	The diagonal matrix of the spectrum of A
$\mathcal{V}$	A set of vertices.
$\mathcal{E}$	A set of pairs of vertices, called edges.
$\mathcal{G} = (\mathcal{V}, \mathcal{E})$	A graph $\mathcal{G}$ with vertices $\mathcal{V}$ and edges $\mathcal{E}$.
$\mathcal{E}$, $\mathcal{E}_\mathcal{G}$	The incidence matrix of the graph $\mathcal{G}$.
$\lambda_2(\mathcal{G})$	The algebraic connectivity of the graph $\mathcal{G}$.
Σ_i	The i-th agent in a multi-agent system.
Σ	The collection of all agents in a multi-agent system.
$\mathcal{O}(n)$	Big-O notation for algorithm run time complexity

We will also use the following acronyms:

Acronym	**Meaning**
LTI	Linear and Time-Invariant
MIMO	Multiple-Input Multiple-Output
SISO	Single-Input Single-Output
TF	Transfer Function
TFM	Transfer Function Matrix
PD	Positive Definite
NP	Non-Polynomial
MAS	Multi-Agent System
PROM	Projection-based Reduced-Order Model
PCM	Partition Characteristic Matrix
PPM	Partition Projection Matrix

Chapter 1

Introduction

1.1 Introduction and Focus

There is currently a rapid growth in the usage of multi-agent systems in many modern technologies, such as robotic flocking and swarming [61], enabling robust operations in the most harsh environments [31]. Other applications include power grids [37], and models in physics, economy and sociology [41], to name a few. As the number of agents increases, multi-agent systems (MAS) may be extremely large-scale, causing analysis and simulation to become computationally infeasible, and presenting new challenges in the design of controllers to such systems.

Multi-agent systems are characterized by their networked structure, where each agent is represented by a node in a graph and edges (and their assigned weights) represent the local interactions between adjacent agents, e.g., local observations or data links [45]. Generally, an agent, is any dynamical system coupled to other systems; however, for large scale MAS, where the scale is determined by the large number of agents, a multi-type agent model seems less relevant. Therefore, in this study, we only consider MAS compromised of a set of functionally-homogeneous agents, i.e., all agents have the same dynamical model up to some specified parameters (Figure 1.1). The most extensively studied MAS are *consensus models* [51]. In a consensus model, all agents try to achieve the same state as adjacent agents using a local control law. Under some conditions, depending on the specific model, the entire ensemble may converge to the same state, and consensus or agreement is obtained [45].

The unique network structure of MAS allows to model and analyze global properties of such systems using graph theoretic tools [45]. Explicit relations have been found between properties of consensus models and their underlying graph structure: the system $\mathcal{H}_2$-performance has been found to be a function of cycle-completing edges [69], and system $\mathcal{H}_p$-norms were relates directly to zeta functions of the graph Laplacian [57]. The combined forces of control theory and graph theory have also provided new powerful methods for controlling MAS

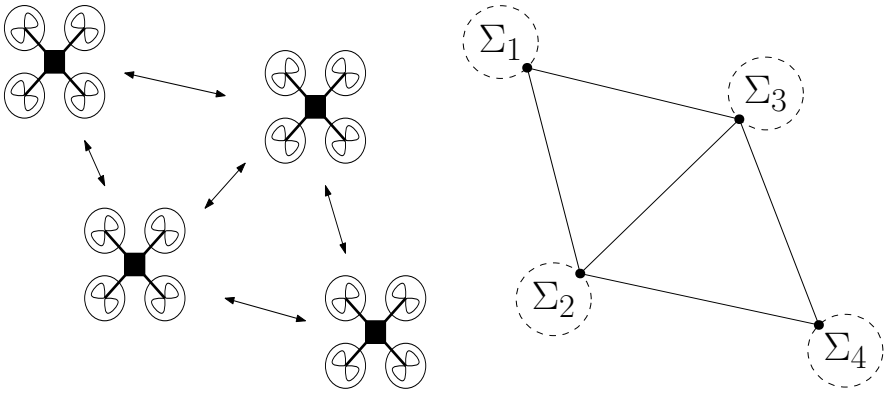

(a) An example of a multi-agent system consisting of four drones interacting over a network.

(b) The multi-drone system is modeled by a graph where each node represents an agent-subsystem and each edge represents an interaction between adjacent agents.

Figure 1.1: A representation of a multi-agent system.

[56]; however, as the complexity and size of such networked systems increases, the design and synthesis of controllers become computationally infeasible, and reduced order controllers are required.

Model-order reduction is an essential tool for the design and study of large-scale with various scientific and engineering applications such as weather forecast schemes [44] or the design of trajectories of spacial probes sent to other planets [62]. Of particular interest is the study of model reduction for the implementation of controllers for large-scale systems. Internal model principle implies that the order of the controller is at least as the order of the plant [22], as reflected in the solution of $\mathcal{H}_2$ and $\mathcal{H}_\infty$ control problems [19, 27, 38]. In order to implement low-order controllers for large scale systems, model reduction of the design model or full-order controller is commonly performed [32, 39].

A widely-used family of reduced-order models are the *projection-based reduced order models* (PROMs) [1, 24]. Well established PROM producing methods, such as *balanced truncation* [3], preserve stability, guarantee minimality and provide *a priori* reduction error bounds [48]. These methods, however, may be unfeasible for very large-scale systems due to their computational complexity [6, 9], and reduced-order control problems of LTI systems introduce a great computational challenge even when the design is carried out off-line [9]. For example, computational methods for solving fixed-order output feedback design problems are proven to be NP-hard [23]. As a result, many works aimed at finding sub-optimal efficient solutions, e.g. by alternating projection methods [28], or Krylov-subspace techniques which are computationally efficient and

suitable for extremely large-scale systems [4]. Such methods, however, may fail to provide stable and minimal reduced order realizations [35].

A great challenge in the study of multi-agent systems is to find efficient reduction methods that guarantee stability and assure minimality of their reduced order realizations, preferably, with optimal or suboptimal reduction errors. For networked systems, as MAS, the interconnection properties of the underlying graph can be related in some cases to the stability, controllability and observability of the system [2]. Therefore, it is desirable that reduced-order models are found that preserve, in some sense, the network structure of the full-order system. If we treat such systems as a general large-scale MIMO system, standard model reduction techniques can be applied; however, the resulting reduced-order system will generally not have the structure of a multi-agent system. Structured model reductions have been developed for systems composed of a small number of interconnected large-scale subsystems [42, 54], and were applied for model reduction of networked power systems [59]. Such methods, however, are not applicable for MAS consisting of large number of low-order agents.

An LTI MAS can be describes as a system with a realization that is a function of the graph. Utilizing this property, *graph-based model reduction* is a family of MAS reduction methods where a graph reduction is performed, rather than a direct model-order reduction. The resulting realization is a function of the reduced-order graph and produces a reduced order model [40], which is a reduced order MAS. In that direction, several recent studies were performed. In [47, 34], PROMs of consensus-type multi-agent models were considered based on graph-contractions over vertex partitions. In [36], removal of cycle completing edges was suggested for model simplification of the consensus protocol. The reduction of second-order network systems with structure preservation using hierarchical $\mathcal{H}_2$ clustering was demonstrated in [12]. A framework for optimal structured model-order reduction of MAS was recently presented in [67]. Here, a convex relaxation technique was derived for the $\mathcal{H}_2$ model reduction of diffusively coupled second-order networks.

While these methods are limited to first or second-order multi-agent models, the goal of this research is to develop efficient graph-based model reduction methods for the general class of LTI MAS. As a first step, we formulate graph-based model reduction as a graph reduction optimization problem. This problem, however, is found to be computationally infeasible. In order to derive efficient sub-optimal solutions of the graph reduction optimization problem, we investigate graph-based model reduction algorithms based on vertex partitions. Vertex partitions have been extensively studied in graph theory in the context of graph clustering and network communities [49, 55, 58], and graph contractions over vertex partitions are widely used as a combinatorial graph reduction tool. It has also been observed in previous studies that partition-based PROMs maintain an MAS structure [47, 34], i.e., the PROM is an MAS defined over a reduced order graph.

An important part of this research is a thorough study of vertex partitions and of graph contractions, reduced-order graphs based on vertex partitions. We construct a sub-class of vertex partitions denoted as “edge-induced partitions”,

and derive a spectral analysis theorem for reduced-order graph Laplacian matrices resulting from graph contractions. Novel efficient algorithms are provided for finding two types of a Laplacian interlacing contractions.

In a second part of this work, we reexamine the well known PROMs and their realizations. A new product form is derived for the reduction error system of these reduced models, an analytic $\mathcal{H}_\infty$ reduction error bound is derived, and an $\mathcal{H}_\infty$ bound optimization problem is defined. We then utilize edge-induced partitions to obtain an efficient suboptimal model reduction method for MAS. We introduce the notion of edge-induced PROMs, PROMs which are constructed over edge-induced partitions of the graph. This graph-based model reduction method allows us to derive sub-optimal but efficient PROMs of MAS based on the derived $\mathcal{H}_\infty$ reduction error bound.

Notation

First, we use some standard notation from set theory. The cardinality (or size) of a set A is denoted by $|A|$. The set $\mathbb{R}$ denotes the real numbers, the set $\mathbb{C}$ denotes the complex numbers, and the set $\mathbb{Z}$ denotes the integers. The integer set $\{1,\ldots,n\} \subset \mathbb{Z}$ is denoted as $[1,n]$. We use the $\mathcal{O}()$ notation ("big O notation"), whose precise meaning is the following. Let f and g be functions that map positive numbers to positive numbers. We write $f(x) \in O(g(x))$ if there exists $M > 0$ and $x_0 > 0$ such that $f(x) < Mg(x)$ for all $x > x_0$.

Second, we use standard notation from linear algebra and matrix analysis [30]. The vector $\mathbf{0}_d$ denotes the d-dimensional zero vector. The vector $\mathbb{1}_d$ denotes the d-dimensional all-ones vector. In both cases, the subscript may be omitted when the dimension is clear. The vector $\hat{\mathrm{e}}_i^{(d)}$ will denote the i-th standard basis vector, i.e., $\hat{\mathrm{e}}_i^{(d)} \in \mathbb{R}^d$ and $\left[\hat{\mathrm{e}}_i^{(d)}\right]_j = \delta_{ij}$, where δ_{ij} is Dirac's delta. The identity matrix of size $d \times d$ will be denoted I_d. For two matrices A and B, $\mathrm{Diag}(A,B)$ is a block diagonal matrix with A,B on the diagonal. The entries of a matrix A are denoted $[A]_{ij}$. For two matrices A, B, we'll let $A \otimes B$ denote the corresponding Kronecker product.

The spectrum of a real matrix $A \in \mathbb{R}^{n\times n}$ is the set of eigenvalues $\lambda(A) = \{\lambda_k(A)\}_{k=1}^n$ where $\lambda_k(A) \in \mathbb{C}$ is the kth eigenvalue of A. The corresponding eigenvectors are $\{u_k(A)\}_{k=1}^n$. For a symmetric matrix we have an eigenvalue decomposition $A = U(A)\Lambda(A)U^T(A)$, where $U(A) = [u_1(A), u_2(A), \ldots, u_n(A)]$ is an orthonormal matrix and $\Lambda(A) = \mathrm{Diag}(\lambda(A)) \in \mathbb{R}^{n\times n}$. A symmetric matrix is *positive-definite* if $\lambda_i(A) > 0$ for $i \in [1,n]$ and is denoted as $A \succ 0$. If A, B are both square symmetric matrices of the same dimension, we'll write $A \succeq B$ if $A - B$ is positive semi-definite. Moreover, we'll write $A \succ B$ if $A - B$ is positive-definite. If A is a map from a linear space to itself, then we denote its minimal singular value by $\sigma_{min}(A)$, and its maximal singular value by $\sigma_{max}(A)$. Similarly, if all of A's eigenvalues are real, we'll let $\lambda_{\min}(A)$ be the minimal eigenvalue of A, and $\lambda_{\max}(A)$ be the maximal value of A. If U is a linear subspace of $\mathbb{R}^n$, we'll let $U^\perp$ be its orthogonal complement. The Euclidean norm of a vector x will be denoted by $\|x\|$. The 2-norm of a matrix A is $\|A\|_2 = \sigma_{max}(A)$. The

Frobenius norm of a matrix $A \in \mathbb{R}^{m\times n}$ is $\|A\|_{\mathcal{F}} = \sqrt{\mathrm{Tr}\left\{A^T A\right\}}$.

We also go over several acronyms repeatedly used throughout the thesis. Namely, multi-agent systems will be abbreviated as MAS, single-input single-output systems will be called SISO systems, where multiple-input multiple-output systems will be called MIMO systems. Projection-based reduced order models will be called PROMs. Lastly, linear and time-invariant systems will be denoted as LTI systems, and their transfer function will be abbreviated as TF.

1.2 Background

In this section, we present an overview of system theory and model reduction theory, along with some basic notions from graph theory introduce used throughout the thesis.

1.2.1 System Theory

An LTI system Σ is a mapping $u(t) \mapsto y(t)$ from the inputs $u(t) \in \mathbb{R}^{n_u}$ to the outputs $y(t) \in \mathbb{R}^{n_y}$. A realization $\Sigma := (A, B, C, D)$ is the dynamical system,

$$\begin{cases} \dot{x}(t) &= Ax(t) + Bu(t) \\ y(t) &= Cx(t) + Du(t) \end{cases}, \tag{1.1}$$

where $x(t) \in \mathbb{R}^{n_x}$ is the system state, and the matrices $A \in \mathbb{R}^{n_x \times n_x}$, $B \in \mathbb{R}^{n_x \times n_u}$, $C \in \mathbb{R}^{n_y \times n_x}$ and $D \in \mathbb{R}^{n_y \times n_u}$ are the system parameters. The corresponding transfer function matrix (TFM) representation of Σ is given as

$$\hat{\Sigma}(s) = C\left(sI_n - A\right)^{-1} B + D. \tag{1.2}$$

Hereafter, the notation $\hat{\Sigma}$ will be used, without the explicit dependence on s, to denote the TFM of a system Σ.

A realization $\Sigma := (A, B, C, D)$ is *minimal* if it is controllable and observable. The order of a system is its *McMillan degree*, denoted as $\deg(\Sigma)$, which is the order of any minimal realization of Σ [15]. For a *strictly-proper* system $D = 0$. The system Σ is stable if A is *Hurwitz*, i.e., $\lambda(A) \subset \mathbb{C}^-$, where $\mathbb{C}^-$ is the open left-half complex plane and $\lambda(A) = \{\lambda_i\}_{i=1}^n$ is the spectrum of A [18, p. 37].

For a *minimal realization* of a stable system, the controllability and observability Gramians X_c and X_o are positive-definite matrices which are the unique solutions to the Lyapunov equations

$$\begin{cases} AX_c + X_c A^T + BB^T &= 0 \\ A^T X_o + X_o A + C^T C &= 0 \end{cases}. \tag{1.3}$$

If $\Sigma := (A, B, C, D)$ is a *minimal* then for any invertible matrix T, also $\Sigma := \left(TAT^{-1}, TB, CT^{-1}, D\right)$ is a *minimal realization* of Σ. We can always find an invertible matrix T_b such that the realization $\Sigma := \left(T_b A T_b^{-1}, T_b B, C T_b^{-1}, D\right)$

is a *balanced realization*, i.e., $X_c = X_o$ [48]. The *Hankel singular values* (HSVs) of Σ are the singular-values of the matrix $X_c X_o$, and for any minimal realization $\sigma_i(X_c X_o) > 0$ for $i \in [1, n]$ [6].

The two most studied system norms are the $\mathcal{H}_2$-norm and the $\mathcal{H}_\infty$-norm [17]. The $\mathcal{H}_2$-norm of a system Σ is

$$\|\Sigma\|_{\mathcal{H}_2} = \left(\frac{1}{2\pi} \int_{-\infty}^{\infty} \left\| \hat{\Sigma}(j\omega) \right\|_{\mathcal{F}}^2 d\omega \right)^{\frac{1}{2}}. \tag{1.4}$$

For a strictly-proper and stable system the $\mathcal{H}_2$ norm is finite and it can be calculated from the controllability or observability Gramians X_c and X_o

$$\|\Sigma\|_{\mathcal{H}_2} = \sqrt{\mathrm{Tr}\left(B^T X_o B\right)} = \sqrt{\mathrm{Tr}\left(C X_c C^T\right)}. \tag{1.5}$$

The $\mathcal{H}_2$-norm can also be interperted as a measure of the steady-state LTI output dispersion as a function of the input noise power

$$\|\Sigma\|_{\mathcal{H}_2} = \lim_{t \to \infty} E\left[y^T(t)\, y(t) \right]. \tag{1.6}$$

The $\mathcal{H}_\infty$-norm of a system Σ is

$$\|\Sigma\|_{\mathcal{H}_\infty} = \sup_{\omega \in \mathbb{R}} \sigma_{max}\left(\hat{\Sigma}(j\omega) \right). \tag{1.7}$$

1.2.2 Model Reduction

A *reduced-order model* of Σ is any system with realization $\Sigma_r := (A_r, B_r, C_r, D_r)$ mapping $u(t) \mapsto y_r(t)$, with $u(t) \in \mathbb{R}^{n_u}$ and $y_r(t) \in \mathbb{R}^{n_y}$, such that $\deg(\Sigma_r) < \deg(\Sigma)$. Reduction error analysis can be performed by constructing an augmented error system,

$$\Sigma_e = \Sigma - \Sigma_r, \tag{1.8}$$

with realization $\Sigma_e := (A_e, B_e, C_e, D_e)$, where $x_e(t) = \begin{bmatrix} x^\top(t) & x_r^\top(t) \end{bmatrix}^\top$, $y_e(t) = y(t) - y_r(t)$, $A_e = \mathrm{Diag}(A, A_r)$, $B_e = \begin{bmatrix} B^\top & B_r^\top \end{bmatrix}^\top$, $C_e = \begin{bmatrix} C & -C_r \end{bmatrix}$ and $D_e = D - D_r$. The reduction error can then be quantified using any system norm $\|\Sigma_e\|$ with the two most studied model reduction system norms being the $\mathcal{H}_2$-norm and the $\mathcal{H}_\infty$-norm.

A family of reduction producing methods are *projection-based reduced-order models* (PROMs). Given a system Σ with minimal realization $\Sigma := (A, B, C, D)$, a projection-based reduction is a system Σ_r with realization

$$\Sigma_r := \left(U^T A V, U^T B, C V, D \right),$$

for any two matrices $U, V \in \mathbb{R}^{n \times r}$ such that UV^T is a projection matrix [24]. Recall that a matrix $\Pi \in \mathbb{C}^{n \times r}$ is called a *projection* whenever $\Pi = \Pi^2$. If

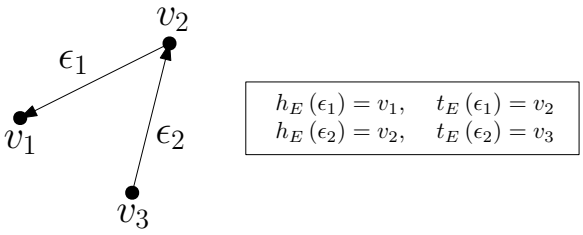

Figure 1.2: An example of head and tail assignment.

$U = V$ the PROM is denoted as *orthogonal*, otherwise it is said to be *oblique* [1].

Given a system Σ with a *balanced realization*

$$\Sigma := \left(\begin{bmatrix} A_{11} & A_{12} \\ A_{21} & A_{22} \end{bmatrix}, \begin{bmatrix} B_1 \\ B_2 \end{bmatrix}, \begin{bmatrix} C_1 & C_2 \end{bmatrix}, D \right),$$

a *balanced truncation* is the reduced system Σ_r with realization $\Sigma_r := (A_{11}, B_1, C_1, D)$ [48]. The HSVs of Σ_r are then the r smallest HSVs of Σ and the $\mathcal{H}_\infty$ reduction error is bounded by

$$\|\Sigma_e\|_{\mathcal{H}_\infty} \leq 2 \sum_{k=1}^{n-r} \sigma_i(\Sigma), \tag{1.9}$$

where $\{\sigma_i\}_{i=1}^n$ are in ascending order [20]. In fact, this classical balanced truncation model reduction scheme is a prime example of employing oblique PROMs [48].

1.2.3 Graph Theory

A graph $\mathcal{G} = (\mathcal{V}, \mathcal{E}, \mathcal{W})$ of order n with m edges consists of a vertex set $\mathcal{V}(\mathcal{G}) = [1, n]$, an edge set $\mathcal{E}(\mathcal{G}) = \{\epsilon_k\}_{k=1}^m$ with $\epsilon_k \in \mathcal{V}^2$, and a set of edge weights, $\mathcal{W}(\mathcal{G}) = \{w_k\}_{k=1}^m$ with $w_i \in \mathbb{R}$. Two nodes $u, v \in \mathcal{V}(\mathcal{G})$ are *adjacent* if they are the endpoints of an edge $\{u, v\}$, and we denote this by $u \sim v$. The neighborhood $\mathcal{N}_v(\mathcal{G})$ is the set of all nodes adjacent to v in $\mathcal{G}$. The degree of a node v, denoted $d_v(\mathcal{G})$, is the number of nodes adjacent to it, $d_v(\mathcal{G}) = |\mathcal{N}_v(\mathcal{G})|$. A *path* in a graph is a sequence of distinct adjacent nodes. A *simple cycle* is a path with an additional edge such that the first and last vertices are repeated. A graph $\mathcal{G}$ is *connected* if we can find a path between any pair of nodes. We denote $\mathcal{G} \backslash \mathcal{V}_R$ as the graph obtained from $\mathcal{G}$ by removing all nodes $v \in \mathcal{V}_R \subset \mathcal{V}$ from $\mathcal{V}(G)$ and removing all edges in $\mathcal{E}(\mathcal{G})$ adjacent to v.

Given a graph $\mathcal{G} = (\mathcal{V}, \mathcal{E}, \mathcal{W})$, we assign an orientation to the edges using head and tail functions, $h_\mathcal{E}, t_\mathcal{E} : \mathcal{E} \to \mathcal{V}$ where $h_\mathcal{E}(\epsilon_k)$ and $t_\mathcal{E}(\epsilon_k)$ return, respectively,

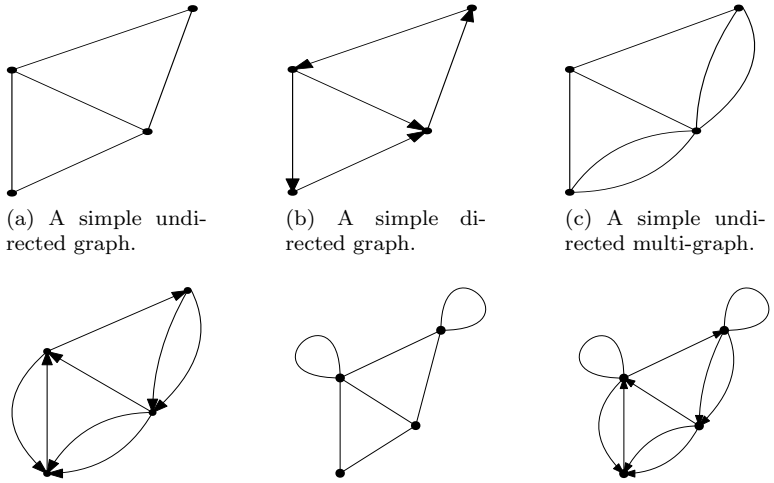

(a) A simple undirected graph.

(b) A simple directed graph.

(c) A simple undirected multi-graph.

(d) A simple directed multi-graph.

(e) An undirected graph with two self-loops.

(f) A directed multi-graph with two self-loops.

Figure 1.3: Examples of the different graph classes.

the *head* and *tail* nodes of edge ϵ_k (Fig. 1.2). If $\mathcal{G}$ is an *undirected graph* then the head and tail of each edge are arbitrary; if $\mathcal{G}$ is a *directed graph* (digraph) then the head and tail define the edge direction. A *self-loop* is an edge $\epsilon_k \in \mathcal{E}$ such that $h_{\mathcal{E}}(\epsilon_k) = t_{\mathcal{E}}(\epsilon_k)$, and *duplicate edges* are any pair $\epsilon_i, \epsilon_j \in \mathcal{E}$ such that $i \neq j$, $t_{\mathcal{E}}(\epsilon_i) = t_{\mathcal{E}}(\epsilon_j)$ and $h_{\mathcal{E}}(\epsilon_i) = h_{\mathcal{E}}(\epsilon_j)$. A *simple graph* does not include self-loops. A *multi-graph* is a graph that includes duplicate edges. Figure 1.3 provides examples of the different graph classes. The head and tail functions can be used to define the *incidence matrix* $E(\mathcal{G})$.

Definition 1.1 (Incidence matrix)**.** *Let $\mathcal{G} = (\mathcal{V}, \mathcal{E})$ with head and tail functions $h_{\mathcal{E}}$ and $t_{\mathcal{E}}$. Then the corresponding incidence matrix, $E(\mathcal{G}) \in \mathbb{R}^{|\mathcal{V}| \times |\mathcal{E}|}$, is defined with entries*

$$[E(\mathcal{G})]_{ij} = \begin{cases} 1 & h_{\mathcal{E}}(\epsilon_j) = v_i \\ -1 & t_{\mathcal{E}}(\epsilon_j) = v_i \\ 0 & \textit{otherwise} \end{cases} \tag{1.10}$$

Subgraphs, spanning trees and co-trees are key concepts in graph theory which will be used throughout the thesis.

Definition 1.2 (Subgraph)**.** *A subgraph $\mathcal{G}_S = (\mathcal{V}_S, \mathcal{E}_S)$ of a graph $\mathcal{G} = (\mathcal{V}, \mathcal{E})$, denoted as $\mathcal{G}_S \subseteq \mathcal{G}$, is any graph such that $\mathcal{V}_S \subseteq \mathcal{V}$ and $\mathcal{E}_S \subseteq \mathcal{E} \cap \mathcal{V}_S^2$. An induced subgraph $\mathcal{G}[\mathcal{V}_S]$ is a subgraph $\mathcal{G}_S \subseteq \mathcal{G}$ such that $\mathcal{E}_S = \mathcal{E}(\mathcal{G}) \cap \mathcal{V}_S^2$. An induced subgraph $\mathcal{G}[\mathcal{V}_S]$ is a connected component of $\mathcal{G}$ if it is connected and no node in $\mathcal{V}_S$ is adjacent to a node in $\mathcal{V}(\mathcal{G}) \setminus \mathcal{V}_S$.*

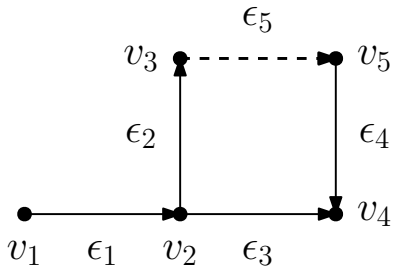

Figure 1.4: An example of a signed path vector. The tree edges are $\mathcal{E}(\mathcal{T}) = \{\epsilon_1, \epsilon_2, \epsilon_3, \epsilon_4\}$, and the sole co-tree edge is $\epsilon_1(\mathcal{C}) = \epsilon_5$ (dashed) with the corresponding signed-path vector $t_1 = [0, 1, -1, 1]^T$.

Definition 1.3 (Spanning tree and co-tree)**.** *A spanning tree $\mathcal{T}(\mathcal{G})$ of a connected graph $\mathcal{G} = (\mathcal{V}, \mathcal{E})$ is any connected subgraph $\mathcal{G}_S = (\mathcal{V}, \mathcal{E}_S)$ with a minimal number of edges. The set $\mathbb{T}(\mathcal{G})$ denotes all spanning trees of a connected graph $\mathcal{G}$. For $\mathcal{T} \in \mathbb{T}(\mathcal{G})$, the* co-tree *graph $\mathcal{G} \backslash \mathcal{E}(\mathcal{T})$ is denoted as $\mathcal{C}(\mathcal{T})$ [25].*

Based on the tree and co-tree representation of the graph, each co-tree edge can be described by a corresponding *signed-path vector* defined below, with an example given in Figure 1.4. We will find signed-path vectors useful in our graph theoretical derivations.

Definition 1.4 (Signed path vector)**.** *Consider a graph $\mathcal{G}$ and its spanning tree $\mathcal{T} \in \mathbb{T}(\mathcal{G})$ with co-tree $\mathcal{C}(\mathcal{T})$, with arbitrary head and tail assigned to the end-nodes of each edge in $\mathcal{E}(\mathcal{G})$. For each edge $\epsilon_j \in \mathcal{E}(\mathcal{C})$ there is a path from head to tail in $\mathcal{T}$, and we define a corresponding signed path vector $t_j \in \mathbb{R}^{|\mathcal{E}(\mathcal{T})|}$, $[t_j]_k = 1$ if $\epsilon_k(\mathcal{T})$ is along the path, $[t_j]_k = -1$ if $\epsilon_k(\mathcal{T})$ is opposite to the path, and $[t_j]_k = 0$ otherwise.*

The most commonly studied matrices in algebraic graph theory are the *adjacency matrix* $A(\mathcal{G}) \in \mathbb{R}^{|\mathcal{V}|\times|\mathcal{V}|}$, the *Laplacian matrix* $L(\mathcal{G}) \in \mathbb{R}^{|\mathcal{V}|\times|\mathcal{V}|}$ and the *normalized Laplacian matrix* $\mathcal{L}(\mathcal{G}) \in \mathbb{R}^{|\mathcal{V}|\times|\mathcal{V}|}$, all of which are real symmetric matrices. They are defined below, where each row and column is indexed by a vertex in the graph $\mathcal{G}$ [25],

$$[A(\mathcal{G})]_{uv} = \begin{cases} 1, & u \sim v \\ 0, & \text{otherwise} \end{cases},$$

$$[L(\mathcal{G})]_{uv} = \begin{cases} d_u(\mathcal{G}), & u = v \\ -1 & u \sim v \\ 0, & \text{otherwise} \end{cases},$$

and

$$[\mathcal{L}(\mathcal{G})]_{uv} = \begin{cases} 1, & u = v \\ -\left(\sqrt{d_u(\mathcal{G})\, d_v(\mathcal{G})}\right)^{-1} & u \sim v \\ 0, & \text{otherwise} \end{cases} .$$

For a simple undirected graph, the Laplacian matrix $L(\mathcal{G}) \in \mathbb{R}^{|\mathcal{V}|\times|\mathcal{V}|}$ can be written as

$$L(\mathcal{G}) = E(\mathcal{G})\, W(\mathcal{G})\, E(\mathcal{G})^T , \tag{1.11}$$

where $W(\mathcal{G})$ is a diagonal matrix with edge weights along the diagonal [25].

1.3 Contributions and Thesis Outline

The following overview presents the outline of this thesis and briefly summarizes its contributions. The second chapter of the thesis deals with graph theoretical derivations of graph contractions, the third chapter studies PROMs and the fourth chapter applies results from these two chapters to the model reduction of multi-agent systems, the fifth and final chapter summarizes the work.

Chapter 2 - Graph Contractions and Their Spectral Interlacing Properties

In this chapter we investigate the combinatorial operation of graph contractions. We show how classes of graph contractions where the edges of the graph are the basis for the contraction operation are a result of a combinatorial operation on the vertices of the graph. We construct, for the first time, the relations between algebraic representations of graphs, such as incidence and Laplacian matrices, and those of contracted graphs. We then derive a general interlacing graph reduction theorem based on a set-theoretical extension of the min-max theorem. A class of edge-matching graph contractions is defined, and utilizing the extension of the min-max theorem it is proven how two types of edge-matching contractions provide Laplacian and normalized Laplacian interlacing. An $\mathcal{O}(mn)$ algorithm is provided for finding a normalized Laplacian interlacing contraction and an $\mathcal{O}\left(n^2 + nm\right)$ algorithm is provided for finding a Laplacian interlacing contraction of a given graph with n vertices and m edges.

Chapter 3 - Product Form of Projection-Based Model Reduction

In this chapter, we reexamine the well known orthogonal PROMs and their realizations. A novel product form is derived for the reduction error system of these reduced models, and it is shown that any such PROM can be obtained from a sequence of 1-dimensional projection reductions. Investigating the error system product form, we then define interface-invariant PROMs, model order reductions with projection-invariant input and output matrices, and it is shown that

for such PROMs the error product systems are strictly proper. Furthermore, exploiting this structure, an analytic $\mathcal{H}_\infty$ reduction error bound is obtained and an $\mathcal{H}_\infty$ bound optimization problem is defined.

Chapter 4 - Model Reduction of Multi-Agent Systems by Graph Contractions

Based on the edge-based contractions derived in Chapter 2, in this chapter we introduce the notion of edge-induced PROMs. These are PROMs which are constructed over edge-induced partitions of the graph. This graph-based model reduction method allows us to derive sub-optimal but efficient PROMs of MAS utilizing the PROM $\mathcal{H}_\infty$ bound derived in Chapter 3. The resulting algorithm is demonstrated on a large-scale consensus model.

Chapter 5 - Summary

This final chapter provides some conclusive remarks, both summarizing the thesis and hinting at possible future directions of research.

1.4 Publications

The research presented in this thesis has been presented in the following publications

- N. Leiter and D. Zelazo, Graph-based model reduction of the controlled consensus protocol, in IFAC World Congress, Toulouse, France, 2017.
- N. Leiter and D. Zelazo, Edge-matching graph contractions and their interlacing properties, Linear Algebra and its Applications, vol. 612, pp. 289-317, 2021.

Some material in this thesis is also contained in the following manuscripts, submitted for review:

- N. Leiter and D. Zelazo, Product Form of Projection-Based Model Reduction and its Application to Multi-Agent Systems, submitted to Automatica.

Chapter 2

Graph Contractions and Their Spectral Interlacing Properties

Graphs are mathematical objects composed of a set of vertices and a set of interconnecting edges. As simple as they are constructed, the study of graphs has developed into a formal branch of mathematics, known as graph theory, with numerous applications in computer science, biology and social science, to mention a few. Partitioning of the graph vertices combined with node and edge contractions along those partitions lead to a reduced order graph known as a graph contraction.

Graph contractions have ambiguous definitions in graph theory studies, and in this chapter we try to formalize this important combinatorial operation. In this process we construct edge-induced partitions, that will lead us in the following chapters to efficient graph-based model reductions. We also explore edge-matching contractions, a class of graph contractions with a one-to-one correspondence of a subset of edges in the full order graph to those in the contracted graph. Additionally, we construct, for the first time, the relations between algebraic representations of graphs, such as incidence and Laplacian matrices, and those of contracted graphs. Finally, based on a novel min-max theorem, it is then shown how two types of such edge-matching contractions provide eigenvalue interlacing of Laplacian-type graph matrices.

2.1 Introduction

The effect of combinatorial operations on graph spectra is an evolving branch of graph theory, linking together combinatorial graph theory with the spectral analysis of the algebraic structures of graphs, e.g., Fiedler's seminal results on the Laplacian algebraic connectivity [21]. In general, there is an interest to

understand how certain graph reduction operations relate to spectral and combinatorial properties. Of particular interest are reductions that satisfy an *interlacing* property between algebraic graph representations such as graph matrices. Interlacing properties of graph matrices have shown to have combinatorial interpretations: Haemers used adjacency and Laplacian interlacing to provide combinatorial results on the chromatic number and spectral bounds [29], and the neighborhood reassignment operation was shown to provide interlacing of the normalized Laplacian [66].

Partitioning the vertices of a graph is a combinatorial operation extensively studied in graph theory in the context of graph clustering [55] and network communities [49], and for spectral clustering methods [50]. However, there are only sparse results relating graph contractions based on vertex partitions and spectral interlacing. Chen et al. provided an interlacing result on normalized Laplacians based on a certain class of edge-based graph contractions [11].

In this work, we explore interlacing of reduced graph matrices and derive a general spectral interlacing theorem for reduced graphs based on an extension of the min-max theorem. In order to find classes of interlacing reduced graphs, we conduct a rigorous combinatorial analysis of graph contractions. The outcome of this analysis includes edge-induced partitions, and edge-matching contractions, a class of graph contractions with a one-to-one correspondence of a subset of edges in the full order graph to those in the contracted graph. An additional novel result of this analysis, is the construction of several relations between algebraic representations of graphs, such as incidence and Laplacian matrices, and those of contracted graphs.

Utilizing the graph theoretical derivations and the interlacing theorem, we show how two type of edge-matching contractions lead to interlacing of the normalized-Laplacian and Laplacian graph matrices. Two algorithms are then constructed for finding, if they exist, such contractions.

The remaining sections of this chapter are as follows. In Section 2.2 we formulate the graph contraction operation for simple undirected graphs, define edge-induced graph contractions, and introduce the class of edge-matching graph contractions. Section 2.3, investigates several relations between algebraic representations of graphs, such as incidence and Laplacian matrices, and those of contracted graphs. In Section 2.4, the interlacing graph reduction problem is presented, and solved for two sub-classes of edge-matching contractions for the Laplacian and normalized-Laplacian matrices. Section 2.5 provides case studies of the interlacing methods, and Section 2.6 concludes this chapter.

2.2 Graph Contractions

Graph contractions are a graph reduction method based on partitions of the vertex set. They are a useful algorithmic tool applied to a variety of graph-theoretical problems, e.g., for obtaining the connected components [13] or finding all spanning trees of a graph [46, 65]. We now define several graph operations required for vertex partitions and graph contractions and derive results that will

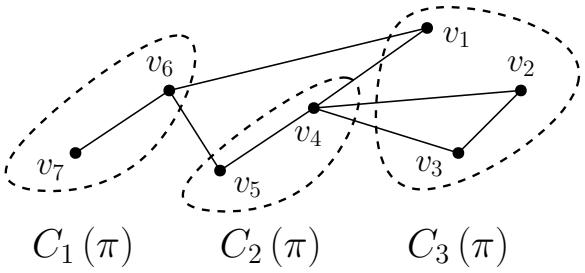

Figure 2.1: An example of a graph and a 3-partition $\pi_3(\mathcal{V})$ of its vertices into three cells $C_1 = \{v_1, v_2, v_3\}$, $C_2 = \{v_4, v_5\}$ and $C_3 = \{v_6, v_7\}$. The corresponding cell neighborhoods are $\mathcal{N}_{C_1}(\mathcal{G}) = \{v_1, v_5\}$, $\mathcal{N}_{C_2}(\mathcal{G}) = \{v_1, v_2, v_3, v_6\}$ and $\mathcal{N}_{C_3}(\mathcal{G}) = \{v_4, v_6\}$.

allow us to relate graph contractions and graph interlacing. Hereafter in this chapter $\mathcal{G} = (\mathcal{V}, \mathcal{E})$ is a simple connected graph of order n.

For an integer r satisfying $1 \leq r \leq n$, an *r-partition* of a vertex set $\mathcal{V}$ of order n, denoted $\pi_r(\mathcal{V})$, is a set of r cells $\{C_i\}_{i=1}^r$ such that $C_i \cap C_j = \emptyset$ and $\cup_{i=1}^r C_i = \mathcal{V}$, and we denote the ith cell of a partition π as $C_i(\pi)$. The *cell neighborhood* $\mathcal{N}_{C_i}(\mathcal{G})$ is defined as $\mathcal{N}_{C_i} \triangleq \{\cup_{v \in C_i} \mathcal{N}_v(\mathcal{G})\} \setminus C_i$ (Figure 2.1).

For $r = n$, $C_i(\pi_n) = i$ is the *identity partition*, which contains n singletons (a cell with a single vertex). An *atom partition* $\pi_{n-1}(\mathcal{V})$ contains $n-2$ singletons and a single 2-vertex cell. The set of all r-partitions of $\mathcal{V}$ is denoted by $\Pi_r(\mathcal{V})$, and the set of all partitions of $\mathcal{V}$ is $\Pi(\mathcal{V}) \triangleq \cup_{r=1}^n \Pi_r(\mathcal{V})$. For a graph $\mathcal{G} = (\mathcal{V}, \mathcal{E})$, we may denote $\pi_r(\mathcal{V})$ and $\Pi_r(\mathcal{V})$ as $\pi_r(\mathcal{G})$ and $\Pi_r(\mathcal{G})$.

For a graph with n_{cc} connected components, we define the *connected components partition* $\pi_{cc}(\mathcal{G})$ as the partition $\pi_{cc}(\mathcal{G}) = \{C_i\}_{i=1}^{n_{cc}}$, such that $\mathcal{G}[C_i]$ is the ith connected components of $\mathcal{G}$ (Figure 2.2).

Definition 2.1 (Partition function)**.** *For a graph $\mathcal{G}$ and r-partition $\pi \in \Pi_r(\mathcal{G})$, the* partition function *is a map $f_\pi : \mathcal{V}(\mathcal{G}) \to [1, r]$ from each node in $\mathcal{V}$ to its cell index, i.e., $f_\pi(v) \triangleq \{i \in [1, r] \,|C_i(\pi) \cap v \neq \emptyset\}$. More generally, for a subset $\mathcal{V}_S \subseteq \mathcal{V}(\mathcal{G})$ we have $f_\pi(\mathcal{V}_S) \triangleq \{i \in [1, r] \,|C_i(\pi) \cap \mathcal{V}_S \neq \emptyset\}$.*

The partition function allows us to precisely define the *quotient* and the *graph contraction*, and their notations which are used interchangeably in the literature.

Definition 2.2 (Quotient)**.** *The quotient of a graph $\mathcal{G}$ over a partition $\pi \in \Pi_r(\mathcal{G})$, denoted by $\mathcal{G}/\pi$, is the multi-graph of order r with an edge $\{u, v\}$ for each edge between nodes in $C_u(\pi)$ and $C_v(\pi)$, i.e., $\mathcal{G}/\pi = \left([1, r], \{\tilde{\epsilon}_j\}_{j=1}^{|\mathcal{E}|}\right)$ with*

$$\tilde{\epsilon}_j = \{f_\pi(h_\mathcal{E}(\epsilon_j)), f_\pi(t_\mathcal{E}(\epsilon_j))\},$$

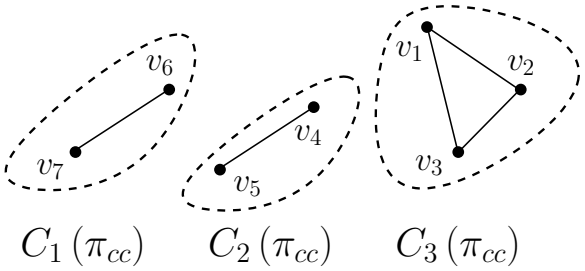

Figure 2.2: An example of a graph and its connected components partition $\pi_{cc}(\mathcal{G})$ with three components $C_1 = \{v_1, v_2, v_3\}$, $C_2 = \{v_4, v_5\}$ and $C_3 = \{v_6, v_7\}$.

where $\epsilon_j \in \mathcal{E}(\mathcal{G})$ *and* $h_{\mathcal{E}}(\epsilon), t_{\mathcal{E}}(\epsilon) : \mathcal{E}(\mathcal{G}) \to \mathcal{V}(\mathcal{G})$ *assign a head and a tail to the end-nodes of each edge (thus,* $\epsilon = (h_{\mathcal{E}}(\epsilon), t_{\mathcal{E}}(\epsilon))$*).*

Definition 2.3 (Graph contraction)**.** *The graph contraction of* $\mathcal{G}$ *over* π *is the simple graph denoted as* $\mathcal{G} /\!\!/ \pi$ *which is obtained from the quotient* $\mathcal{G}/\pi$ *by removing all self-loops and redundant duplicate edges. Equivalently,* $\mathcal{G} /\!\!/ \pi = ([1, r], \mathcal{E}_r)$ *with*

$$\mathcal{E}_r = \left\{ \tilde{\epsilon} \in [1, r]^2 \,|\tilde{\epsilon} \in \mathcal{E}(\mathcal{G}/\pi), h_{\mathcal{E}}(\tilde{\epsilon}) \neq t_{\mathcal{E}}(\tilde{\epsilon}) \right\}.$$

If π is an atom partition we call $\mathcal{G} /\!\!/ \pi$ an *atom contraction*. For example, consider the partition of $\pi = \{\{v_1\}, \{v_2\}, \{v_3\}, \{v_4, v_5\}\}$, for the graph $\mathcal{G}$ shown in Figure 2.3. The quotient $\mathcal{G}/\pi$ and the graph contraction $\mathcal{G} /\!\!/ \pi$ are shown in Figure 2.3. Notice that this is an example of an atom partition and atom contraction.

Node removal is the simplest graph-reduction method. However, in some cases the same reduced graph can be obtained either from node-removal or from a graph contraction. We define here these contractions as *node-removal equivalent contractions*.

Definition 2.4 (Node-removal equivalent contraction)**.** *For the graph* $\mathcal{G}$ *and its contraction* $\mathcal{G} /\!\!/ \pi$*, we say that* $\mathcal{G} /\!\!/ \pi$ *is* node-removal equivalent *if there is a subset* $\mathcal{V}_S \subset \mathcal{V}(\mathcal{G})$ *such that* $\mathcal{G} /\!\!/ \pi = \mathcal{G} \backslash \mathcal{V}_S$*.*

Cycles play an important role in the properties of graphs, and we define here a cycle-invariant graph contraction as a contraction that preserves the cycle structure of the full graph. To the best of our knowledge, such a relation between contractions and cycles has not been previously defined.

Definition 2.5 (Cycle-invariant contraction)**.** *Consider a graph* $\mathcal{G}$ *and its contraction* $\mathcal{G} /\!\!/ \pi$*, then we say that the contraction* $\mathcal{G} /\!\!/ \pi$ *is* cycle-invariant *if there is one-to-one mapping between the set of simple cycles of the full-order graph and the set of simple cycles of the contracted graph.*

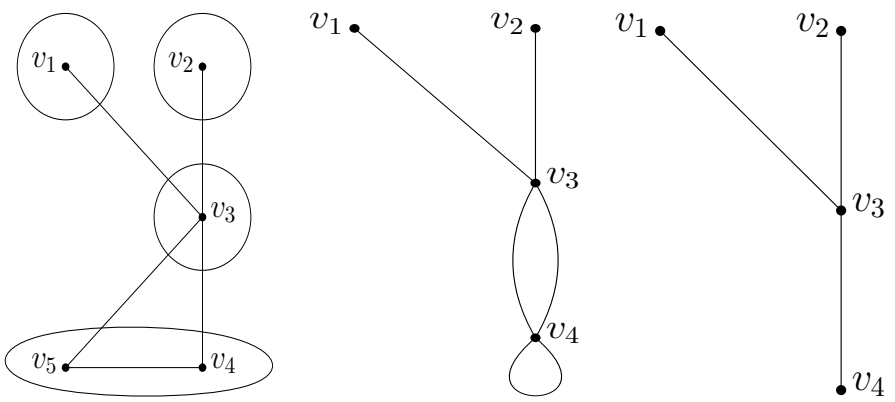

(a) Full order graph $\mathcal{G}$ and its vertex partition π.

(b) The graph quotient $\mathcal{G}\backslash\pi$

(c) The graph contraction $\mathcal{G} /\!\!/ \pi$.

Figure 2.3: Full order graph and its quotient and contraction over the vertex partition $\pi = \{\{v_1\}, \{v_2\}, \{v_3\}, \{v_4, v_5\}\}$.

For example, consider the partition $\pi = \{\{v_1, v_2, v_3\}, \{v_4\}, \{v_5\}\}$ for the graph shown in Figure 2.4. The resulting contraction over the graph is cycle-invariant (Definition 2.5) with the cycle $v_3v_4v_5v_3$ of $\mathcal{G}$ mapped to the cycle $v_1v_2v_3v_1$ of $\mathcal{G} /\!\!/ \pi$, and is also node-removal equivalent (Definition 2.4) with $\mathcal{V}_S = \{v_1, v_2\}$. Notice that if the edge $\{v_1, v_5\}$ were added in Figure 2.4, the same contraction would *not* be a cycle-invariant contraction; however, it would still be node-removal equivalent with $\mathcal{V}_S = \{v_1, v_2\}$.

We derive the following three lemmas that provide combinatorial results related to graph contractions: The first lemma (Lemma 2.1) shows that the contraction of a subgraph obtained by removal of edges is a subgraph of the graph contraction over the same partition. The second lemma (Lemma 2.2) relates the connectivity of a graph contraction to the neighborhoods of the graph. The third lemma (Lemma 2.3) dictates that if a graph is connected then any of its contractions is connected.

Lemma 2.1 (Subgraph contraction lemma)**.** *Consider a graph $\mathcal{G}$ and its subgraph $\mathcal{G}_R = \mathcal{G}\backslash\mathcal{E}_R$ for $\mathcal{E}_R \subseteq \mathcal{E}(\mathcal{G})$. Then for any $\pi \in \Pi(\mathcal{G})$, $\mathcal{G}_R /\!\!/ \pi \subseteq \mathcal{G} /\!\!/ \pi$.*

Proof. For any $\tilde{\epsilon} \in \mathcal{E}(\mathcal{G}_R /\!\!/ \pi)$ we can find $\epsilon \in \mathcal{E}(\mathcal{G}_R)$ such that $\tilde{\epsilon} = \{f_\pi(h_\mathcal{E}(\epsilon)), f_\pi(t_\mathcal{E}(\epsilon))\}$. Since $\mathcal{E}(\mathcal{G}_R) \subseteq \mathcal{E}(\mathcal{G})$, therefore $\epsilon \in \mathcal{E}(\mathcal{G})$ and $\{f_\pi(h_\mathcal{E}(\epsilon)), f_\pi(t_\mathcal{E}(\epsilon))\} \in \mathcal{E}(\mathcal{G} /\!\!/ \pi)$. We conclude that $\mathcal{E}(\mathcal{G}_R /\!\!/ \pi) \subseteq \mathcal{E}(\mathcal{G} /\!\!/ \pi)$, and since $\mathcal{V}(\mathcal{G}_R /\!\!/ \pi) = \mathcal{V}(\mathcal{G} /\!\!/ \pi)$ we obtain that $\mathcal{G}_R /\!\!/ \pi \subseteq \mathcal{G} /\!\!/ \pi$. □

Lemma 2.2. *Consider a graph $\mathcal{G}$ and its contraction $\mathcal{G} /\!\!/ \pi$ for $\pi \in \Pi(\mathcal{G})$. Then $\forall u \in \mathcal{V}(\mathcal{G}), \forall \tilde{u} \in \mathcal{V}(\mathcal{G} /\!\!/ \pi)$, we have $u \in \mathcal{N}_{C_{\tilde{u}}}(\mathcal{G})$ if and only if $f_\pi(u) \sim \tilde{u}$.*

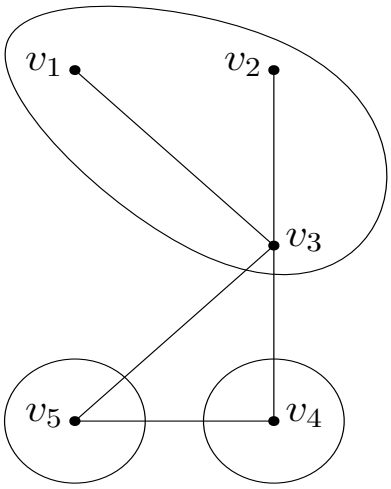

(a) Full order graph $\mathcal{G}$ and its vertex partition $\pi = \{\{v_1, v_2, v_3\}, \{v_4\}, \{v_5\}\}$.

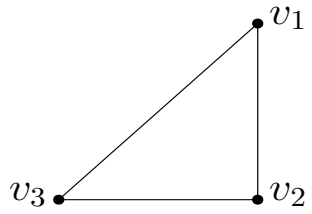

(b) Cycle invariant graph and node-removal equivalent contraction $\mathcal{G} /\!\!/ \pi$.

Figure 2.4: Full order graph and its cycle-invariant and node-removal equivalent contraction.

Proof. If $u \in \mathcal{N}_{C_{\tilde{u}}}$ then $\exists v \in C_{\tilde{u}}$ such that $u \sim v$ with $\epsilon = \{u, v\} \in \mathcal{E}(\mathcal{G})$, and therefore $\{f_\pi(u), f_\pi(v)\} = \{f_\pi(u), \tilde{u}\} \in \mathcal{E}(\mathcal{G} /\!\!/ \pi)$ and $f_\pi(u) \sim \tilde{u}$. If $f_\pi(u) \sim \tilde{u}$, then $\exists v \in C_{\tilde{u}}$ such that $u \sim v$ and therefore $u \in \mathcal{N}_{C_{\tilde{u}}}$. □

Lemma 2.3. *If a graph $\mathcal{G}$ is connected then its graph contraction $\mathcal{G} /\!\!/ \pi$ is connected.*

Proof. If $\mathcal{G}$ is connected then $\forall u, v \in \mathcal{V}$, there is a path $uu_1u_2 \dots u_pv$. For any $\tilde{u}, \tilde{v} \in \mathcal{V}(\mathcal{G} /\!\!/ \pi)$ we can find $u, v \in \mathcal{V}$ such that $f_\pi(u) = \tilde{u}$ and $f_\pi(v) = \tilde{v}$. If we then apply the partition function on the path $uu_1u_2 \dots u_pv$ we obtain a walk (including self loops) in $\mathcal{G} /\!\!/ \pi$, $\tilde{u} f_\pi(u_1) f_\pi(u_2) \dots f_\pi(u_p) \tilde{v}$, therefore, $\mathcal{G} /\!\!/ \pi$ is a connected graph. □

Based on Lemma 2.2, the following proposition relates the degree of a node in a contracted graph to its cell-neighborhood.

Proposition 2.1 (Degree-contraction)**.** *Consider a graph $\mathcal{G}$ and its contraction $\mathcal{G} /\!\!/ \pi$ for $\pi \in \Pi(\mathcal{G})$. Then $\forall \tilde{v} \in \mathcal{V}(\mathcal{G} /\!\!/ \pi)$, $d_{\tilde{v}}(\mathcal{G} /\!\!/ \pi) = |f_\pi(\mathcal{N}_{C_{\tilde{v}}}(\mathcal{G}))|$.*

Proof. From Definition 2.1 we have

$$f_\pi(\mathcal{N}_{C_{\tilde{v}}}(\mathcal{G})) = \{i \in [1, r] \,|C_i(\pi) \cap \mathcal{N}_{C_{\tilde{v}}}(\mathcal{G}) \neq \emptyset\},$$

and from Lemma 2.2 we obtain that $\forall \tilde{u}, \tilde{v} \in \mathcal{V}(\mathcal{G} /\!\!/ \pi)$, $\tilde{v} \sim \tilde{u}$ if and only if $\tilde{u} \in f_\pi(\mathcal{N}_{C_{\tilde{v}}})$ such that $f_\pi(\mathcal{N}_{C_{\tilde{v}}}) = \mathcal{N}_{\tilde{v}}(\mathcal{G} /\!\!/ \pi)$, and therefore, $d_{\tilde{v}}(\mathcal{G} /\!\!/ \pi) = |f_\pi(\mathcal{N}_{C_{\tilde{v}}})|$. □

2.2.1 Graph Contraction Posets

Partially-ordered sets (posets) are an essential concept in order theory, and a useful tool in proving graph-theoretical results [8]. Based on the one-to-one correspondence between graph contractions and vertex partitions, we show how graph contractions fall under the definition of a poset. We then establish contraction chains and their corresponding contraction sequences as a basis for proving cases of graph matrices interlacing.

Two partitions $\pi_{r_1}, \pi_{r_2} \in \Pi(\mathcal{V})$ may comply with a *refinement* relation and sets of partitions can construct *chains*, totally-ordered subsets of the posets.

Definition 2.6 (Refinement)**.** *Consider two partitions $\pi_{r_1}, \pi_{r_2} \in \Pi(\mathcal{V})$ of a vertex set $\mathcal{V}$ where $r_1 \leq r_2 \leq |\mathcal{V}|$. Then we say π_{r_2} is a* refinement *of π_{r_1} if $\forall j \in \{1, 2, \ldots, r_2\}$ we can find $i \in \{1, 2, \ldots, r_1\}$ such that $C_j(\pi_{r_2}) \subseteq C_i(\pi_{r_1})$, and we denote $\pi_{r_2} \leq \pi_{r_1}$. If $\pi_{r_2} \leq \pi_{r_1}$ and $r_1 < r_2$ we denote $\pi_{r_2} < \pi_{r_1}$. An N-*chain *is a partition set $\chi(\mathcal{V}) = \{\pi_{r_i}\}_{i=1}^{N} \subseteq \Pi(\mathcal{V})$ such that $\pi_{r_1} < \pi_{r_2} < \ldots < \pi_{r_N}$.*

If two partitions $\pi_{r_1}, \pi_{r_2} \in \Pi(\mathcal{V})$ comply with the refinement relation, we can construct the *coarsening* partition $\delta(\pi_{r_2}, \pi_{r_1}) \in \Pi_{r_1}(\mathcal{V}_{r_2})$ with

$$C_j(\delta(\pi_{r_2}, \pi_{r_1})) = \{k \in \{1, 2, \ldots, r_2\} \,|C_k(\pi_{r_2}) \subseteq C_j(\pi_{r_1})\}.$$

We can now define the coarsening sequence.

Definition 2.7 (Coarsening sequence)**.** *Consider a vertex set $\mathcal{V}$ and its N-*chain *$\chi(\mathcal{V}) \subseteq \Pi(\mathcal{V})$. Then we define the coarsening sequence as $\Delta(\chi) = \{\delta_i\}_{i=1}^{N-1}$ with $\delta_i \triangleq \delta(\pi_{r_{i+1}}, \pi_{r_i})$.*

The refinement relation is reflexive, anti-symmetric and transitive, therefore, the set of partitions together with the refinement relation, $(\Pi(\mathcal{V}), \leq)$, falls under the definition of a finite *partial-ordered set* (poset). Let $\mathcal{G} = (\mathcal{V}, \mathcal{E})$, we define the contraction set

$$\mathcal{G} /\!\!/ \Pi \triangleq \{\mathcal{G} /\!\!/ \pi | \pi \in \Pi(\mathcal{V})\},$$

and define the contraction binary relation $\mathcal{G} /\!\!/ \pi_{r_1} \leq \mathcal{G} /\!\!/ \pi_{r_2}$ if $\pi_{r_1} \leq \pi_{r_2}$. Since there is a one-to-one correspondence between $(\mathcal{G} /\!\!/ \Pi, \leq)$ and $(\Pi(\mathcal{V}), \leq)$, the contraction set with the contraction binary relation, $(\mathcal{G} /\!\!/ \Pi, \leq)$, is also a poset, and for each N-chain $\chi \subseteq \Pi(\mathcal{V})$ there is a corresponding *contraction chain* ,

$$\mathcal{G} /\!\!/ \chi = \{\mathcal{G} /\!\!/ \pi_{r_i}\}_{i=1}^{N} \subseteq \mathcal{G} /\!\!/ \Pi.$$

For each coarsening sequence $\Delta(\chi)$ we can then define a corresponding contraction sequence, a series of graphs where each graph in the series is a graph contraction of the former graph over the coarsening partition in the coarsening sequence.

Definition 2.8 (Contraction sequence)**.** *Consider a graph $\mathcal{G}$ and an N-chain $\chi(\mathcal{V}) \subseteq \Pi(\mathcal{V}(\mathcal{G}))$ with coarsening sequence $\Delta(\chi) = \{\delta_i\}_{i=1}^{N-1}$. Then we define the* contraction sequence *$\mathcal{G} /\!\!/ \Delta(\chi) \triangleq \{\mathcal{G}_i\}_{i=0}^{N-1}$ with $\mathcal{G}_i = \mathcal{G}_{i-1} /\!\!/ \delta_{N-i}$ and $\mathcal{G}_0 = \mathcal{G} /\!\!/ \pi_{r_N}$.*

Proposition 2.2. *Consider a graph $\mathcal{G}$ and its partition $\pi \in \Pi(\mathcal{G})$, and let $\chi = \{\pi_{r_i}\}_{i=1}^{N} \subseteq \Pi(\mathcal{V})$ be a chain with $\pi_{r_1} = \pi$ and corresponding contraction sequence $\mathcal{G} /\!\!/ \Delta(\chi) = \{\mathcal{G}_i\}_{i=0}^{N-1}$. Then $\mathcal{G}_{N-1} = \mathcal{G} /\!\!/ \pi$.*

Proof. It is sufficient to prove for any two-chain $\pi = \pi_{r_1} < \pi_{r_2}$ with $\Delta(\chi) = \delta(\pi_{r_2}, \pi_{r_1})$, i.e., $\mathcal{G} /\!\!/ \pi = (\mathcal{G} /\!\!/ \pi_{r_2}) /\!\!/ \delta(\pi_{r_2}, \pi_{r_1})$, and extend by induction for $N > 2$. The order of $\mathcal{G}_0 = \mathcal{G} /\!\!/ \pi_{r_2}$ is r_2 and from the coarsening sequence (Definition 2.7) we get that the order of $\mathcal{G}_1 = (\mathcal{G} /\!\!/ \pi_{r_2}) /\!\!/ \delta(\pi_{r_2}, \pi_{r_1})$ is $r_1 = |\pi|$, therefore, $\mathcal{V}(\mathcal{G}_1) = \mathcal{V}(\mathcal{G} /\!\!/ \pi)$. It is left to show that $\mathcal{E}(\mathcal{G}_1) = \mathcal{E}(\mathcal{G} /\!\!/ \pi)$. Let $\tilde{\epsilon} \in \mathcal{E}(\mathcal{G} /\!\!/ \pi)$ then $\exists \epsilon \in \mathcal{E}_{\mathcal{G}}$ such that $\tilde{\epsilon} = f_{\pi}(\epsilon)$. Now let $\epsilon_1 = f_{\pi_{r_2}}(\epsilon)$ and $\epsilon_2 = f_{\delta}(\epsilon_1)$, from the coarsening sequence (Definition 2.7) we then obtain that the end nodes of ϵ_2 are the end nodes of $\tilde{\epsilon}$, therefore, $\mathcal{E}(\mathcal{G}_1) = \mathcal{E}(\mathcal{G} /\!\!/ \pi)$. □

Corollary 2.1 (Atom-contraction sequence)**.** *Consider a graph $\mathcal{G}$ and its partition $\pi \in \Pi_r(\mathcal{G})$ for $r < n$. Then there exists a chain $\chi(\mathcal{V}) = \{\pi_{r_i}\}_{i=1}^{n-r+1} \subseteq \Pi(\mathcal{V}_n)$ such that $\mathcal{G} /\!\!/ \Delta(\chi) = \{\mathcal{G}_i\}_{i=0}^{n-r}$ is an atom contraction sequence, i.e., $\delta\left(\pi_{r_{i+1}}, \pi_{r_i}\right)$ is an atom-partition.*

Proof. Choose $\pi_{r_1} = \pi(\mathcal{V}_n)$, and then construct π_{r_2} by extracting a singleton from a non-singleton cell of π. Continue to extract singleton cells until all cells are singletons, i.e., $\pi_{r_N} = \pi_n(\mathcal{V}_n)$. The number of singleton extractions of non-singleton cells in an r-partition is $n - r$, therefore, $N = n - r + 1$. □

For example, consider the 2-chain $\chi(\mathcal{V}_5) = \{\pi_2, \pi_3\}$ with

$$\pi_2(\mathcal{V}_5) = \left\{ \underbrace{\{v_1, v_2, v_3\}}_{C_1}, \underbrace{\{v_4, v_5\}}_{C_2} \right\}, \text{ and } \pi_3(\mathcal{V}_5) = \left\{ \underbrace{\{v_1, v_2\}}_{C_1}, \underbrace{\{v_3\}}_{C_2}, \underbrace{\{v_4, v_5\}}_{C_3} \right\}.$$

We have $C_1(\pi_3), C_2(\pi_3) \subseteq C_1(\pi_2)$ and $C_3(\pi_3) \subseteq C_2(\pi_2)$, therefore, $\pi_3 < \pi_2$. We can then construct the *coarsening sequence* $\Delta(\chi) = \delta(\pi_3, \pi_2)$ with $\delta(\pi_3, \pi_2) = \{\underbrace{\{1, 2\}}_{C_1}, \underbrace{\{3\}}_{C_2}\}$. The resulting graph contraction sequence is presented in Figure 2.5.

2.2.2 Edge-Based Graph Contractions

Graph contractions are defined over vertex partitions. However, there is also an edge-based approach to perform graph contractions. Our contribution here is the definition of edge-induced partitions and their utility as a combinatorial relation between edge-based contractions and vertex-based contractions.

Definition 2.9 (Edge-induced partition)**.** *Consider a graph $\mathcal{G}$ and an edge contraction set $\mathcal{E}_{cs} \subset \mathcal{E}(\mathcal{G})$ with $|\mathcal{E}_{cs}| = n - r$. Then we define the* edge-induced partition $\pi_c(\mathcal{G}, \mathcal{E}_{cs})$ *as the connected components partition of the graph*

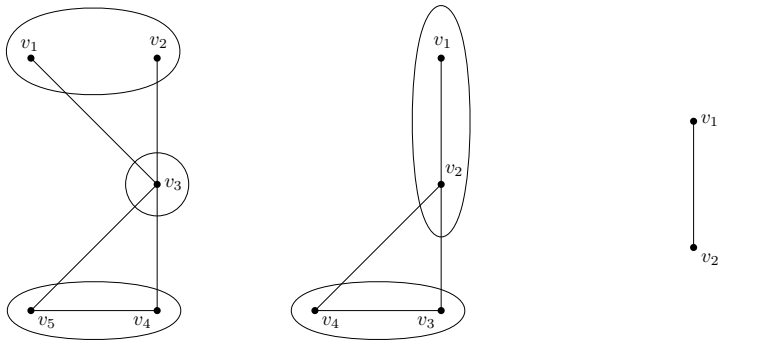

Figure 2.5: Graph contraction sequence.

$\mathcal{G}_c(\mathcal{G}, \mathcal{E}_{cs}) = (\mathcal{V}(\mathcal{G}), \mathcal{E}_{cs})$, *i.e.,* $\pi_c(\mathcal{G}, \mathcal{E}_{cs}) = \pi_{cc}(\mathcal{G}_c(\mathcal{G}, \mathcal{E}_{cs}))$. *The set of all edge contraction sets of cardinality* p *is defined as*

$$\Xi_p(\mathcal{G}) \triangleq \{\mathcal{E}_{cs} \subset \mathcal{E}(\mathcal{G}) \,|\, |\mathcal{E}_{cs}| = p\}.$$

With the edge contraction partition definition we can define an edge-based graph contraction.

Definition 2.10 (Edge-based graph contraction)**.** *Consider a graph* $\mathcal{G}$ *and an edge contraction set* $\mathcal{E}_{cs} \in \Xi_{n-r}(\mathcal{G})$ *for* $r < n$*. Then the edge-based contraction is defined as the contraction over the edge-induced partition, i.e.,* $\mathcal{G} /\!\!/ \mathcal{E}_{cs} = \mathcal{G} /\!\!/ \pi_c(\mathcal{G}, \mathcal{E}_{cs})$.

In this work we find that a class of edge-matching contractions has interlacing properties.

Definition 2.11 (Edge-matching contraction)**.** *Consider a graph* $\mathcal{G}$ *and an edge contraction set* $\mathcal{E}_{cs} \in \Xi_{n-r}(\mathcal{G})$ *for* $r < n$*. Then* $\mathcal{G} /\!\!/ \mathcal{E}_{cs}$ *is an edge-matching contraction if there is one-to-one correspondence between* $\mathcal{E}(\mathcal{G}) \setminus \mathcal{E}_{cs}$ *and* $\mathcal{E}(\mathcal{G} /\!\!/ \mathcal{E}_{cs})$.

A graph contraction cannot create new edges, therefore, edge-matching (Definition 2.11) is equivalent to $|\mathcal{E}(\mathcal{G}) \setminus \mathcal{E}_{cs}| = |\mathcal{E}(\mathcal{G} /\!\!/ \mathcal{E}_{cs})|$.

Proposition 2.3. *Consider a graph* $\mathcal{G}$ *and an edge contraction set* $\mathcal{E}_{cs} \in \Xi_{n-r}(\mathcal{G})$*. Then if* $\mathcal{G} /\!\!/ \mathcal{E}_{cs}$ *is cycle-invariant (Definition 2.5) it is also edge-matching (Definition 2.11).*

Proof. If $\mathcal{G} /\!\!/ \mathcal{E}_{cs}$ is cycle-invariant then from Definition 2.5 the edges in $\mathcal{E}_{cs}$ are not part of any cycle of $\mathcal{G}$. Therefore, the contraction does not map any two edges in $\mathcal{E}(\mathcal{G}) \setminus \mathcal{E}_{cs}$ to a single edge in $\mathcal{E}(\mathcal{G} /\!\!/ \mathcal{E}_{cs})$, otherwise they would have been part of a cycle with an edge in $\mathcal{E}_{cs}$, and we obtain that $|\mathcal{E}(\mathcal{G}) \setminus \mathcal{E}_{cs}| = |\mathcal{E}(\mathcal{G} /\!\!/ \mathcal{E}_{cs})|$. □

Proposition 2.4. *Consider a graph $\mathcal{G}$ and a node $v \in \mathcal{V}(G)$, and let $\pi_{cc}(\mathcal{G}\backslash v)$ be the connected component partition of $\mathcal{G}\backslash v$, then for $C_i \in \pi_{cc}(\mathcal{G}\backslash v)$ and $\mathcal{E}_{cs} = \mathcal{E}(\mathcal{G}[C_i \cup v])$, the contraction $\mathcal{G} /\!\!/ \mathcal{E}_{cs}$ is node-removal equivalent (Definition 2.4) with $\mathcal{V}_S = C_i$, and is also edge-matching (Definition 2.11).*

Proof. Since C_i is a connected component of $\mathcal{G}\backslash\mathcal{E}(\mathcal{G}[\mathcal{N}_v \cup v])$ then v is the only node in any path between C_i and $\mathcal{V}(\mathcal{G}) \setminus \{C_i \cup v\}$, therefore, by choosing $\mathcal{V}_S = C_i$ the graph $\mathcal{G}\backslash C_i$ removes all edges $\mathcal{E}(\mathcal{G}[C_i])$ and all edges connecting C_i to $\mathcal{V}(\mathcal{G})\backslash C_i$ which are the edges between C_i and v and we obtain that $\mathcal{G}\backslash C_i = \mathcal{G} /\!\!/ \mathcal{E}(\mathcal{G}[C_i \cup v])$, i.e., the contraction $\mathcal{G} /\!\!/ \mathcal{E}_{cs}$ is node-removal equivalent (Definition 2.4). Furthermore, contracting all edges $\mathcal{E}(\mathcal{G}[C_i \cup v])$ does not effect any other edges in $\mathcal{G}$ such that $|\mathcal{E}(\mathcal{G})\backslash\mathcal{E}_{cs}| = |\mathcal{E}(\mathcal{G} /\!\!/ \mathcal{E}_{cs})|$ and we obtain that $\mathcal{G} /\!\!/ \mathcal{E}_{cs}$ is edge-matching. □

We can choose a subset of tree edges to create a tree-based contraction of a graph.

Definition 2.12 (tree-based contraction)**.** *Consider a graph $\mathcal{G}$ and its spanning tree $\mathcal{T} \in \mathbb{T}(\mathcal{G})$ with an edge contraction set $\mathcal{E}_{cs} \in \Xi_{n-r}(\mathcal{T})$. Then $\mathcal{G} /\!\!/ \mathcal{E}_{cs}$ is a tree-based contraction.*

For example, the graph contraction $\mathcal{G} /\!\!/ \pi$ presented in Figure 2.4 can also be performed as an edge-based contraction $\mathcal{G} /\!\!/ \mathcal{E}_{cs}$ with $\mathcal{E}_{cs} = \{\{v_1, v_3\}, \{v_2, v_3\}\}$ and a tree-based contraction (Definition 2.12).

If the contraction edge set is a subset of the edges of a spanning tree, then the contracted tree edges will form a spanning tree of the contracted graph.

Proposition 2.5. *Consider a graph $\mathcal{G}$ and its spanning tree $\mathcal{T} \in \mathbb{T}(\mathcal{G})$ with an edge contraction set $\mathcal{E}_{cs} \in \Xi_{n-r}(\mathcal{T})$. Then $\mathcal{T} /\!\!/ \mathcal{E}_{cs} \in \mathbb{T}(\mathcal{G} /\!\!/ \mathcal{E}_{cs})$, i.e., $\mathcal{T} /\!\!/ \mathcal{E}_{cs}$ is a tree of order r of the contracted graph.*

Proof. A tree of order n has $n-1$ edges, and by contracting $n-r$ tree edges we are left with $(n-1)-(n-r)$ edges, such that $|\mathcal{E}(\mathcal{T} /\!\!/ \mathcal{E}_{cs})| = r-1$. It is left to show that $\mathcal{T} /\!\!/ \mathcal{E}_{cs}(\mathcal{T}) \subseteq \mathcal{G} /\!\!/ \mathcal{E}_{cs}(\mathcal{T})$. From Lemma 2.3 we obtain that $\mathcal{T} /\!\!/ \mathcal{E}_{cs}$ is connected, therefore, $\mathcal{T} /\!\!/ \mathcal{E}_{cs}$ is a connected graph of order r with $r-1$ edges, which is a tree of order r. Since $\mathcal{E}_{cs}(\mathcal{T}) \subseteq \mathcal{E}(\mathcal{G})$ we have $\pi_c(\mathcal{T}, \mathcal{E}_{cs}(\mathcal{T})) = \pi_c(\mathcal{G}, \mathcal{E}_{cs}(\mathcal{T}))$, and since $\mathcal{T} = \mathcal{G}\backslash\mathcal{E}(\mathcal{C})$ we obtain from the subgraph contraction lemma (Lemma 2.1) that $\mathcal{T} /\!\!/ \pi_c(\mathcal{T}, \mathcal{E}_{cs}(\mathcal{T})) \subseteq \mathcal{G} /\!\!/ \pi_c(\mathcal{T}, \mathcal{E}_{cs}(\mathcal{T}))$ and conclude that $\mathcal{T} /\!\!/ \mathcal{E}_{cs}(\mathcal{T}) \subseteq \mathcal{G} /\!\!/ \mathcal{E}_{cs}(\mathcal{T})$, and therefore, $\mathcal{T} /\!\!/ \mathcal{E}_{cs}(\mathcal{T}) \in \mathbb{T}(\mathcal{G} /\!\!/ \mathcal{E}_{cs})$. □

Proposition 2.6. *Consider a graph $\mathcal{G}$ and an edge contraction set $\mathcal{E}_{cs} \in \Xi_{n-r}(\mathcal{G})$. Then $\forall \tilde{v} \in \mathcal{V}(\mathcal{G} /\!\!/ \mathcal{E}_{cs})$*

$$d_{\tilde{v}}(\mathcal{G} /\!\!/ \mathcal{E}_{cs}) \leq \left(\sum_{v \in C_{\tilde{v}}(\pi)} d_v(\mathcal{G}) \right) - 2\left(|C_{\tilde{v}}(\pi)| - 1\right), \tag{2.1}$$

where $\pi = \pi_c(\mathcal{G}, \mathcal{E}_{cs})$.

Proof. From Proposition 2.1 we obtain that $d_{\tilde{v}}(\mathcal{G} /\!\!/ \pi) = |f_\pi(\mathcal{N}_{C_{\tilde{v}}})|$. We have $|f_\pi(\mathcal{N}_{C_{\tilde{v}}})| \leq |\mathcal{N}_{C_{\tilde{v}}}|$ and since $C_{\tilde{v}}(\pi) \in \pi_c$ is a connected component of $\mathcal{G}$ we get

$$|\mathcal{N}_{C_{\tilde{v}}}| \leq \left(\sum_{v \in C_{\tilde{v}}(\pi)} d_v(\mathcal{G}) \right) - 2\left|\mathcal{E}\left(\mathcal{G}\left[C_{\tilde{v}}(\pi)\right]\right)\right|.$$

The number of edges in the cell $|\mathcal{E}(\mathcal{G}[C_{\tilde{v}}(\pi)])|$ is at least the number of spanning tree edges, therefore, $|\mathcal{E}(\mathcal{G}[C_{\tilde{v}}(\pi)])| \geq |C_{\tilde{v}}(\pi)| - 1$, and we obtain that

$$d_{\tilde{v}}(\mathcal{G} /\!\!/ \mathcal{E}_{cs}) \leq \left(\sum_{v \in C_{\tilde{v}}(\pi)} d_v(\mathcal{G}) \right) - 2\left(|C_{\tilde{v}}(\pi)| - 1\right),$$

completing the proof. □

Corollary 2.2. *Consider a graph $\mathcal{G}$ and an edge contraction set $\mathcal{E}_{cs} \in \Xi_{n-r}(\mathcal{G})$ for $r < n$. Then if $\mathcal{G} /\!\!/ \mathcal{E}_{cs}$ is cycle-invariant (Definition 2.4) then $\forall \tilde{v} \in \mathcal{V}(\mathcal{G} /\!\!/ \mathcal{E}_{cs})$,*

$$d_{\tilde{v}}(\mathcal{G} /\!\!/ \mathcal{E}_{cs}) = \left(\sum_{v \in C_{\tilde{v}}(\pi)} d_v(\mathcal{G}) \right) - 2\left(|C_{\tilde{v}}(\pi)| - 1\right), \tag{2.2}$$

where $\pi = \pi_c(\mathcal{G}, \mathcal{E}_{cs})$.

Proof. Since $\forall \tilde{v} \in \mathcal{V}(\mathcal{G} /\!\!/ \mathcal{E}_{cs})$ $C_{\tilde{v}}(\pi)$ is a connected component of $\mathcal{G}$, and $\mathcal{G} /\!\!/ \mathcal{E}_{cs}$ is cycle-invariant then $|f_\pi(\mathcal{N}_{C_{\tilde{v}}})| = |\mathcal{N}_{C_{\tilde{v}}}|$ and $\mathcal{G}[C_{\tilde{v}}(\pi)]$ is a tree of order $|C_{\tilde{v}}(\pi)|$, such that from Proposition 2.1 we obtain that

$$d_{\tilde{v}}(\mathcal{G} /\!\!/ \mathcal{E}_{cs}) = \left(\sum_{v \in C_{\tilde{v}}(\pi)} d_v(\mathcal{G}) \right) - 2\left(|C_{\tilde{v}}(\pi)| - 1\right).$$

□

Corollary 2.3. *If a graph $\mathcal{G}$ is a tree then $\mathcal{G} /\!\!/ \mathcal{E}_{cs}$ is edge-matching for any $\mathcal{E}_{cs} \in \Xi_{n-r}(\mathcal{G})$.*

Proof. If $\mathcal{G}$ is a tree then $\mathcal{G} /\!\!/ \mathcal{E}_{cs}$ is cycle-invariant for any $\mathcal{E}_{cs} \in \Xi_{n-r}(\mathcal{G})$ and from Proposition 2.3 we obtain that $\mathcal{G} /\!\!/ \mathcal{E}_{cs}$ is edge-matching. □

In the following section we investigate the algebraic relations between the algebraic representations of graphs and contracted graphs.

2.3 The Algebraic Representation of Contracted Graphs

The algebraic representation of graphs, such as Laplacian matrices, finds numerous applications [16]. Less known are the algebraic representations of graph contractions as a function of the full order graph representation. In this section, we derive, for the first time, several graph representations of contracted graphs such as the incidence matrix, Laplacian and normalized-Laplacian matrices and the Tucker representation.

The following definitions will be used throughout this section. We start by defining the *partition characteristic matrix* (PCM) and the *partition projection matrix* (PPM), which are the algebraic representations of vertex partitions and will be building blocks for following representations of graph contractions. They will also be useful in our application of graph contractions for model reduction of MAS.

Definition 2.13 (Partition projection matrix)**.** *Given an r-partition* $\pi = \{C_i\}_{i=1}^r$*, we define* $P_\pi \in \mathbb{R}^{n\times r}$*, the* partition characteristic matrix *(PCM) with entries* $[P_\pi]_{ij} = 1$ *if* $i \in C_j$*, and* 0 *otherwise, i.e., for* $v_i \in \mathcal{V}$ *and* $v_j^r \in \mathcal{V}_r$

$$[P_\pi]_{ij} = \begin{cases} 1 & f_\pi(v_i) = v_j^r \\ 0 & o.w. \end{cases} \tag{2.3}$$

The corresponding partition projection matrix (PPM) is

$$P(\pi) \triangleq P_\pi D^{-\frac{1}{2}}(\pi), \tag{2.4}$$

where

$$D(\pi) \triangleq P_\pi^T P_\pi. \tag{2.5}$$

We now define several algebraic structures related to the edges of a graph that will be required for the following derivations.

Definition 2.14 (Edge contraction function)**.** *Consider a graph* $\mathcal{G}$ *and its graph contraction* $\mathcal{G}/\!\!/\pi$ *with head and tail functions* $h_\mathcal{E}, t_\mathcal{E}$ *and* $h_{\mathcal{E}_r}, t_{\mathcal{E}_r}$ *respectively, where* $\mathcal{E}_r \triangleq \mathcal{E}(\mathcal{G}/\!\!/\pi)$*. Then the* edge contraction function $p : \mathcal{E}(\mathcal{G}) \times \mathcal{E}(\mathcal{G}/\!\!/\pi) \to \{\pm 1, 0\}$ *is defined such that*

$$p(\epsilon, \epsilon^r) = \begin{cases} 1 & f_\pi(h_\mathcal{E}(\epsilon)) = h_{\mathcal{E}_r}(\epsilon^r) \text{ and } f_\pi(t_\mathcal{E}(\epsilon)) = t_{\mathcal{E}_r}(\epsilon^r) \\ -1 & f_\pi(h_\mathcal{E}(\epsilon)) = t_{\mathcal{E}_r}(\epsilon^r) \text{ and } f_\pi(t_\mathcal{E}(\epsilon)) = h_{\mathcal{E}_r}(\epsilon^r) \\ 0 & \text{otherwise.} \end{cases} \tag{2.6}$$

Definition 2.15 (Edge contraction matrix)**.** *Consider a graph* $\mathcal{G} = (\mathcal{V}, \mathcal{E})$ *and its graph contraction* $\mathcal{G}/\!\!/\pi = (\mathcal{V}_r, \mathcal{E}_r)$*, and let* $\mathcal{E}_S \subseteq \mathcal{E}$ *and* $\mathcal{E}_{S_r} \subseteq \mathcal{E}_r$*. Then the edge contraction matrix* $P_{(\mathcal{E}_S, \mathcal{E}_{S_r})} \in \mathbb{R}^{|\mathcal{E}_S|\times|\mathcal{E}_{S_r}|}$ *is defined such that*

$$\left[P_{(\mathcal{E}_S, \mathcal{E}_{S_r})}\right]_{km} = p(\epsilon_k, \epsilon_m^r), \tag{2.7}$$

for $\epsilon_k \in \mathcal{E}_S$ and $\epsilon_k^r \in \mathcal{E}_{S_r}$. The corresponding normalized edge contraction matrix is defined as

$$U_{(\mathcal{E}_S,\mathcal{E}_{S_r})} \triangleq P_{(\mathcal{E}_S,\mathcal{E}_{S_r})} D^{\dagger}_{(\mathcal{E}_S,\mathcal{E}_{S_r})} \tag{2.8}$$

with

$$D_{(\mathcal{E}_S,\mathcal{E}_{S_r})} \triangleq P^T_{(\mathcal{E}_S,\mathcal{E}_{S_r})} P_{(\mathcal{E}_S,\mathcal{E}_{S_r})}. \tag{2.9}$$

The matrix $D_{(\mathcal{E}_S,\mathcal{E}_{S_r})}$ has a combinatorial interpretation given here.

Proposition 2.7. *Consider a graph $\mathcal{G} = (\mathcal{V}, \mathcal{E})$ and its graph contraction $\mathcal{G}/\!\!/\pi = (\mathcal{V}_r, \mathcal{E}_r)$, and let $\mathcal{E}_S \subseteq \mathcal{E}$ and $\mathcal{E}_{S_r} \subseteq \mathcal{E}_r$. Then $D_{(\mathcal{E}_S,\mathcal{E}_{S_r})}$ is diagonal where each entry on the diagonal is the number of edges of $\mathcal{E}_S$ mapped to each edge of $\mathcal{E}_{S_r}$, i.e.,*

$$\left[D_{(\mathcal{E}_S,\mathcal{E}_{S_r})}\right]_{ii} = \left|\{\epsilon \in \mathcal{E}_S\} \left| f_\pi(\epsilon) = \epsilon_i^r \right.\right|. \tag{2.10}$$

Proof. Let $p_i \in \mathbb{R}^{|\mathcal{E}_{S_r}|}$ be the i'th column of $P_{(\mathcal{E}_S,\mathcal{E}_{S_r})}$ corresponding to $\epsilon_i^r \in \mathcal{E}_{S_r}$, then $\left[D_{(\mathcal{E}_S,\mathcal{E}_{S_r})}\right]_{ij} = p_i^T p_j = \sum_{k=1}^{|\mathcal{E}|} p(\epsilon_k, \epsilon_i^r)\, p\left(\epsilon_k, \epsilon_j^r\right)$. For $i \neq j$ if $p(\epsilon_k, \epsilon_i^r) = \pm 1$ then $p\left(\epsilon_k, \epsilon_j^r\right) = 0$, such that $\left[D_{(\mathcal{E}_S,\mathcal{E}_{S_r})}\right]_{ij} = 0$. For $i = j$ $p(\epsilon_k, \epsilon_i^r) = \pm 1$ if $f_\pi(\epsilon_k) = \epsilon_i^r$ and we get $p_i^T p_i = \sum_{k=1}^{|\mathcal{E}|} p^2(\epsilon_k, \epsilon_i^r) = |\{\epsilon \in \mathcal{E}_S | f_\pi(\epsilon) = \epsilon_i^r\}|$. □

Based on the above definitions, in the following subsection we derive algebraic representations of the incidence matrix of graph contractions.

2.3.1 The Contracted Incidence Matrix

We start this subsection by deriving the algebraic representation of the incidence matrix of the quotient graph (Definition 2.2) $E(\mathcal{G}/\pi)$ as the product of the incidence matrix $E(\mathcal{G})$ of the original graph and the PCM P_π.

Proposition 2.8 (Quotient incidence matrix)**.** *Consider a graph $\mathcal{G} = (\mathcal{V}, \mathcal{E})$ with incidence matrix $E(\mathcal{G})$ (Definition 1.1) and partition $\pi \in \Pi_r(\mathcal{G})$ for $r < n$ and PCM P_π. Then incidence matrix of the quotient $\mathcal{G}/\pi$ takes the form*

$$E(\mathcal{G}/\pi) = P_\pi^T E(\mathcal{G}). \tag{2.11}$$

Proof. Let $e_j \in \mathbb{R}^n$ be the j'th column of $E(\mathcal{G})$ corresponding to edge $\epsilon_j \in \mathcal{E}(\mathcal{G})$,

$$[e_j]_k = \begin{cases} 1 & h_{\mathcal{E}}(\epsilon_j) = v_k \\ -1 & t_{\mathcal{E}}(\epsilon_j) = v_k \\ 0 & o.w. \end{cases}, \tag{2.12}$$

and let $p_i \in \mathbb{R}^n$ be the i'th column of P_π corresponding to the i'th cell $C_i \in \pi$,

$$[p_i]_k = \begin{cases} 1 & v_k \in C_i \\ 0 & o.w. \end{cases}. \tag{2.13}$$

From the product of (2.13) and (2.12) we obtain that

$$p_i^T e_j = \begin{cases} -1 & t_{\mathcal{E}}(\epsilon_j) \in C_i,\ h_{\mathcal{E}}(\epsilon_j) \notin C_i \\ 1 & t_{\mathcal{E}}(\epsilon_j) \notin C_i,\ h_{\mathcal{E}}(\epsilon_j) \in C_i \\ 0 & t_{\mathcal{E}}(\epsilon_j) \in C_i,\ h_{\mathcal{E}}(\epsilon_j) \in C_i \\ 0 & t_{\mathcal{E}}(\epsilon_j) \notin C_i,\ h_{\mathcal{E}}(\epsilon_j) \notin C_i \end{cases}. \tag{2.14}$$

Now let $\mathcal{G}/\pi$ be the quotient of $\mathcal{G}$ over π with edge set $\tilde{\mathcal{E}} = \mathcal{E}(\mathcal{G}/\pi)$, then the jth column of $E(\mathcal{G}/\pi)$, $\tilde{e}_j \in \mathbb{R}^r$, takes the form

$$[\tilde{e}_j]_k = \begin{cases} -1 & t_{\tilde{\mathcal{E}}}(\tilde{\epsilon}_j) = v_k^r,\ h_{\tilde{\mathcal{E}}}(\tilde{\epsilon}_j) \neq v_k^r \\ 1 & t_{\tilde{\mathcal{E}}}(\tilde{\epsilon}_j) \neq v_k^r,\ h_{\tilde{\mathcal{E}}}(\tilde{\epsilon}_j) = v_k^r \\ 0 & t_{\tilde{\mathcal{E}}}(\tilde{\epsilon}_j) = v_k^r,\ h_{\tilde{\mathcal{E}}}(\tilde{\epsilon}_j) = v_k^r \\ 0 & t_{\tilde{\mathcal{E}}}(\tilde{\epsilon}_j) \neq v_k^r,\ h_{\tilde{\mathcal{E}}}(\tilde{\epsilon}_j) \neq v_k^r \end{cases}. \tag{2.15}$$

As according to Definition 2.2, $t_{\tilde{\mathcal{E}}}(\tilde{\epsilon}_j) = v_k^r$ for $\tilde{\epsilon}_j \in \tilde{\mathcal{E}}$ and $v_k^r \in \mathcal{V}(\mathcal{G}/\pi)$ if and only if $t_{\mathcal{E}}(\epsilon_j) \in C_i$ for $\epsilon_j \in \mathcal{E}$ and $C_i \in \pi$, and similarly all other conditions in (2.14) and (2.15) are equivalent, therefore, we conclude that $[\tilde{e}_j]_k = p_i^T e_j$, and $E(\mathcal{G}/\pi) = P_\pi^T E(\mathcal{G})$. □

Proposition 2.9 (Graph contraction incidence matrix)**.** *Let $\mathcal{G} = (\mathcal{V}, \mathcal{E})$ and $\mathcal{G} /\!\!/ \pi = (\mathcal{V}_r, \mathcal{E}_r)$ with head and tail functions $h_{\mathcal{E}}, t_{\mathcal{E}}$ and $h_{\mathcal{E}_r}, t_{\mathcal{E}_r}$ respectively, for $\pi \in \Pi_r(\mathcal{G})$. Then the contracted graph incidence matrix $E(\mathcal{G} /\!\!/ \pi)$ takes the form*

$$E(\mathcal{G} /\!\!/ \pi) = P_\pi^T E(\mathcal{G}) U_{(\mathcal{E}, \mathcal{E}_r)}. \tag{2.16}$$

Proof. From Proposition 2.8 we obtain that $E(\mathcal{G}/\pi) = P_\pi^T E(\mathcal{G})$. It is left to show that $E(\mathcal{G} /\!\!/ \pi) = E(\mathcal{G}/\pi) U_{(\mathcal{E}, \mathcal{E}_r)}$. Let $e_j^r \in \mathbb{R}^r$ be the jth column of $E(\mathcal{G} /\!\!/ \pi)$ corresponding to edge $\epsilon_j^r \in \mathcal{E}_r$,

$$\left[e_j^r\right]_k = \begin{cases} 1 & h_{\mathcal{E}_r}\left(\epsilon_j^r\right) = v_k^r \\ -1 & t_{\mathcal{E}}\left(\epsilon_j^r\right) = v_k^r \\ 0 & o.w. \end{cases}. \tag{2.17}$$

Now let $\mathcal{G}/\pi = \left(\mathcal{V}_r, \tilde{\mathcal{E}}\right)$, then the jth column of $E(\mathcal{G}/\pi)$, $\tilde{e}_j \in \mathbb{R}^r$, takes the form

$$[\tilde{e}_j]_k = \begin{cases} -1 & t_{\tilde{\mathcal{E}}}(\tilde{\epsilon}_j) = v_k^r,\ h_{\tilde{\mathcal{E}}}(\tilde{\epsilon}_j) \neq v_k^r \\ 1 & t_{\tilde{\mathcal{E}}}(\tilde{\epsilon}_j) \neq v_k^r,\ h_{\tilde{\mathcal{E}}}(\tilde{\epsilon}_j) = v_k^r \\ 0 & t_{\tilde{\mathcal{E}}}(\tilde{\epsilon}_j) = v_k^r,\ h_{\tilde{\mathcal{E}}}(\tilde{\epsilon}_j) = v_k^r \\ 0 & t_{\tilde{\mathcal{E}}}(\tilde{\epsilon}_j) \neq v_k^r,\ h_{\tilde{\mathcal{E}}}(\tilde{\epsilon}_j) \neq v_k^r \end{cases}. \tag{2.18}$$

From Definition 2.3 the contracted graph is $\mathcal{G} /\!\!/ \pi = ([1, r], \mathcal{E}_r)$ where

$$\mathcal{E}_r = \left\{ \epsilon^r \in [1, r]^2 \,|\, \epsilon^r \in \mathcal{E}(\mathcal{G}/\pi), h_{\mathcal{E}}(\epsilon^r) \neq t_{\mathcal{E}}(\epsilon^r) \right\}.$$

Taking the product of $E(\mathcal{G}/\pi)$ and $U_{(\mathcal{E},\mathcal{E}_r)}$ (Definition 2.15) we get

$$\left[E(\mathcal{G}/\pi)U_{(\mathcal{E},\mathcal{E}_r)}\right]_{jk} = \frac{1}{d(\epsilon_k^r)}\sum_{t=1}^{|\mathcal{E}|} p(\epsilon_t,\epsilon_k^r)\left[\tilde{e}_t\right]_k = \begin{cases} 1 & h_{\mathcal{E}_r}\left(\epsilon_j^r\right) = v_k^r \\ -1 & t_{\mathcal{E}}\left(\epsilon_j^r\right) = v_k^r \\ 0 & o.w. \end{cases},$$

where from Proposition 2.7 we have $d(\epsilon_k^r) = \left[D_{(\mathcal{E}_S,\mathcal{E}_{S_r})}\right]_{kk}$ and we obtain that $\left[E(\mathcal{G}/\pi)U_{(\mathcal{E},\mathcal{E}_r)}\right]_{jk} = \left[e_j^r\right]_k$ such that $E(\mathcal{G}/\!/\pi) = P_\pi^T E(\mathcal{G})U_{(\mathcal{E},\mathcal{E}_r)}$.

□

2.3.2 The Contracted Laplacian Matrix

The Laplacian matrix plays a key role in algebraic graph theory. We recall that for a simple undirected graph, the Laplacian matrix $L(\mathcal{G}) \in \mathbb{R}^{|\mathcal{V}|\times|\mathcal{V}|}$ can be constructed as

$$L(\mathcal{G}) = E(\mathcal{G})E(\mathcal{G})^T.$$

In this section we present the general algebraic relation between the Laplacian of the full graph $\mathcal{G}$ and the Laplacian of the contracted graph $\mathcal{G}_r = \mathcal{G}/\!/\pi$. We will also investigate the *edge Laplacian matrix* and the *normalized Laplacian matrix* of graph contractions.

Definition 2.16 (Edge Laplacian matrix)**.** *Consider a graph $\mathcal{G} = (\mathcal{V},\mathcal{E})$ with head and tail functions $h_\mathcal{E}, t_\mathcal{E}$, and incidence matrix $E(\mathcal{G})$ (Definition 1.1) then the edge Laplacian $L_e(\mathcal{G}) \in \mathbb{R}^{|\mathcal{E}|\times|\mathcal{E}|}$ is defined as [68]*

$$L_e(\mathcal{G}) \triangleq E^T(\mathcal{G})E(\mathcal{G}).$$

Definition 2.17 (Normalized Laplacian matrix)**.** *Let $\mathcal{G} = (\mathcal{V},\mathcal{E})$ be a simple connected graph with Laplacian $L(\mathcal{G})$. Then the normalized Laplacian matrix $\mathcal{L}(\mathcal{G}) \in \mathbb{R}^{|\mathcal{V}|\times|\mathcal{V}|}$ is defined as*

$$\mathcal{L}(\mathcal{G}) \triangleq D^{-\frac{1}{2}}(\mathcal{G})L(\mathcal{G})D^{-\frac{1}{2}}(\mathcal{G})$$

where $D(\mathcal{G}) \in \mathbb{R}^{|\mathcal{V}|\times|\mathcal{V}|}$ is the degree matrix, a diagonal matrix with entries $[D(\mathcal{G})]_{ii} = d(v_i)$.

The following theorem provides the algebraic representations of the three Laplacian matrices of a graph contraction as a function of algebraic representations of the full-order graph.

Theorem 2.1 (Contracted Laplacian matrices)**.** *Consider a graph $\mathcal{G} = (\mathcal{V},\mathcal{E})$ and its contraction $\mathcal{G}_r = \mathcal{G}/\!/\pi$, for $\pi \in \Pi_r(\mathcal{G})$, with head and tail functions $h_\mathcal{E}, t_\mathcal{E}$ and $h_{\mathcal{E}_r}, t_{\mathcal{E}_r}$ respectively. Then the contracted graph Laplacian matrices take the forms*

$$L(\mathcal{G}_r) = P_\pi^T E(\mathcal{G})U_{(\mathcal{E},\mathcal{E}_r)}U_{(\mathcal{E},\mathcal{E}_r)}^T E^T(\mathcal{G})P_\pi, \tag{2.19}$$

$$L_e(\mathcal{G}_r) = U_{(\mathcal{E},\mathcal{E}_r)}^T L_e(\mathcal{G}/\pi)U_{(\mathcal{E},\mathcal{E}_r)}, \tag{2.20}$$

$$\mathcal{L}(\mathcal{G}_r) = D^{-\frac{1}{2}}(\mathcal{G}_r)P_\pi^T E(\mathcal{G})U_{(\mathcal{E},\mathcal{E}_r)}U_{(\mathcal{E},\mathcal{E}_r)}^T E^T(\mathcal{G})P_\pi D^{-\frac{1}{2}}(\mathcal{G}_r). \tag{2.21}$$

Proof. The Laplacian matrix of the contracted graph is $L(\mathcal{G}_r) = E(\mathcal{G}_r) E^T(\mathcal{G}_r)$ and with $E(\mathcal{G}_r) = P_\pi^T E(\mathcal{G}) U_{(\mathcal{E},\mathcal{E}_r)}$ from Proposition 2.9, the reduced Laplacian matrix $L(\mathcal{G}_r) = E(\mathcal{G}_r) E^T(\mathcal{G}_r)$ takes the form

$$L(\mathcal{G}_r) = P_\pi^T E(\mathcal{G}) U_{(\mathcal{E},\mathcal{E}_r)} U_{(\mathcal{E},\mathcal{E}_r)}^T E^T(\mathcal{G}) P_\pi.$$

Similarly $L_e(\mathcal{G}_r) \triangleq E^T(\mathcal{G}_r) E(\mathcal{G}_r)$ with $E(\mathcal{G}_r) = P_\pi^T E(\mathcal{G}) U_{(\mathcal{E},\mathcal{E}_r)}$ takes the form

$$L_e(\mathcal{G}_r) = U_{(\mathcal{E},\mathcal{E}_r)}^T E^T(\mathcal{G}) P_\pi P_\pi^T E(\mathcal{G}) U_{(\mathcal{E},\mathcal{E}_r)},$$

and

$$\begin{aligned}\mathcal{L}(\mathcal{G}_r) &\triangleq D^{-\frac{1}{2}}(\mathcal{G}_r) L(\mathcal{G}_r) D^{-\frac{1}{2}}(\mathcal{G}_r) \\ &= D^{-\frac{1}{2}}(\mathcal{G}_r) P_\pi^T E(\mathcal{G}) U_{(\mathcal{E},\mathcal{E}_r)} U_{(\mathcal{E},\mathcal{E}_r)}^T E^T(\mathcal{G}) P_\pi D^{-\frac{1}{2}}(\mathcal{G}_r).\end{aligned}$$

□

2.3.3 The Graph Contraction Tucker Representation

Trees and cycle-completing edges are the building blocks of any connected graph, and the edges of a graph can be ordered accordingly as defined be the *tree partition matrix*.

Definition 2.18 (Edge selection matrix)**.** *Consider a graph $\mathcal{G} = (\mathcal{V}, \mathcal{E})$ with a subset of edges $\mathcal{E}_S \subseteq \mathcal{E}(\mathcal{G})$. Then we define the edge selection matrix $M(\mathcal{E}, \mathcal{E}_S)$ where*

$$[M(\mathcal{E}, \mathcal{E}_S)]_{ij} = \begin{cases} 1 & \epsilon_i(\mathcal{E}) = \epsilon_j(\mathcal{E}_S) \\ 0 & o.w., \end{cases} \tag{2.22}$$

for $i = 1, \ldots, |\mathcal{E}|$ and $j = 1, \ldots, |\mathcal{E}_S|$.

Definition 2.19 (Tree partition matrix)**.** *Let $\mathcal{G} = (\mathcal{V}, \mathcal{E})$ be a simple connected graph and let $\mathcal{T} \in \mathbb{T}(\mathcal{G})$ be a tree of $\mathcal{G}$ with co-tree $\mathcal{C}(\mathcal{T})$. Then we define the* tree partition matrix *as the permutation*

$$M_{\mathcal{T}} = [M(\mathcal{E}, \mathcal{E}_{\mathcal{T}}), M(\mathcal{E}, \mathcal{E}_{\mathcal{C}})]. \tag{2.23}$$

The tree and co-tree structure of the graph is described by the Tucker representation [53, p.113].

Definition 2.20 (Tucker representation)**.** *The* Tucker representation *of the co-tree is the matrix $T_{(\mathcal{T},\mathcal{C})} \in \mathbb{R}^{|\mathcal{E}(\mathcal{T})| \times |\mathcal{E}(\mathcal{C})|}$ where the jth column of $T_{(\mathcal{T},\mathcal{C})}$ is the signed path vector (Definition 1.4) $t_j \in \mathbb{R}^{|\mathcal{E}(\mathcal{T})|}$ of the corresponding edge $\epsilon_j \in \mathcal{E}(\mathcal{C})$.*

Proposition 2.10 (Incidence matrix tree mapping)**.** *Let $\mathcal{G} = (\mathcal{V}, \mathcal{E})$ be a simple connected graph with head and tail functions, $h_{\mathcal{E}}, t_{\mathcal{E}}$, and let $\mathcal{T} \in \mathbb{T}(\mathcal{G})$ be a tree of $\mathcal{G}$ with co-tree $\mathcal{C}(\mathcal{T})$. Then the incidence matrix takes the form [69]*

$$E(\mathcal{G}) = E(\mathcal{T}) R_{(\mathcal{T},\mathcal{C})} M_{\mathcal{T}}^T, \tag{2.24}$$

where $R_{(\mathcal{T},\mathcal{C})} \triangleq \left[I_{|\mathcal{E}_{\mathcal{T}}|}\ T_{(\mathcal{T},\mathcal{C})}\right]$.

Proof. From Definition 2.19 we obtain that $[E(\mathcal{T})\ E(\mathcal{C})] = E(\mathcal{G})\, M_{\mathcal{T}}$, $M_{\mathcal{T}}$ is a permutation matrix and therefore $M_{\mathcal{T}} M_{\mathcal{T}}^T = I_{|\mathcal{E}_{\mathcal{T}}|}$and we get $E(\mathcal{G}) = [E(\mathcal{T})\ E(\mathcal{C})]\, M_{\mathcal{T}}^T$. From the Tucker representation (Definition 2.20) we obtain that $E(\mathcal{C}) = E(\mathcal{T})\, T_{(\mathcal{T},\mathcal{C})}$. The rank of an incidence matrix of a connected graph of order n is $n-1$ [25], therefore, $E(\mathcal{T}) \in \mathbb{R}^{n\times n-1}$ has full column rank and $L_e(\mathcal{T}) = E(\mathcal{T})^T E(\mathcal{T})$ is invertible, such that $T_{(\mathcal{T},\mathcal{C})} = L_e^{-1}(\mathcal{T})\, E(\mathcal{T})^T E(\mathcal{C})$ and we obtain that $[E(\mathcal{T})\ E(\mathcal{C})] = E(\mathcal{T})\left[I_{|\mathcal{E}_{\mathcal{T}}|}\, T_{(\mathcal{T},\mathcal{C})}\right]$. □

Proposition 2.11. *Let $\mathcal{G}$ and $\mathcal{G}_r = \mathcal{G}/\!\!/\pi$ with head and tail functions $h_{\mathcal{E}}, t_{\mathcal{E}}$ and $h_{\mathcal{E}_r}, t_{\mathcal{E}_r}$ respectively, and let $\mathcal{T} \in \mathbb{T}(\mathcal{G})$ and $\mathcal{T}_r \in \mathbb{T}(\mathcal{G}_r)$ with co-trees $\mathcal{C}$ and $\mathcal{C}_r$ respectively. If we reorder the edge sets $\mathcal{E}$ and $\mathcal{E}_r$ according to the permutations $M_{\mathcal{T}}$ and $M_{\mathcal{T}_r}$, then the edge contraction matrix of the permuted sets $\mathcal{E}'$ and $\mathcal{E}_r'$ takes the form*

$$P_{(\mathcal{E}',\mathcal{E}_r')} = \begin{bmatrix} P_{(\mathcal{E}_{\mathcal{T}},\mathcal{E}_{\mathcal{T}_r})} & P_{(\mathcal{E}_{\mathcal{T}},\mathcal{E}_{\mathcal{C}_r})} \\ P_{(\mathcal{E}_{\mathcal{C}},\mathcal{E}_{\mathcal{T}_r})} & P_{(\mathcal{E}_{\mathcal{C}},\mathcal{E}_{\mathcal{C}_r})} \end{bmatrix}, \tag{2.25}$$

and the normalized edge contraction matrix takes the form

$$U_{(\mathcal{E},'\mathcal{E}_r')} = \begin{bmatrix} P_{(\mathcal{E}_{\mathcal{T}},\mathcal{E}_{\mathcal{T}_r})} D_{\mathcal{T}_r}^{-1} & P_{(\mathcal{E}_{\mathcal{T}},\mathcal{E}_{\mathcal{C}_r})} D_{\mathcal{C}_r}^{\dagger} \\ P_{(\mathcal{E}_{\mathcal{C}},\mathcal{E}_{\mathcal{T}_r})} D_{\mathcal{T}_r}^{-1} & P_{(\mathcal{E}_{\mathcal{C}},\mathcal{E}_{\mathcal{C}_r})} D_{\mathcal{C}_r}^{\dagger} \end{bmatrix}, \tag{2.26}$$

with $D_{\mathcal{T}_r} \triangleq P_{(\mathcal{E}_{\mathcal{T}},\mathcal{E}_{\mathcal{T}_r})}^T P_{(\mathcal{E}_{\mathcal{T}},\mathcal{E}_{\mathcal{T}_r})} + P_{(\mathcal{E}_{\mathcal{C}},\mathcal{E}_{\mathcal{T}_r})}^T P_{(\mathcal{E}_{\mathcal{C}},\mathcal{E}_{\mathcal{T}_r})}$ and $D_{\mathcal{C}_r} \triangleq P_{(\mathcal{E}_{\mathcal{T}},\mathcal{E}_{\mathcal{C}_r})}^T P_{(\mathcal{E}_{\mathcal{T}},\mathcal{E}_{\mathcal{C}_r})} + P_{(\mathcal{E}_{\mathcal{C}},\mathcal{E}_{\mathcal{C}_r})}^T P_{(\mathcal{E}_{\mathcal{C}},\mathcal{E}_{\mathcal{C}_r})}$.

Proof. The edge contraction matrix $P_{(\mathcal{E},'\mathcal{E}_r')}$ is obtained by applying the tree partition matrices $M_{\mathcal{T}}$ and $M_{\mathcal{T}_r}$ on $P_{(\mathcal{E},\mathcal{E}_r)}$,

$$\begin{aligned} P_{(\mathcal{E},'\mathcal{E}_r')} &= M_{\mathcal{T}}^T P_{(\mathcal{E},\mathcal{E}_r)} M_{\mathcal{T}_r} \\ &= \left[M(\mathcal{E},\mathcal{E}_{\mathcal{T}}), M(\mathcal{E},\mathcal{E}_{\mathcal{C}})\right]^T P_{(\mathcal{E},\mathcal{E}_r)} \left[M(\mathcal{E}_r,\mathcal{E}_{\mathcal{T}_r}), M(\mathcal{E}_r,\mathcal{E}_{\mathcal{C}_r})\right], \\ &= \begin{bmatrix} M^T(\mathcal{E},\mathcal{E}_{\mathcal{T}})\, P_{(\mathcal{E},\mathcal{E}_r)} M(\mathcal{E}_r,\mathcal{E}_{\mathcal{T}_r}) & M^T(\mathcal{E},\mathcal{E}_{\mathcal{T}})\, P_{(\mathcal{E},\mathcal{E}_r)} M(\mathcal{E}_r,\mathcal{E}_{\mathcal{C}_r}) \\ M^T(\mathcal{E},\mathcal{E}_{\mathcal{C}})\, P_{(\mathcal{E},\mathcal{E}_r)} M(\mathcal{E}_r,\mathcal{E}_{\mathcal{T}_r}) & M^T(\mathcal{E},\mathcal{E}_{\mathcal{C}})\, P_{(\mathcal{E},\mathcal{E}_r)} M(\mathcal{E}_r,\mathcal{E}_{\mathcal{C}_r}) \end{bmatrix}. \end{aligned}$$

Since $\mathcal{E}_{\mathcal{T}}, \mathcal{E}_{\mathcal{C}} \subseteq \mathcal{E}$ and $\mathcal{E}_{\mathcal{T}_r}, \mathcal{E}_{\mathcal{C}_r} \subseteq \mathcal{E}_r$, then from Definition 2.18 and Definition 2.15 we obtain that

$$M^T(\mathcal{E},\mathcal{E}_{\mathcal{T}})\, P_{(\mathcal{E},\mathcal{E}_r)} M(\mathcal{E}_r,\mathcal{E}_{\mathcal{T}_r}) = P_{(\mathcal{E}_{\mathcal{T}},\mathcal{E}_{\mathcal{T}_r})}, \tag{2.27}$$

$$M^T(\mathcal{E},\mathcal{E}_{\mathcal{T}})\, P_{(\mathcal{E},\mathcal{E}_r)} M(\mathcal{E}_r,\mathcal{E}_{\mathcal{C}_r}) = P_{(\mathcal{E}_{\mathcal{T}},\mathcal{E}_{\mathcal{C}_r})}, \tag{2.28}$$

$$M^T(\mathcal{E},\mathcal{E}_{\mathcal{C}})\, P_{(\mathcal{E},\mathcal{E}_r)} M(\mathcal{E}_r,\mathcal{E}_{\mathcal{T}_r}) = P_{(\mathcal{E}_{\mathcal{C}},\mathcal{E}_{\mathcal{T}_r})} \tag{2.29}$$

and

$$M^T(\mathcal{E},\mathcal{E}_{\mathcal{C}})\, P_{(\mathcal{E},\mathcal{E}_r)} M(\mathcal{E}_r,\mathcal{E}_{\mathcal{C}_r}) = P_{(\mathcal{E}_{\mathcal{C}},\mathcal{E}_{\mathcal{C}_r})}. \tag{2.30}$$

Expanding $D_{\left(\mathcal{E}',\mathcal{E}'_r\right)}$ with $P_{\left(\mathcal{E},'\mathcal{E}'_r\right)} = M_{\mathcal{T}}^T P_{(\mathcal{E},\mathcal{E}_r)} M_{\mathcal{T}_r}$ we obtain

$$\begin{aligned} D_{\left(\mathcal{E}',\mathcal{E}'_r\right)} &= \left(M_{\mathcal{T}}^T P_{(\mathcal{E},\mathcal{E}_r)} M_{\mathcal{T}_r}\right)^T \left(M_{\mathcal{T}}^T P_{(\mathcal{E},\mathcal{E}_r)} M_{\mathcal{T}_r}\right) \\ &= M_{\mathcal{T}_r}^T P_{(\mathcal{E},\mathcal{E}_r)}^T M_{\mathcal{T}} M_{\mathcal{T}}^T P_{(\mathcal{E},\mathcal{E}_r)} M_{\mathcal{T}_r} \\ &= M_{\mathcal{T}_r}^T P_{(\mathcal{E},\mathcal{E}_r)}^T P_{(\mathcal{E},\mathcal{E}_r)} M_{\mathcal{T}_r} \\ &= \left[M\left(\mathcal{E}_r,\mathcal{E}_{\mathcal{T}_r}\right), M\left(\mathcal{E}_r,\mathcal{E}_{\mathcal{C}_r}\right)\right]^T D_{(\mathcal{E},\mathcal{E}_r)} \left[M\left(\mathcal{E}_r,\mathcal{E}_{\mathcal{T}_r}\right), M\left(\mathcal{E}_r,\mathcal{E}_{\mathcal{C}_r}\right)\right], \end{aligned}$$

and since $D_{(\mathcal{E},\mathcal{E}_r)}$ is diagonal we get that $D_{\left(\mathcal{E}',\mathcal{E}'_r\right)} = \mathrm{Diag}\left(D_{\mathcal{T}_r}, D_{\mathcal{C}_r}\right)$ with

$$D_{\mathcal{T}_r} \triangleq P_{(\mathcal{E}_{\mathcal{T}},\mathcal{E}_{\mathcal{T}_r})}^T P_{(\mathcal{E}_{\mathcal{T}},\mathcal{E}_{\mathcal{T}_r})} + P_{(\mathcal{E}_{\mathcal{C}},\mathcal{E}_{\mathcal{T}_r})}^T P_{(\mathcal{E}_{\mathcal{C}},\mathcal{E}_{\mathcal{T}_r})}$$

and

$$D_{\mathcal{C}_r} \triangleq P_{(\mathcal{E}_{\mathcal{T}},\mathcal{E}_{\mathcal{C}_r})}^T P_{(\mathcal{E}_{\mathcal{T}},\mathcal{E}_{\mathcal{C}_r})} + P_{(\mathcal{E}_{\mathcal{C}},\mathcal{E}_{\mathcal{C}_r})}^T P_{(\mathcal{E}_{\mathcal{C}},\mathcal{E}_{\mathcal{C}_r})}.$$

We notice that $D_{\mathcal{T}_r}$ is regular and $D_{\mathcal{C}_r}$ may be singular. Expanding

$$U_{\left(\mathcal{E},'\mathcal{E}'_r\right)} = P_{\left(\mathcal{E}',\mathcal{E}'_r\right)} D^{\dagger}_{\left(\mathcal{E}',\mathcal{E}'_r\right)}$$

completes the proof. □

Proposition 2.12. *Let $\mathcal{G} = (\mathcal{V},\mathcal{E})$, $\mathcal{T} \in \mathbb{T}(\mathcal{G})$ and $\mathcal{E}_{cs} \in \Xi_{n-r}(\mathcal{T})$, and let $\mathcal{G}_r = \mathcal{G} /\!\!/ \mathcal{E}_{cs}$, with $\mathcal{T}_r = \mathcal{T} /\!\!/ \mathcal{E}_{cs}$ and $\mathcal{C}_r = \mathcal{C}(\mathcal{T}_r)$. Then $P_{(\mathcal{E}_{\mathcal{T}},\mathcal{E}_{\mathcal{T}_r})} = M\left(\mathcal{E}_{\mathcal{T}},\mathcal{E}_{\mathcal{T}}\backslash\mathcal{E}_{cs}\right)$ and $P_{(\mathcal{E}_{\mathcal{T}},\mathcal{E}_{\mathcal{C}_r})} = 0$. If in addition $\mathcal{G} /\!\!/ \mathcal{E}_{cs}$ is cycle-invariant (Definition 2.5) then $U_{(\mathcal{E},\mathcal{E}_r)} = P_{(\mathcal{E},\mathcal{E}_r)} = M\left(\mathcal{E},\mathcal{E}\backslash\mathcal{E}_{cs}\right)$, where $M\left(\mathcal{E},\mathcal{E}\backslash\mathcal{E}_{cs}\right) = M_{\mathcal{T}} P_{\left(\mathcal{E}',\mathcal{E}'_r\right)} M_{\mathcal{T}_r}^T$ and*

$$P_{\left(\mathcal{E}',\mathcal{E}'_r\right)} = Diag\left(M\left(\mathcal{E}_{\mathcal{T}},\mathcal{E}_{\mathcal{T}}\backslash\mathcal{E}_{cs}\right), I_{|\mathcal{E}_{\mathcal{C}}|}\right).$$

Proof. We have $\mathcal{E}_{\mathcal{T}} = \mathcal{E}_{cs}^* \cup \mathcal{E}_{cs}$ where $\mathcal{E}_{cs}^* \triangleq \mathcal{E}_{\mathcal{T}}\backslash\mathcal{E}_c$. Since $\mathcal{T}_r = \mathcal{T} /\!\!/ \mathcal{E}_{cs}$ from Proposition 2.5 we get that there is a one-to-one correspondence between $\mathcal{E}_{cs}^*$ and $\mathcal{E}_{\mathcal{T}_r}$ such that $P_{(\mathcal{E}_{\mathcal{T}},\mathcal{E}_{\mathcal{C}_r})} = 0$ and $\left[P_{(\mathcal{E}_{\mathcal{T}},\mathcal{E}_{\mathcal{T}_r})}\right]_{ij} = 1$ if $\epsilon_i(\mathcal{E}_{\mathcal{T}}) = \epsilon_j(\mathcal{E}_{cs}^*)$ and zero otherwise, which is exactly how $M\left(\mathcal{E}_{\mathcal{T}},\mathcal{E}_{\mathcal{T}}\backslash\mathcal{E}_{cs}\right)$ is defined (Definition 2.18). If $\mathcal{G} /\!\!/ \mathcal{E}_{cs}$ is *cycle-invariant* then there is one-to-one correspondense between $\mathcal{C}$ and $\mathcal{C}_r$ such that $P_{(\mathcal{E}_{\mathcal{C}},\mathcal{E}_{\mathcal{C}_r})} = I_{|\mathcal{E}_{\mathcal{C}}|}$ and $P_{(\mathcal{E}_{\mathcal{C}},\mathcal{E}_{\mathcal{T}_r})} = 0$. We then get from Proposition that $D_{\mathcal{T}_r} = I_{|\mathcal{E}_{\mathcal{T}_r}|}$ and $D_{\mathcal{C}_r} = I_{|\mathcal{E}_{\mathcal{C}}|}$ and

$$U_{\left(\mathcal{E},'\mathcal{E}'_r\right)} = P_{\left(\mathcal{E}',\mathcal{E}'_r\right)} = \begin{bmatrix} M\left(\mathcal{E}_{\mathcal{T}},\mathcal{E}_{\mathcal{T}}\backslash\mathcal{E}_{cs}\right) & O_{|\mathcal{E}_{\mathcal{T}_r}|\times|\mathcal{E}_C|} \\ O_{|\mathcal{E}_C|\times|\mathcal{E}_{\mathcal{T}_r}|} & I_{|\mathcal{E}_{\mathcal{C}}|} \end{bmatrix}. \tag{2.31}$$

Multiplying by $M_{\mathcal{T}}$ and $M_{\mathcal{T}_r}$ we get $U_{(\mathcal{E},\mathcal{E}_r)} = P_{(\mathcal{E},\mathcal{E}_r)} = M\left(\mathcal{E},\mathcal{E}\backslash\mathcal{E}_{cs}\right)$ where $M\left(\mathcal{E},\mathcal{E}\backslash\mathcal{E}_{cs}\right) = M_{\mathcal{T}} P_{\left(\mathcal{E}',\mathcal{E}'_r\right)} M_{\mathcal{T}_r}^T$. □

Proposition 2.10 allows us to derive the following Tucker representation of graph contractions.

Theorem 2.2 (Contracted Tucker representation)**.** *Let $\mathcal{G}=(\mathcal{V},\mathcal{E})$ and $\mathcal{G}/\!\!/\pi=(\mathcal{V}_r,\mathcal{E}_r)$, $\pi\in\Pi_r(\mathcal{G})$, with head and tail functions $h_{\mathcal{E}},t_{\mathcal{E}}$ and $h_{\mathcal{E}_r},t_{\mathcal{E}_r}$ respectively, and let $\mathcal{T}\in\mathbb{T}(\mathcal{G})$ and $\mathcal{T}_r\in\mathbb{T}(\mathcal{G}/\!\!/\pi)$ with cycle completing graphs $\mathcal{C}(\mathcal{T})$ and $\mathcal{C}_r=\mathcal{C}(\mathcal{T}_r)$. Then the contracted tree graph and contracted cycle-completing graph incidence matrices take the forms*

$$E(\mathcal{T}_r)=P_\pi^T E(\mathcal{T})\,U_{(\mathcal{T},\mathcal{T}_r)}, \tag{2.32}$$

and

$$E(\mathcal{C}_r)=P_\pi^T E(\mathcal{T})\,U_{(\mathcal{T},\mathcal{C}_r)}, \tag{2.33}$$

and the Tucker representation of the graph contraction is

$$T_{(\mathcal{T}_r,\mathcal{C}_r)}=L_\pi^{-1}(\mathcal{T},\mathcal{T}_r)\,U_{(\mathcal{T},\mathcal{T}_r)}^T L_e(\mathcal{T}/\pi)\,U_{(\mathcal{T},\mathcal{C}_r)}, \tag{2.34}$$

where

$$L_e(\mathcal{T}/\pi)=E^T(\mathcal{T})\,P_\pi P_\pi^T E(\mathcal{T}) \tag{2.35}$$

is the edge Laplacian of the quotient $\mathcal{T}/\pi$ and we define

$$L_\pi(\mathcal{T},\mathcal{T}_r)\triangleq U_{(\mathcal{T},\mathcal{T}_r)}^T L_e(\mathcal{T}/\pi)\,U_{(\mathcal{T},\mathcal{T}_r)} \tag{2.36}$$

and

$$U_{(\mathcal{T},\mathcal{T}_r)}\triangleq\left(P_{(\mathcal{E}_\mathcal{T},\mathcal{E}_{\mathcal{T}_r})}+T_{(\mathcal{T},\mathcal{C})}P_{(\mathcal{E}_\mathcal{C},\mathcal{E}_{\mathcal{T}_r})}\right)D_{\mathcal{T}_r}^{-1}, \tag{2.37}$$

$$U_{(\mathcal{T},\mathcal{C}_r)}\triangleq\left(P_{(\mathcal{E}_\mathcal{T},\mathcal{E}_{\mathcal{C}_r})}+T_{(\mathcal{T},\mathcal{C})}P_{(\mathcal{E}_\mathcal{C},\mathcal{E}_{\mathcal{C}_r})}\right)D_{\mathcal{C}_r}^{\dagger}. \tag{2.38}$$

Proof. Using

$$E(\mathcal{G}_r)=P_\pi^T E(\mathcal{G})\,U_{(\mathcal{E},\mathcal{E}_r)},$$
$$E(\mathcal{G}_r)=\left[E(\mathcal{T}_r)\;E(\mathcal{C}_r)\right]M_{\mathcal{T}_r}^T$$

and

$$E(\mathcal{G})=E(\mathcal{T})\,R_{(\mathcal{T},\mathcal{C})}M_\mathcal{T}^T$$

we get

$$\left[E(\mathcal{T}_r)\;E(\mathcal{C}_r)\right]M_{\mathcal{T}_r}^T=P_\pi^T E(\mathcal{T})\,R_{(\mathcal{T},\mathcal{C})}M_\mathcal{T}^T U_{(\mathcal{E},\mathcal{E}_r)}.$$

Multiplying by $M_{\mathcal{T}_r}$ and with

$$M_{\mathcal{T}_r}^T M_{\mathcal{T}_r}=I_{|\mathcal{E}_{\mathcal{T}_r}|}$$

and

$$U_{(\mathcal{E}',\mathcal{E}_r')}=M_\mathcal{T}^T U_{(\mathcal{E},\mathcal{E}_r)}M_{\mathcal{T}_r}$$

the normalized edge reduction matrix (Eq. (2.26)) we get

$$\left[E(\mathcal{T}_r)\;E(\mathcal{C}_r)\right]=P_\pi^T E(\mathcal{T})\,R_{(\mathcal{T},\mathcal{C})}U_{(\mathcal{E}',\mathcal{E}_r')}. \tag{2.39}$$

Expanding $R_{(\mathcal{T},\mathcal{C})}$ and $U_{(\mathcal{E}',\mathcal{E}_r')}$ we get $E(\mathcal{T}_r)=P_\pi^T E(\mathcal{T})\,U_{(\mathcal{T},\mathcal{T}_r)}$ and $E(\mathcal{C}_r)=P_\pi^T E(\mathcal{T})\,U_{(\mathcal{T},\mathcal{C}_r)}$ with $U_{(\mathcal{T},\mathcal{T}_r)}$ and $U_{(\mathcal{T},\mathcal{C}_r)}$ given in Eq.(2.37) and Eq.(2.38). Expanding the Tucker representation of the contracted graph

$$T_{(\mathcal{T}_r,\mathcal{C}_r)}=L_e^{-1}(\mathcal{T}_r)\,E(\mathcal{T}_r)^T E(\mathcal{C}_r), \tag{2.40}$$

with Eq.(2.32) and Eq.(2.33) we obtain Eq. (2.3.5). □

Proposition 2.13. *Let $\mathcal{G} = (\mathcal{V}, \mathcal{E})$, $\mathcal{T} \in \mathbb{T}(\mathcal{G})$ and $\mathcal{E}_{cs} \in \Xi_{n-r}(\mathcal{T})$, and let $\mathcal{G}_r = \mathcal{G} /\!\!/ \mathcal{E}_{cs}$, with $\mathcal{T}_r = \mathcal{T} /\!\!/ \mathcal{E}_{cs}$ and $\mathcal{C}_r = \mathcal{C}(\mathcal{T}_r)$. Then if $\mathcal{G} /\!\!/ \mathcal{E}_{cs}$ is cycle-invariant (Definition 2.5) then the Tucker representation of the graph contraction is*

$$T_{(\mathcal{T}_r,\mathcal{C}_r)} = M^T(\mathcal{E}_\mathcal{T}, \mathcal{E}_\mathcal{T} \backslash \mathcal{E}_{cs}) T_{(\mathcal{T},\mathcal{C})}. \tag{2.41}$$

Proof. From Proposition 2.12 we obtain that $P_{(\mathcal{E}_\mathcal{T},\mathcal{E}_{\mathcal{T}_r})} = M(\mathcal{E}_\mathcal{T}, \mathcal{E}_\mathcal{T} \backslash \mathcal{E}_{cs})$ and $P_{(\mathcal{E}_\mathcal{T},\mathcal{E}_{\mathcal{C}_r})} = 0$, and since $\mathcal{G} /\!\!/ \mathcal{E}_{cs}$ is *cycle-invariant* then $P_{(\mathcal{E}_\mathcal{C},\mathcal{E}_{\mathcal{T}_r})} = 0$ and $P_{(\mathcal{E}_\mathcal{C},\mathcal{E}_{\mathcal{C}_r})} = I_{|\mathcal{E}_\mathcal{C}|}$. From Theorem 2.2 we then obtain

$$\begin{aligned} U_{(\mathcal{T},\mathcal{T}_r)} &= M(\mathcal{E}_\mathcal{T}, \mathcal{E}_\mathcal{T} \backslash \mathcal{E}_{cs}), \\ U_{(\mathcal{T},\mathcal{C}_r)} &= T_{(\mathcal{T},\mathcal{C})}, \\ E(\mathcal{T}_r) &= P_\pi^T E(\mathcal{T}) M(\mathcal{E}_\mathcal{T}, \mathcal{E}_\mathcal{T} \backslash \mathcal{E}_{cs}), \\ E(\mathcal{C}_r) &= P_\pi^T E(\mathcal{T}) T_{(\mathcal{T},\mathcal{C})} \end{aligned}$$

and

$$T_{(\mathcal{T}_r,\mathcal{C}_r)} = L_\pi^{-1}(\mathcal{T}) M^T(\mathcal{E}_\mathcal{T}, \mathcal{E}_\mathcal{T} \backslash \mathcal{E}_{cs}) L_e(\mathcal{T}/\mathcal{E}_{cs}) T_{(\mathcal{T},\mathcal{C})}.$$

We notice that

$$I_{|\mathcal{E}_\mathcal{T}|} = M(\mathcal{E}_\mathcal{T}, \mathcal{E}_\mathcal{T} \backslash \mathcal{E}_{cs}) M^T(\mathcal{E}_\mathcal{T}, \mathcal{E}_\mathcal{T} \backslash \mathcal{E}_{cs}) + M(\mathcal{E}_\mathcal{T}, \mathcal{E}_{cs}) M^T(\mathcal{E}_\mathcal{T}, \mathcal{E}_{cs})$$

such that

$$\begin{aligned} T_{(\mathcal{T}_r,\mathcal{C}_r)} &= M^T(\mathcal{E}_\mathcal{T}, \mathcal{E}_\mathcal{T} \backslash \mathcal{E}_{cs}) T_{(\mathcal{T},\mathcal{C})} \\ &\quad + L_\pi^{-1}(\mathcal{T}) M^T(\mathcal{E}_\mathcal{T}, \mathcal{E}_\mathcal{T} \backslash \mathcal{E}_{cs}) L_e(\mathcal{T}/\mathcal{E}_{cs}) M(\mathcal{E}_\mathcal{T}, \mathcal{E}_{cs}) M^T(\mathcal{E}_\mathcal{T}, \mathcal{E}_{cs}) T_{(\mathcal{T},\mathcal{C})}. \end{aligned}$$

We have

$$L_e(\mathcal{T}/\mathcal{E}_{cs}) M(\mathcal{E}_\mathcal{T}, \mathcal{E}_{cs}) = E^T(\mathcal{T}/\mathcal{E}_{cs}) E(\mathcal{T}/\mathcal{E}_{cs}) M(\mathcal{E}_\mathcal{T}, \mathcal{E}_{cs})$$

and from Proposition 2.8 we obtain that $E(\mathcal{T}/\mathcal{E}_{cs}) M(\mathcal{E}_\mathcal{T}, \mathcal{E}_{cs}) = 0$, such that

$$T_{(\mathcal{T}_r,\mathcal{C}_r)} = M^T(\mathcal{E}_\mathcal{T}, \mathcal{E}_\mathcal{T} \backslash \mathcal{E}_{cs}) T_{(\mathcal{T},\mathcal{C})}.$$

□

2.3.4 Summary of Definitions of Graph Contraction Algebraic Representations

For clarity and easiness of reading, Table 2.1 summarizes summarizes definitions of graph contraction algebraic representations used throughout this chapter.

Table 2.1: Summary of definitions of graph contraction algebraic representations.

Definition	Symbol	Expression
Partition characteristic matrix	P_π	$[P_\pi]_{ij} = \begin{cases} 1 & f_\pi(v_i) = v_j^r \\ 0 & \text{o.w.} \end{cases}$ for $v_i \in \mathcal{V}$ and $v_j^r \in \mathcal{V}_r$.
Partition projection matrix	$P(\pi)$	$P(\pi) = P_\pi D^{-\frac{1}{2}}(\pi)$ where $D(\pi) = P_\pi^T P_\pi$
Edge contraction matrix	$P_{(\mathcal{E}_S, \mathcal{E}_{S_r})}$	$\left[P_{(\mathcal{E}_S, \mathcal{E}_{S_r})}\right]_{km} = p(\epsilon_k, \epsilon_m^r)$, for $\epsilon_k \in \mathcal{E}_S$ and $\epsilon_k^r \in \mathcal{E}_{S_r}$.
Normalized edge contraction matrix	$U_{(\mathcal{E}_S, \mathcal{E}_{S_r})}$	$U_{(\mathcal{E}_S, \mathcal{E}_{S_r})} = P_{(\mathcal{E}_S, \mathcal{E}_{S_r})} D^\dagger_{(\mathcal{E}_S, \mathcal{E}_{S_r})}$ where $D_{(\mathcal{E}_S, \mathcal{E}_{S_r})} = P^T_{(\mathcal{E}_S, \mathcal{E}_{S_r})} P_{(\mathcal{E}_S, \mathcal{E}_{S_r})}$
Incidence matrix	$E(\mathcal{G})$	$[E(\mathcal{G})]_{ij} = \begin{cases} 1 & h_\mathcal{E}(\epsilon_j) = v_i \\ -1 & t_\mathcal{E}(\epsilon_j) = v_i \\ 0 & \text{otherwise} \end{cases}$
Laplacian matrix	$L(\mathcal{G})$	$L(\mathcal{G}) = E(\mathcal{G}) E^T(\mathcal{G})$
Edge Laplacian matrix	$L_e(\mathcal{G})$	$L_e(\mathcal{G}) = E^T(\mathcal{G}) E(\mathcal{G})$
Normalized Laplacian matrix	$\mathcal{L}(\mathcal{G})$	$\mathcal{L}(\mathcal{G}) = D^{-\frac{1}{2}}(\mathcal{G}) L(\mathcal{G}) D^{-\frac{1}{2}}(\mathcal{G})$ where $[D(\mathcal{G})]_{ii} = d(v_i)$
Edge selection matrix	$M(\mathcal{E}, \mathcal{E}_S)$	$[M(\mathcal{E}, \mathcal{E}_S)]_{ij} = \begin{cases} 1 & \epsilon_i(\mathcal{E}) = \epsilon_j(\mathcal{E}_S) \\ 0 & \text{o.w.,} \end{cases}$ for $i = 1, \ldots, \lvert\mathcal{E}\rvert$ and $j = 1, \ldots, \lvert\mathcal{E}_S\rvert$

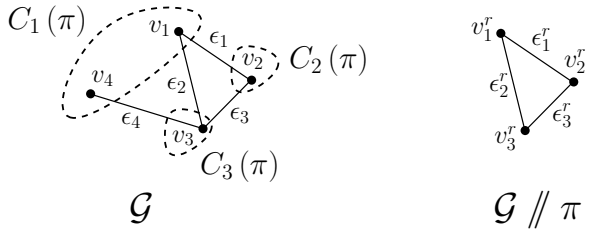

Figure 2.6: An example of a graph $\mathcal{G}$ and its contraction $\mathcal{G} /\!\!/ \pi$ over a 3-partition $\pi(\mathcal{G}) = \{C_1, C_2, C_3\}$ with $C_1 = \{v_1, v_4\}$, $C_2 = \{v_2\}$ and $C_3 = \{v_3\}$.

2.3.5 An Illustrative Example

The following example illustrates the above definitions and derivations of algebraic representations for graph contractions. Consider a graph $\mathcal{G} = (\mathcal{V}, \mathcal{E})$ of order 4 and its graph contraction $\mathcal{G} /\!\!/ \pi$, shown in Figure 2.6.

The corresponding PCM and PPM (Definition 2.13) are given in Table 2.2. The edges $\mathcal{E}(\mathcal{G})$ are (with assigned direction) $\epsilon_1 = (v_1, v_2)$, $\epsilon_2 = (v_1, v_3)$, $\epsilon_3 = (v_2, v_3)$ and $\epsilon_4 = (v_3, v_4)$, and the edges $\mathcal{E}_r = \mathcal{E}(\mathcal{G} /\!\!/ \pi)$ are (with assigned direction) $\epsilon_1^r = (v_1, v_2)$, $\epsilon_2^r = (v_1, v_3)$, $\epsilon_3^r = (v_2, v_3)$. The resulting edge contraction matrix and the normalized edge contraction matrix (Definition 2.15) for this example are given in Table 2.2

We now examine for the same graph contraction example (Figure 2.6) the incidence and Laplacian matrices of the graph and contracted graph (Table 2.3). It can be verified that as according to Proposition 2.9 and Theorem 2.1 that

$$E(\mathcal{G} /\!\!/ \pi) = P_\pi^T E(\mathcal{G}) U_{(\mathcal{E},\mathcal{E}_r)}$$

and

$$L(\mathcal{G}_r) = P_\pi^T E(\mathcal{G}) U_{(\mathcal{E},\mathcal{E}_r)} U_{(\mathcal{E},\mathcal{E}_r)}^T E^T(\mathcal{G}) P_\pi$$
$$L_e(\mathcal{G}_r) = U_{(\mathcal{E},\mathcal{E}_r)}^T L_e(\mathcal{G}/\pi) U_{(\mathcal{E},\mathcal{E}_r)}$$

where P_π and $U_{(\mathcal{E},\mathcal{E}_r)}$ are given in Table 2.2.

In order to demonstarte the Tucker representation of the graph contraction we choose a spanning tree $\mathcal{T}$ with edges $\epsilon_1(\mathcal{E}(\mathcal{T})) = (v_1, v_2)$, $\epsilon_2(\mathcal{E}(\mathcal{T})) = (v_2, v_3)$ and $\epsilon_3(\mathcal{E}(\mathcal{T})) = (v_3, v_4)$. The co-tree $\mathcal{C}$ edges are then $\epsilon_1(\mathcal{E}(\mathcal{C})) = (v_1, v_3)$. The spanning tree $\mathcal{T}_r$ of the reduced graph $\mathcal{G} /\!\!/ \pi$ has edges $\epsilon_1(\mathcal{E}(\mathcal{T}_r)) = (v_1^r, v_2^r)$ and $\epsilon_2(\mathcal{E}(\mathcal{T}_r)) = (v_2^r, v_3^r)$ and the co-tree $\mathcal{C}_r$ edges are then $\epsilon_1(\mathcal{E}(\mathcal{C}_r)) = (v_1^r, v_3^r)$. The Tucker representations $T_{(\mathcal{T},\mathcal{C})}$ and $T_{(\mathcal{T}_r,\mathcal{C}_r)}$ of the full graph and the graph contraction are given in Table 2.2. It can be verified that as according to Theorem 2.2 that

$$T_{(\mathcal{T}_r,\mathcal{C}_r)} = L_\pi^{-1}(\mathcal{T}) U_{(\mathcal{T},\mathcal{T}_r)}^T L_e(\mathcal{T}/\pi) U_{(\mathcal{T},\mathcal{C}_r)} \cdot,$$

Table 2.2: Example of the PCM, PPM and (normalized) edge contraction matrix of a graph contraction.

Algebraic representation	Symbol	Value
PCM	P_π	$\begin{bmatrix} 1 & 0 & 0 \\ 0 & 1 & 0 \\ 0 & 0 & 1 \\ 0 & 0 & -1 \end{bmatrix}$
PPM	$P(\pi)$	$\begin{bmatrix} \frac{1}{\sqrt{2}} & 0 & 0 \\ 0 & 1 & 0 \\ 0 & 0 & 1 \\ \frac{1}{\sqrt{2}} & 0 & 0 \end{bmatrix}$
Edge contraction matrix	$P_{(\mathcal{E},\mathcal{E}_r)}$	$\begin{bmatrix} 1 & 0 & 0 \\ 0 & 1 & 0 \\ 0 & 0 & 1 \\ 0 & -1 & 0 \end{bmatrix}$
Normalized edge contraction matrix	$U_{(\mathcal{E},\mathcal{E}_r)}$	$\begin{bmatrix} 1 & 0 & 0 \\ 0 & \frac{1}{2} & 0 \\ 0 & 0 & 1 \\ 0 & -\frac{1}{2} & 0 \end{bmatrix}$

In the next section we derive efficient algorithms for finding Laplacian-interlacing graph contractions, based on a novel min-max interlacing theorem.

2.4 Interlacing Graph Contractions

The interlacing property of matrices has been extensively studied with classic algebraic results such as the Poincare separation theorem [5, p. 119], and matrix combinatorial results such as the relation of equitable partitions with tight interlacing [26]. Here we study what types of reduced graphs have interlacing graph matrices. We start by defining spectral interlacing. The spectrum of a real symmetric matrix $A \in \mathbb{R}^{n\times n}$ is the set of eigenvalues $\{\lambda_k(A)\}_{k=1}^n$. In this chapter we always take λ_k as the kth eigenvalue of A in ascending order.

Definition 2.21 (Interlacing)**.** *Let $A \in \mathbb{R}^{n\times n}$ and $B \in \mathbb{R}^{r\times r}$ be real symmetric matrices with $0 < r < n$. Then the eigenvalues of B* interlace *the eigenvalues of A, denoted $B \propto A$, if $\lambda_k(A) \le \lambda_k(B) \le \lambda_{n-r+k}(A)$ for $k = 1, 2, \ldots, r$. The interlacing is tight if $\lambda_k(A) = \lambda_k(B)$ or $\lambda_k(B) = \lambda_{n-r+k}(A)$ for $k = 1, 2, \ldots, r$.*

It is straight forward to show that interlacing is a transitive property.

Proposition 2.14. *Let $A_1 \in \mathbb{R}^{n_1\times n_1}$, $A_2 \in \mathbb{R}^{n_2\times n_2}$ and $A_3 \in \mathbb{R}^{n_3\times n_3}$ be real symmetric matrices with $0 < n_3 < n_2 < n_1$. If $A_3 \propto A_2$ and $A_2 \propto A_1$, then $A_3 \propto A_1$.*

Table 2.3: Example of incidence and Laplacian matrices and the Tucker representation of a graph contraction.

Algebraic representation	Symbol	Value
Incidence matrix	$E(\mathcal{G})$	$\begin{bmatrix} -1 & -1 & 0 & 0 \\ 1 & 0 & -1 & 0 \\ 0 & 1 & 1 & -1 \\ 0 & 0 & 0 & 1 \end{bmatrix}$
Incidence matrix	$E(\mathcal{G} /\!\!/ \pi)$	$\begin{bmatrix} -1 & 1 & 0 \\ 1 & 0 & -1 \\ 0 & -1 & 1 \end{bmatrix}$
Laplacian matrix	$L(\mathcal{G})$	$\begin{bmatrix} 2 & -1 & -1 & 0 \\ -1 & 2 & -1 & 0 \\ -1 & -1 & 3 & -1 \\ 0 & 0 & -1 & 1 \end{bmatrix}$
Laplacian matrix	$L(\mathcal{G} /\!\!/ \pi)$	$\begin{bmatrix} 2 & -1 & -1 \\ -1 & 2 & -1 \\ -1 & -1 & 2 \end{bmatrix}$
Edge Laplacian matrix	$L_e(\mathcal{G})$	$\begin{bmatrix} 2 & 1 & -1 & 0 \\ 1 & 2 & 1 & -1 \\ -1 & 1 & 2 & -1 \\ 0 & -1 & -1 & 2 \end{bmatrix}$
Edge Laplacian matrix	$L_e(\mathcal{G} /\!\!/ \pi)$	$\begin{bmatrix} 2 & 1 & -1 \\ 1 & 2 & 1 \\ -1 & 1 & 2 \end{bmatrix}$
Tucker representation	$T_{(\mathcal{T},\mathcal{C})}$	$\begin{bmatrix} 1 & 1 & 0 \end{bmatrix}^T$
Tucker representation	$T_{(\mathcal{T}_r,\mathcal{C}_r)}$	$\begin{bmatrix} 1 & 1 \end{bmatrix}^T$

Proof. From $A_3 \propto A_2$ and $A_2 \propto A_1$ we have $\lambda_k(A_2) \leq \lambda_k(A_3) \leq \lambda_{n_2-n_3+k}(A_2)$ for $k = 1, 2, \ldots, n_3$ and $\lambda_l(A_1) \leq \lambda_l(A_2) \leq \lambda_{n_1-n_2+l}(A_1)$ for $l = 1, 2, \ldots, n_2$. From $l = k$ we get $\lambda_k(A_1) \leq \lambda_k(A_2) \leq \lambda_k(A_3)$, and from $l = n_2 - n_3 + k$ we get $\lambda_k(A_3) \leq \lambda_{n_2-n_3+k}(A_2) \leq \lambda_{n_1-n_3+k}(A_1)$, such that $\lambda_k(A_1) \leq \lambda_k(A_3) \leq \lambda_{n_1-n_3+k}(A_1)$ for $k = 1, 2, \ldots, n_3$ and we obtain that $A_3 \propto A_1$. □

We now extend the notion of spectral interlacing properties to graphs. For a given graph $\mathcal{G}$ of order n with m edges, and a real symmetric matrix associated to the graph, $M(\mathcal{G}) \in \mathbb{R}^{n\times n}$, the interlacing graph reduction problem is to find a graph $\mathcal{G}_r$ of order $r < n$ such that the eigenvalues of $M(\mathcal{G}_r)$ interlace the eigenvalues of $M(\mathcal{G})$.

Definition 2.22 (Interlacing graphs)**.** *Consider two graphs $\mathcal{G}_n$ and $\mathcal{G}_r$ of order n and r respectively, with $n > r$, and let $M(\mathcal{G}) \in \mathbb{R}^{n\times n}$ be any real symmetric matrix associated with the graph $\mathcal{G}$. We say that the two graphs are* M-interlacing *if $M(\mathcal{G}_r) \propto M(\mathcal{G}_n)$, and denote the property by $\mathcal{G}_r \propto_M \mathcal{G}_n$.*

A problem arising naturally from the definition of interlacing graphs is the interlacing graph reduction problem.

Problem 2.1 (Interlacing graph reduction)**.** *Consider a graph $\mathcal{G}_n$ of order n and let $M(\mathcal{G}) \in \mathbb{R}^{n\times n}$ be any real symmetric matrix associated with the graph $\mathcal{G}$. Find a graph $\mathcal{G}_r$ of a given order $r < n$ such that $\mathcal{G}_r \propto_M \mathcal{G}_n$.*

Finding a solution to Problem 2.1 may be numerically intractable for a moderate number of nodes, as the number c_r of simple connected graphs of order r increases exponentially according to the recurrence $\sum_k \binom{r}{k} k c_k 2^{\binom{r-k}{2}} = r2^{\binom{r}{2}}$ for $r \geq 1$ [64, p.87], e.g., for $r = 1, \ldots, 6$, $c_r = 1$, 1, 4, 38, 728, 26704.

A powerful tool for proving interlacing results is the Courant-Fischer theorem, e.g., that a symmetric matrix and a principle submatrix of that matrix interlace [29], which leads to an adjacency interlacing theorem for node-removal graph reductions:

Theorem 2.3 (Adjacency interlacing node-removal)**.** *Consider a graph $\mathcal{G}$ and a node subset $\mathcal{V}_S \subset \mathcal{V}(\mathcal{G})$. Then $\mathcal{G}\backslash\mathcal{V}_S \propto_A \mathcal{G}$.*

Proof. The matrix $A(\mathcal{G}\backslash\mathcal{V}_S)$ is a principle submatrix of $A(\mathcal{G})$, therefore, $\mathcal{G}\backslash\mathcal{V}_S \propto_A \mathcal{G}$. □

Utilizing the Courant-Fischer theorem [33] and the following $\min - \max$ inequalities (Proposition 2.15) an interlacing graph reduction theorem is derived. We first introduce some notations to simplify the statement. A k-dimensional subspace of $\mathbb{R}^n$ is denoted as $\mathcal{F}_n^{(k)}$. For an r-dimensional subspace $\mathcal{F}_n^{(r)}$, we define the injective map $p_{\mathcal{F}_n^{(r)}} : \mathbb{R}^r \to \mathbb{R}^n$, such that $x \in \mathbb{R}^r \mapsto y \in \mathcal{F}_n^{(r)}$.

Theorem 2.4 (Courant-Fischer)**.** *Consider a real symmetric matrix $M \in \mathbb{R}^{n\times n}$, then for $k \in [1, n]$*

$$\lambda_k(M) = \max_{\mathcal{F}_n^{(n-k+1)}} \min_{\substack{x\in\mathcal{F}_n^{(n-k+1)} \\ x\neq 0}} R(M, x), \tag{2.42}$$

and

$$\lambda_k(M) = \min_{\mathcal{F}_n^{(k)}} \max_{\substack{x \in \mathcal{F}_n^{(k)} \\ x \neq 0}} R(M,x), \tag{2.43}$$

where $R(M,x) \triangleq \frac{x^T M x}{x^T x}$ *is the Rayleigh quotient.*

Proposition 2.15. *Consider a subspace* $\mathcal{F}_n^{(r)}$ *for* $r < n$*, and let* $f(x) : \mathbb{R}^n \to \mathbb{R}$ *be a real-valued function that attains a minimum and a maximum on* $\mathbb{R}^n \setminus \{0\}$*. Then the following holds for* $k \in [1, r]$*:*

i) $$\max_{\mathcal{F}_n^{(n-k+1)}} \min_{\substack{x \in \mathcal{F}_n^{(n-k+1)} \\ x \neq 0}} f(x) \leq \max_{\mathcal{F}_r^{(r-k+1)}} \min_{\substack{\tilde{x} \in \mathcal{F}_r^{(r-k+1)} \\ \tilde{x} \neq 0}} f\left(p_{\mathcal{F}_n^{(r)}}(\tilde{x})\right),$$

ii) $$\min_{\mathcal{F}_n^{(n-r+k)}} \max_{\substack{x \in \mathcal{F}_n^{(n-r+k)} \\ x \neq 0}} f(x) \geq \min_{\mathcal{F}_r^{(k)}} \max_{\substack{\tilde{x} \in \mathcal{F}_r^{(k)} \\ \tilde{x} \neq 0}} f\left(p_{\mathcal{F}_n^{(r)}}(\tilde{x})\right).$$

Proof. We first prove (i). Let $s \equiv n - k + 1$. For all $\mathcal{F}_n^{(s)} \subseteq \mathbb{R}^n$

$$\begin{aligned} \min_{\substack{x \in \mathcal{F}_n^{(s)} \\ x \neq 0}} f(x) &= \min \left\{ \min_{\substack{x \in \mathcal{F}_n^{(s)} \cap \mathcal{F}_n^{(r)} \\ x \neq 0}} f(x), \min_{\substack{x \in \mathcal{F}_n^{(s)} \setminus \left\{\mathcal{F}_n^{(s)} \cap \mathcal{F}_n^{(r)}\right\} \\ x \neq 0}} f(x) \right\} \\ &\leq \min_{\substack{x \in \mathcal{F}_n^{(s)} \cap \mathcal{F}_n^{(r)} \\ x \neq 0}} f(x), \end{aligned} \tag{2.44}$$

and we obtain that

$$\max_{\mathcal{F}_n^{(s)}} \min_{\substack{x \in \mathcal{F}_n^{(s)} \\ x \neq 0}} f(x) \leq \max_{\mathcal{F}_n^{(s)}} \min_{\substack{x \in \mathcal{F}_n^{(s)} \cap \mathcal{F}_n^{(r)} \\ x \neq 0}} f(x). \tag{2.45}$$

Since $k \leq r$ then $s = n - k + 1 > n - r$ and

$$\dim\left(\mathcal{F}_n^{(s)} \cap \mathcal{F}_n^{(r)}\right) \geq s - (n - r), \tag{2.46}$$

therefore,

$$\max_{\mathcal{F}_n^{(s)}} \min_{\substack{x \in \mathcal{F}_n^{(s)} \cap \mathcal{F}_n^{(r)} \\ x \neq 0}} f(x) = \max_{\mathcal{F}_n^{(s-(n-r))} \subseteq \mathcal{F}_n^{(r)}} \min_{\substack{x \in \mathcal{F}_n^{(s-(n-r))} \\ x \neq 0}} f(x). \tag{2.47}$$

For each $\mathcal{F}_n^{(s-(n-r))} \subseteq \mathcal{F}_n^{(r)}$ we can find $\tilde{\mathcal{F}}_r^{(s-(n-r))} \subseteq \mathbb{R}^r$ that is mapped to it by $p_{\mathcal{F}_n^{(r)}}(\tilde{x})$,

$$\tilde{\mathcal{F}}_r^{(s-(n-r))} = \left\{ \tilde{x} \in \mathbb{R}^r | p_{\mathcal{F}_n^{(r)}}(\tilde{x}) \in \mathcal{F}_n^{(s-(n-r))} \right\}, \tag{2.48}$$

such that

$$\min_{\substack{x \in \mathcal{F}_n^{(s-(n-r))} \\ x \neq 0}} f(x) = \min_{\substack{\tilde{x} \in \tilde{\mathcal{F}}_r^{(s-(n-r))} \\ \tilde{x} \neq 0}} f\left(p_{\mathcal{F}_n^{(r)}}(\tilde{x})\right). \tag{2.49}$$

Maximizing over all $\mathcal{F}_n^{(s-(n-r))} \subseteq \mathcal{F}_n^{(r)}$ we obtain

$$\max_{\mathcal{F}_n^{(s-(n-r))} \subseteq \mathcal{F}_n^{(r)}} \min_{\substack{x \in \mathcal{F}_n^{(s-(n-r))} \\ x \neq 0}} f(x) = \max_{\mathcal{F}_r^{(s-(n-r))}} \min_{\substack{\tilde{x} \in \tilde{\mathcal{F}}_r^{(s-(n-r))} \\ \tilde{x} \neq 0}} f\left(p_{\mathcal{F}_n^{(r)}}(\tilde{x})\right), \tag{2.50}$$

and

$$\max_{\mathcal{F}_n^{(n-k+1)}} \min_{\substack{x \in \mathcal{F}_n^{(n-k+1)} \cap \mathcal{F}_n^{(r)} \\ x \neq 0}} f(x) = \max_{\mathcal{F}_r^{(r-k+1)}} \min_{\substack{\tilde{x} \in \tilde{\mathcal{F}}_r^{(r-k+1)} \\ \tilde{x} \neq 0}} f\left(p_{\mathcal{F}_n^{(r)}}(\tilde{x})\right), \tag{2.51}$$

completing the proof of (i).

The proof of (ii) is as follows. Let $s \equiv n - r + k$. For all $\mathcal{F}_n^{(s)} \subseteq \mathbb{R}^n$

$$\begin{aligned} \max_{\substack{x \in \mathcal{F}_n^{(s)} \\ x \neq 0}} f(x) &= \max \left\{ \max_{\substack{x \in \mathcal{F}_n^{(s)} \cap \mathcal{F}_n^{(r)} \\ x \neq 0}} f(x), \max_{\substack{x \in \mathcal{F}_n^{(s)} \setminus \left\{\mathcal{F}_n^{(s)} \cap \mathcal{F}_n^{(r)}\right\} \\ x \neq 0}} f(x) \right\} \\ &\geq \max_{\substack{x \in \mathcal{F}_n^{(s)} \cap \mathcal{F}_n^{(r)} \\ x \neq 0}} f(x), \end{aligned} \tag{2.52}$$

and

$$\min_{\mathcal{F}_n^{(s)}} \max_{\substack{x \in \mathcal{F}_n^{(s)} \\ x \neq 0}} f(x) \geq \min_{\mathcal{F}_n^{(s)}} \max_{\substack{x \in \mathcal{F}_n^{(s)} \cap \mathcal{F}_n^{(r)} \\ x \neq 0}} f(x). \tag{2.53}$$

Since $k \geq 1$ then $s = n - r + k > n - r$ and

$$\dim\left(\mathcal{F}_n^{(s)} \cap \mathcal{F}_n^{(r)}\right) \geq s - (n - r), \tag{2.54}$$

and we can then replace max min with min max in the above proof of (i) and obtain

$$\min_{\mathcal{F}_n^{(n-r+k)}} \max_{\substack{x \in \mathcal{F}_n^{(n-r+k)} \cap \mathcal{F}_n^{(r)} \\ x \neq 0}} f(x) = \min_{\mathcal{F}_r^{(k)}} \max_{\substack{\tilde{x} \in \mathcal{F}_r^{(k)} \\ \tilde{x} \neq 0}} f\left(p_{\mathcal{F}_n^{(r)}}(\tilde{x})\right),$$

completing the proof of (ii). □

Theorem 2.5 (Interlacing graph reduction theorem)**.** *Consider two graphs $\mathcal{G}_n$ and $\mathcal{G}_r$ of order n and r respectively, with $n > r$, and let $M(\mathcal{G}) \in \mathbb{R}^{n\times n}$ be any real symmetric matrix associated with the graph $\mathcal{G}$. If there exists r-dimentional subspaces $\mathcal{A}, \mathcal{B} \subseteq \mathbb{R}^n$ such that $\forall x \in \mathbb{R}^r \setminus \{0\}$*

$$R\left(M\left(\mathcal{G}_n\right), p_{\mathcal{A}}\left(x\right)\right) \leq R\left(M\left(\mathcal{G}_r\right), x\right), \tag{2.55}$$

and

$$R\left(M\left(\mathcal{G}_n\right), p_{\mathcal{B}}\left(x\right)\right) \geq R\left(M\left(\mathcal{G}_r\right), x\right), \tag{2.56}$$

then $\mathcal{G}_r \propto_M \mathcal{G}_n$.

Proof. In order for $\mathcal{G}_n$ and $\mathcal{G}_r$ to be M-interlacing (Definition 2.15) we must prove that $\lambda_k\left(M\left(\mathcal{G}_n\right)\right) \leq \lambda_k\left(M\left(\mathcal{G}_r\right)\right) \leq \lambda_{n-r+k}\left(M\left(\mathcal{G}_n\right)\right)$ for $k \in [1, r]$. From the Courant–Fischer theorem (Theorem 2.4) we have

$$\lambda_k\left(M\left(\mathcal{G}_n\right)\right) = \max_{\mathcal{F}_n^{(n-k+1)}} \min_{\substack{x\in\mathcal{F}_n^{(n-k+1)} \\ x\neq 0}} R\left(M\left(\mathcal{G}_n\right), x\right), \tag{2.57}$$

and from the min-max properties (Proposition 2.15) with $\mathcal{F}_n^{(r)} \equiv \mathcal{A}$ we have for $k \in [1, r]$

$$\lambda_k\left(M\left(\mathcal{G}_n\right)\right) \leq \max_{\mathcal{F}_r^{(r-k+1)}} \min_{\substack{x\in\mathcal{F}_r^{(r-k+1)} \\ x\neq 0}} R\left(M\left(\mathcal{G}_n\right), p_{\mathcal{A}}\left(x\right)\right). \tag{2.58}$$

Since $R\left(M\left(\mathcal{G}_n\right), p_{\mathcal{A}}\left(x\right)\right) \leq R\left(M\left(\mathcal{G}_r\right), x\right)$, therefore,

$$\begin{aligned}\lambda_k\left(M\left(\mathcal{G}_n\right)\right) &\leq \max_{\mathcal{F}_r^{(r-k+1)}} \min_{\substack{x\in\mathcal{F}_r^{(r-k+1)} \\ x\neq 0}} R\left(M\left(\mathcal{G}_r\right), x\right) \\ &= \lambda_k\left(M\left(\mathcal{G}_r\right)\right),\end{aligned} \tag{2.59}$$

and $\lambda_k\left(M\left(\mathcal{G}_n\right)\right) \leq \lambda_k\left(M\left(\mathcal{G}_r\right)\right)$ for $k \in [1, r]$. In order to complete the interlacing proof it is left to show that $\lambda_k\left(M\left(\mathcal{G}_r\right)\right) \leq \lambda_{n-r+k}\left(M\left(\mathcal{G}_n\right)\right)$ for $k \in [1, r]$. From the Courant–Fischer theorem (Theorem 2.4) we get

$$\lambda_{n-r+k}\left(M\left(\mathcal{G}_n\right)\right) = \min_{\mathcal{F}_n^{(n-r+k)}} \max_{\substack{x\in\mathcal{F}_n^{(n-r+k)} \\ x\neq 0}} R\left(M\left(\mathcal{G}_n\right), x\right), \tag{2.60}$$

and from the min-max properties (Proposition 2.15) with $\mathcal{F}_n^{(r)} \equiv \mathcal{B}$ we have

$$\lambda_{n-r+k}\left(M\left(\mathcal{G}_n\right)\right) \geq \min_{\mathcal{F}_r^{(k)}} \max_{\substack{x\in\mathcal{F}_r^{(k)} \\ x\neq 0}} R\left(M\left(\mathcal{G}_n\right), p_{\mathcal{B}}\left(x\right)\right). \tag{2.61}$$

Since $R\left(M\left(\mathcal{G}_n\right), p_{\mathcal{B}}\left(x\right)\right) \geq R\left(M\left(\mathcal{G}_r\right), x\right)$, therefore,

$$\begin{aligned}\lambda_{n-r+k}\left(M\left(\mathcal{G}_n\right)\right) &\geq \min_{\mathcal{F}_r^{(k)}} \max_{\substack{x\in\mathcal{F}_r^{(k)} \\ x\neq 0}} R\left(M\left(\mathcal{G}_r\right), x\right) \\ &= \lambda_k\left(M\left(\mathcal{G}_r\right)\right),\end{aligned} \tag{2.62}$$

and $\lambda_k\left(M\left(\mathcal{G}_n\right)\right) \leq \lambda_{n-r+k}\left(M\left(\mathcal{G}_r\right)\right)$ for $k \in [1, r]$, completing the proof. □

The general interlacing graph reduction problem (Problem 2.1) is combinatorial hard. If we restrict the class of reduced-order graphs to graph contractions then we get the following interlacing graph contraction problem.

Problem 2.2 (interlacing graph contraction)**.** *Consider a graph $\mathcal{G}$ and a real symmetric graph matrix $M(\mathcal{G}) \in \mathbb{R}^{n\times n}$. Then given $r < n$ find $\pi \in \Pi_r(\mathcal{G})$ such that $\mathcal{G} /\!\!/ \pi \propto_M \mathcal{G}$.*

The number of *r-partitions* is $|\Pi_r(\mathcal{G})| = S(n,r)$ where

$$S(n,r) = \sum_{k=1}^{r} (-1)^{r-k} \frac{k^n}{k!\,(r-k)!} \tag{2.63}$$

is the Stirling number of the second kind [64, p.18], which for $r \ll n$ is asymptotically $S(n,r) \sim \frac{r^n}{r!}$. If we restrict the problem to edge-based contractions then the number of partitions is the number of $n-r$ *edge contractions* is

$$|\Xi_{n-r}(\mathcal{G})| = \left(\begin{array}{c} m \\ n-r \end{array} \right),$$

where $m = |\mathcal{E}(\mathcal{G})|$. Finding an interlacing contraction is, therefore, combinatorial hard as well and in the following section we show how cycle-invariant and node-removal equivalent contractions have associated subspaces required by Theorem 2.5 and lead to interlacing graphs. Two algorithms of complexity $\mathcal{O}(mn)$ and $\mathcal{O}\left(n^2+nm\right)$ are then provided for finding, if they exist, a cycle-invariant contraction and a node-removal equivalent contraction respectively for a given graph with n vertices and m edges.

The following subspaces are now defined: the partition subspace, the anti-partition subspace and the node-removal subspace. These will be used for applying the min-max interlacing theorem (Theorem 2.5).

Consider a graph $\mathcal{G} = (\mathcal{V}, \mathcal{E})$ of order n and an r-partition $\pi \in \Pi_r(\mathcal{G})$ and consider a subset $\mathcal{V}_S \subset \mathcal{V}(\mathcal{G})$, $|\mathcal{V}_S| = n - r$ for $r < n$. Then we define the following subspaces of dimension r. The *partition subspace* $\mathcal{F}_\pi \subseteq \mathbb{R}^n$ is the space of all vectors in $\mathbb{R}^n$ such that variables with indexes in the same partition cell are equal,

$$\mathcal{F}_\pi \triangleq \{x \in \mathbb{R}^n | x_j = x_k, \forall j,k \in C_i(\pi), \forall i \in [1,r]\}, \tag{2.64}$$

and the corresponding *partition mapping* $p_{\mathcal{F}_\pi}(\tilde{x}) : \mathbb{R}^r \to \mathbb{R}^n$,

$$[p_{\mathcal{F}_\pi}(\tilde{x})]_k = \{\tilde{x}_i | k \in C_i(\pi)\}. \tag{2.65}$$

We define the *anti-partition subspace* $\tilde{\mathcal{F}}_\pi \subseteq \mathbb{R}^n$ such that for $x \in \tilde{\mathcal{F}}_\pi$ the sum of all vector variables in non-singleton partition cells is zero

$$\tilde{\mathcal{F}}_\pi \triangleq \left\{ x \in \mathbb{R}^n | x_{v_j(C_i(\pi))} = -\frac{x_{v_1(C_i(\pi))}}{|C_i(\pi)|-1}, \begin{array}{c} \forall i \in [1,r], |C_i(\pi)| > 1 \\ \forall j \in [2, |C_i(\pi)|] \end{array} \right\}, \tag{2.66}$$

and the corresponding *anti-partition mapping*, $p_{\tilde{\mathcal{F}}_\pi}(\tilde{x}):\mathbb{R}^r\to\mathbb{R}^n$,

$$\left[p_{\tilde{\mathcal{F}}_\pi}(\tilde{x})\right]_k=\begin{cases}\tilde{x}_k & k=v_1\left(C_i(\pi)\right)\\ -\frac{\tilde{x}_k}{|C_i(\pi)|-1} & k=v_j\left(C_i(\pi)\right),j\geq 2\end{cases}, \tag{2.67}$$

where $v_j\left(C_i(\pi)\right)$ denotes the j'th node of the i'th partition cell.

The *node-removal subspace*, $\mathcal{F}_{\mathcal{V}_S}\subseteq\mathbb{R}^n$, is defined as

$$\mathcal{F}_{\mathcal{V}_S}\triangleq\left\{x\in\mathbb{R}^n|x_i=0,i\in\mathcal{V}_S\right\}, \tag{2.68}$$

and the corresponding *node-removal mapping* $p_{\mathcal{F}_{\mathcal{V}_S}}(\tilde{x}):\mathbb{R}^r\to\mathbb{R}^n$,

$$\left[p_{\mathcal{F}_{\mathcal{V}_S}}(\tilde{x})\right]_k=\begin{cases}\tilde{x}_k & k\notin\mathcal{V}_S\\ 0 & o.w.\end{cases}. \tag{2.69}$$

Proposition 2.16. *Consider a graph $\mathcal{G}$ and an edge-matching and node-removal equivalent contraction $\mathcal{G}/\!\!/\mathcal{E}_{cs}$ (Definitions 2.11&2.9) with $\mathcal{E}_{cs}\in\Xi_{n-r}(\mathcal{G})$ for $r<n$. Then for $\tilde{x}\in\mathbb{R}^r$ we have*

$$R\left(L(\mathcal{G}),p_{\mathcal{F}_\pi}(\tilde{x})\right)\leq R\left(L\left(\mathcal{G}/\!\!/\mathcal{E}_{cs}\right),\tilde{x}\right), \tag{2.70}$$

and

$$R\left(L(\mathcal{G}),p_{\mathcal{F}_{\mathcal{V}_S}}(\tilde{x})\right)\geq R\left(L\left(\mathcal{G}/\!\!/\mathcal{E}_{cs}\right),\tilde{x}\right). \tag{2.71}$$

Proof. Let $x=p_{\mathcal{F}_\pi}(\tilde{x})$ for $\tilde{x}\in\mathbb{R}^r$. The Rayleigh quotients of the Laplacian takes the form [11]

$$R\left(L(\mathcal{G}),x\right)=\frac{\sum\limits_{\{u,v\}\in\mathcal{E}(\mathcal{G})}(x_v-x_u)^2}{\sum\limits_{v\in\mathcal{V}(\mathcal{G})}x_v^2}. \tag{2.72}$$

Separating the edges to $\mathcal{E}_{cs}$ and $\mathcal{E}\backslash\mathcal{E}_{cs}$, the sum $\sum\limits_{\{u,v\}\in\mathcal{E}(\mathcal{G})}(x_v-x_u)^2$ can be written as

$$\sum_{\{u,v\}\in\mathcal{E}(\mathcal{G})}(x_v-x_u)^2=\sum_{\{u,v\}\in\mathcal{E}(\mathcal{G})\backslash\mathcal{E}_{cs}}(x_u-x_v)^2+\sum_{\{u,v\}\in\mathcal{E}_{cs}}(x_u-x_v)^2. \tag{2.73}$$

Therefore, if $x\in\mathcal{F}_\pi$ and $\{u,v\}\in\mathcal{E}_{cs}$ then $\sum\limits_{\{u,v\}\in\mathcal{E}_{cs}}(x_u-x_v)^2=0$ and

$$\sum_{\{u,v\}\in\mathcal{E}}(x_v-x_u)^2=\sum_{\{u,v\}\in\mathcal{E}\backslash\mathcal{E}_{cs}}(x_u-x_v)^2. \tag{2.74}$$

Since $\mathcal{G}/\!\!/\mathcal{E}_{cs}$ is edge-matching (Definition 2.11) there is one-to-one correspondence between $\mathcal{E}(\mathcal{G})\backslash\mathcal{E}_{cs}$ and $\mathcal{E}\left(\mathcal{G}/\!\!/\mathcal{E}_{cs}\right)$ (Proposition 2.3), and substituting the partition lifting $x=p_{\mathcal{F}_\pi}(\tilde{x})$ (Eq. (2.65)) we get

$$\sum_{\{u,v\}\in\mathcal{E}\backslash\mathcal{E}_{cs}}(x_u-x_v)^2=\sum_{\{u,v\}\in\mathcal{E}\left(\mathcal{G}/\!\!/\mathcal{E}_{cs}\right)}(\tilde{x}_u-\tilde{x}_v)^2. \tag{2.75}$$

Rearranging the sums $\sum_{v\in\mathcal{V}} x_v^2$ over the vertices of each partition cell and substituting the partition lifting $x = p_{\mathcal{F}_\pi}(\tilde{x})$ (Eq. (2.65)) we get,

$$\begin{aligned}\sum_{v\in\mathcal{V}(\mathcal{G})} x_v^2 &= \sum_{i=1}^{r}\sum_{v\in C_i(\pi)} x_v^2 \\ &= \sum_{u\in\mathcal{V}(\mathcal{G}/\!\!/\mathcal{E}_{cs})} \tilde{x}_u^2 \left|C_u(\pi)\right|, \end{aligned} \tag{2.76}$$

The Rayleigh quotients of the Laplacian is then

$$R\left(L(\mathcal{G}), p_{\mathcal{F}_\pi}(\tilde{x})\right) = \frac{\sum_{\{u,v\}\in\mathcal{E}(\mathcal{G}/\!\!/\mathcal{E}_{cs})} (\tilde{x}_u - \tilde{x}_v)^2}{\sum_{u\in\mathcal{V}(\mathcal{G}/\!\!/\mathcal{E}_{cs})} \tilde{x}_u^2 \left|C_u(\pi)\right|}, \tag{2.77}$$

and we have $|C_i(\pi)| \geq 1$, therefore,

$$\begin{aligned} R\left(L(\mathcal{G}), p_{\mathcal{F}_\pi}(\tilde{x})\right) &\leq \frac{\sum_{\{u,v\}\in\mathcal{E}(\mathcal{G}/\!\!/\mathcal{E}_{cs})} (\tilde{x}_u - \tilde{x}_v)^2}{\sum_{u\in\mathcal{V}(\mathcal{G}/\!\!/\mathcal{E}_{cs})} \tilde{x}_u^2} \\ &= R\left(L(\mathcal{G}/\!\!/\mathcal{E}_{cs}), \tilde{x}\right). \end{aligned} \tag{2.78}$$

If $\mathcal{G}/\!\!/\mathcal{E}_{cs}$ is node-removal equivalent (Definition 2.4) then by substituting the node-removal lifting $x = p_{\mathcal{F}_{\mathcal{V}_S}}(\tilde{x})$ (Eq. (2.65)) we get

$$\sum_{\{u,v\}\in\mathcal{E}\setminus\mathcal{E}_{cs}} (x_u - x_v)^2 = \sum_{\{u,v\}\in\mathcal{E}(\mathcal{G}/\!\!/\mathcal{E}_{cs})} (\tilde{x}_u - \tilde{x}_v)^2$$

and

$$\sum_{v\in\mathcal{V}(\mathcal{G})} x_v^2 = \sum_{u\in\mathcal{V}(\mathcal{G}/\!\!/\mathcal{E}_{cs})} \tilde{x}_u^2, \tag{2.79}$$

and we obtain that

$$\begin{aligned} R\left(L(\mathcal{G}), p_{\mathcal{F}_{\mathcal{V}_S}}(\tilde{x})\right) &\geq \frac{\sum_{\{u,v\}\in\mathcal{E}\setminus\mathcal{E}_{cs}} (x_v - x_u)^2}{\sum_{v\in\mathcal{V}(\mathcal{G})} x_v^2} \\ &= \frac{\sum_{\{u,v\}\in\mathcal{E}(\mathcal{G}/\!\!/\mathcal{E}_{cs})} (\tilde{x}_u - \tilde{x}_v)^2}{\sum_{u\in\mathcal{V}(\mathcal{G}/\!\!/\mathcal{E}_{cs})} \tilde{x}_u^2} \\ &= R\left(L(\mathcal{G}/\!\!/\mathcal{E}_{cs}), \tilde{x}\right). \end{aligned} \tag{2.80}$$

□

Proposition 2.17. *Consider a graph $\mathcal{G}$ and a cycle invariant contraction $\mathcal{G}/\!\!/\mathcal{E}_{cs}$ (Definition 2.5) with $\mathcal{E}_{cs} \in \Xi_{n-r}(\mathcal{G})$ for $r < n$. Then for $\tilde{x} \in \mathbb{R}^r$ we have*

$$R\left(\mathcal{L}\left(\mathcal{G}\right), p_{\mathcal{F}_\pi}\left(\tilde{x}\right)\right) \leq R\left(\mathcal{L}\left(\mathcal{G} /\!\!/ \mathcal{E}_{cs}\right), \tilde{x}\right), \tag{2.81}$$

and if $\mathcal{G} /\!\!/ \mathcal{E}_{cs}$ is a single edge contraction with $\mathcal{E}_{cs} = \varepsilon_{cs}$ then

$$R\left(\mathcal{L}\left(\mathcal{G}\right), p_{\tilde{\mathcal{F}}_\pi}\left(\tilde{x}\right)\right) \geq R\left(\mathcal{L}\left(\mathcal{G} /\!\!/ \varepsilon_{cs}\right), \tilde{x}\right). \tag{2.82}$$

Proof. The Rayleigh quotient of the normalized-Laplacian takes the form [11]

$$R\left(\mathcal{L}\left(\mathcal{G}\right), x\right) = \frac{\sum\limits_{\{u,v\}\in\mathcal{E}(\mathcal{G})} \left(x_v - x_u\right)^2}{\sum\limits_{v\in\mathcal{V}(\mathcal{G})} x_v^2 d_v\left(\mathcal{G}\right)}. \tag{2.83}$$

Since $\mathcal{G} /\!\!/ \mathcal{E}_{cs}$ is a cycle-invariant contraction it is edge-matching (Proposition 2.3) and there is one-to-one correspondence between $\mathcal{E}\left(\mathcal{G}\right)\setminus\mathcal{E}_{cs}$ and $\mathcal{E}\left(\mathcal{G} /\!\!/ \mathcal{E}_{cs}\right)$ (Proposition 2.3), and substituting the partition mapping $x = p_{\mathcal{F}_\pi}\left(\tilde{x}\right)$ for $\tilde{x} \in \mathbb{R}^r$ (Eq. (2.65)) we get as in Eq. (2.75)

$$\begin{aligned}\sum_{\{u,v\}\in\mathcal{E}(\mathcal{G})} \left(x_v - x_u\right)^2 &= \sum_{\{u,v\}\in\mathcal{E}\setminus\mathcal{E}_{cs}} \left(x_u - x_v\right)^2 \\ &= \sum_{\{u,v\}\in\mathcal{E}(\mathcal{G}/\!\!/\mathcal{E}_{cs})} \left(\tilde{x}_u - \tilde{x}_v\right)^2.\end{aligned} \tag{2.84}$$

Rearranging the sum $\sum\limits_{v\in\mathcal{V}(\mathcal{G})} x_v^2 d_v\left(\mathcal{G}\right)$ over the vertices of each partition cell and substituting the partition lifting $x = p_{\mathcal{F}_\pi}\left(\tilde{x}\right)$ (Eq. (2.65)) we get,

$$\begin{aligned}\sum_{v\in\mathcal{V}(\mathcal{G})} x_v^2 d_v\left(\mathcal{G}\right) &= \sum_{i=1}^{r} \sum_{v\in C_i(\pi)} x_v^2 d_v\left(\mathcal{G}\right), \\ &= \sum_{u\in\mathcal{V}(\mathcal{G}/\!\!/\mathcal{E}_{cs})} \tilde{x}_u^2 \left(\sum_{v\in C_u(\pi)} d_v\left(\mathcal{G}\right)\right).\end{aligned} \tag{2.85}$$

The graph contraction $\mathcal{G} /\!\!/ \mathcal{E}_{cs}$ is cycle-invariant, therefore, from Proposition 2.2 we have $d_u\left(\mathcal{G} /\!\!/ \mathcal{E}_{cs}\right) = \left(\sum\limits_{v\in C_u(\pi)} d_v\left(\mathcal{G}\right)\right) - 2\left(\left|C_u\left(\pi\right)\right| - 1\right)$, and

$$\sum_{v\in\mathcal{V}(\mathcal{G})} x_v^2 d_v\left(\mathcal{G}\right) = \sum_{u\in\mathcal{V}(\mathcal{G}/\!\!/\mathcal{E}_{cs})} \tilde{x}_u^2 \left[d_u\left(\mathcal{G} /\!\!/ \mathcal{E}_{cs}\right) + 2\left(\left|C_u\left(\pi\right)\right| - 1\right)\right]. \tag{2.86}$$

The Rayleigh quotients of the normalized-Laplacian is then

$$R\left(\mathcal{L}\left(\mathcal{G}\right), p_{\mathcal{F}_\pi}\left(\tilde{x}\right)\right) = \frac{\sum\limits_{\{u,v\}\in\mathcal{E}(\mathcal{G}/\!\!/\mathcal{E}_{cs})} \left(\tilde{x}_u - \tilde{x}_v\right)^2}{\sum\limits_{u\in\mathcal{V}(\mathcal{G}/\!\!/\mathcal{E}_{cs})} \tilde{x}_u^2 \left[d_u\left(\mathcal{G} /\!\!/ \mathcal{E}_{cs}\right) + 2\left(\left|C_u\left(\pi\right)\right| - 1\right)\right]}. \tag{2.87}$$

We have $|C_i(\pi)| \geq 1$ such that $2(|C_i(\pi)| - 1) \geq 0$, therefore,

$$R(\mathcal{L}(\mathcal{G}), p_{\mathcal{F}_\pi}(\tilde{x})) \leq \frac{\sum\limits_{\{u,v\}\in\mathcal{E}(\mathcal{G}/\!\!/\mathcal{E}_{cs})} (\tilde{x}_u - \tilde{x}_v)^2}{\sum\limits_{u\in\mathcal{V}(\mathcal{G}/\!\!/\mathcal{E}_{cs})} \tilde{x}_u^2 d_u(\mathcal{G}/\!\!/\mathcal{E}_{cs})} = R(\mathcal{L}(\mathcal{G}/\!\!/\mathcal{E}_{cs}), \tilde{x}). \quad (2.88)$$

Let $\mathcal{G}/\!\!/\varepsilon_{cs}$ be a cycle-invariant edge contraction with corresponding edge contraction partition $\pi \in \Pi_{n-1}(\mathcal{G})$. For an atom-contraction there is only one non-singlet cell, and without loss of generality we can choose it to be $C_{n-1}(\pi) = \{n-1, n\}$ such that the contracted edge is $\varepsilon_{cs} = \{x_{n-1}, x_n\}$, and

$$R(\mathcal{L}(\mathcal{G}), x) = \frac{\sum\limits_{\{u,v\}\in\mathcal{E}\setminus\mathcal{E}_{cs}} (x_u - x_v)^2 + (x_{n-1} - x_n)^2}{\sum\limits_{v=1}^{n-2} x_v^2 d_v(\mathcal{G}) + x_{n-1}^2 d_{n-1}(\mathcal{G}) + x_n^2 d_n(\mathcal{G})}. \quad (2.89)$$

For this atom-contraction we have the anti-partition space $\tilde{\mathcal{F}}_\pi = \{x \in \mathbb{R}^n \,|\, x_{n-1} = -x_n\}$ (Eq. (2.66)) and anti-partition mapping $p_{\tilde{\mathcal{F}}_\pi}(\tilde{x}) : \mathbb{R}^{n-1} \to \mathbb{R}^n$ is (Eq. (2.67))

$$\left[p_{\tilde{\mathcal{F}}_\pi}(\tilde{x})\right]_k = \begin{cases} \tilde{x}_k & k \leq n-1 \\ -\tilde{x}_{n-1} & k = n \end{cases}, \quad (2.90)$$

such that

$$R\left(\mathcal{L}(\mathcal{G}), p_{\tilde{\mathcal{F}}_\pi}(\tilde{x})\right) = \frac{\sum\limits_{\{u,v\}\in\mathcal{E}\setminus\mathcal{E}_{cs}} (\tilde{x}_u - \tilde{x}_v)^2 + 4\tilde{x}_{n-1}^2}{\sum\limits_{v=1}^{n-2} \tilde{x}_v^2 d_v(\mathcal{G}) + \tilde{x}_{n-1}^2 (d_{n-1}(\mathcal{G}) + d_n(\mathcal{G}))}. \quad (2.91)$$

There is one-to-one correspondence between $\mathcal{E}(\mathcal{G})\setminus\varepsilon_{cs}$ and $\mathcal{E}(\mathcal{G}/\!\!/\varepsilon_{cs})$ (Proposition 2.3), therefore, $\sum\limits_{\{u,v\}\in\mathcal{E}\setminus\mathcal{E}_{cs}} (\tilde{x}_u - \tilde{x}_v)^2 = \sum\limits_{\{u,v\}\in\mathcal{E}(\mathcal{G}/\!\!/\varepsilon_{cs})} (\tilde{x}_u - \tilde{x}_v)^2$, and from Proposition 2.2 we get

$$d_v(\mathcal{G}/\!\!/\varepsilon_{cs}) = \begin{cases} d_v(\mathcal{G}) & v \leq n-2 \\ d_{n-1}(\mathcal{G}) + d_n(\mathcal{G}) - 2 & v = n-1 \end{cases}, \quad (2.92)$$

such that

$$\begin{aligned} R\left(\mathcal{L}(\mathcal{G}), p_{\tilde{\mathcal{F}}_\pi}(\tilde{x})\right) &= \frac{\sum\limits_{\{u,v\}\in\mathcal{E}(\mathcal{G}/\!\!/\varepsilon_{cs})} (\tilde{x}_u - \tilde{x}_v)^2 + 4\tilde{x}_{n-1}^2}{\sum\limits_{v\in\mathcal{V}(\mathcal{G}/\!\!/\varepsilon_{cs})} \tilde{x}_v^2 d_v(\mathcal{G}/\!\!/\varepsilon_{cs}) + 2\tilde{x}_{n-1}^2} \\ &= R(\mathcal{L}(\mathcal{G}/\!\!/\varepsilon_{cs}), \tilde{x}) \frac{1 + \frac{4\tilde{x}_{n-1}^2}{\sum_{\{u,v\}\in\mathcal{E}(\mathcal{G}/\!\!/\varepsilon_{cs})} (\tilde{x}_u - \tilde{x}_v)^2}}{1 + \frac{2\tilde{x}_{n-1}^2}{\sum_{v\in\mathcal{V}(\mathcal{G}/\!\!/\varepsilon_{cs})} \tilde{x}_v^2 d_v(\mathcal{G}/\!\!/\varepsilon_{cs})}}. \end{aligned} \quad (2.93)$$

For any $\mathcal{G}$ we have $R\left(\mathcal{L}\left(\mathcal{G}\right),x\right)\leq 2$ [14], therefore,

$$\sum_{\{u,v\}\in\mathcal{E}(\mathcal{G}/\!\!/\varepsilon_{cs})}\left(\tilde{x}_u-\tilde{x}_v\right)^2\leq 2\sum_{v\in\mathcal{V}(\mathcal{G}/\!\!/\varepsilon_{cs})}\tilde{x}_v^2 d_v\left(\mathcal{G}/\!\!/\varepsilon_{cs}\right) \tag{2.94}$$

and

$$\frac{1+\frac{4\tilde{x}_{n-1}^2}{\sum_{\{u,v\}\in\mathcal{E}(\mathcal{G}/\!\!/\varepsilon_{cs})}\left(\tilde{x}_u-\tilde{x}_v\right)^2}}{1+\frac{2\tilde{x}_{n-1}^2}{\sum_{v\in\mathcal{V}(\mathcal{G}/\!\!/\varepsilon_{cs})}\tilde{x}_v^2 d_v\left(\mathcal{G}/\!\!/\varepsilon_{cs}\right)}}\geq 1, \tag{2.95}$$

and we obtain that $R\left(\mathcal{L}\left(\mathcal{G}\right),p_{\tilde{\mathcal{F}}_\pi}\left(\tilde{x}\right)\right)\geq R\left(\mathcal{L}\left(\mathcal{G}/\!\!/\varepsilon_{cs}\right),\tilde{x}\right)$ for any cycle invariant single edge contraction. □

The only graph contraction interlacing result known to the authors has been presented by Chen et. al. [11]:

Theorem 2.6 (normalized-Laplacian interlacing cycle-invariant contraction)**.** *Consider a graph $\mathcal{G}$ and two vetices $u,v\in\mathcal{V}\left(\mathcal{G}\right)$ with corresponding partition $\pi\in\Pi_{n-1}\left(\mathcal{G}\right)$ with only one non-singlet cell $C_{n-1}\left(\pi\right)=\{u,v\}$. Then if $\mathcal{N}_u\left(\mathcal{G}\right)\cap\{\mathcal{N}_v\left(\mathcal{G}\right)\cup v\}=\varnothing$ the atom contraction is normalized-Laplacian interlacing, i.e., $\mathcal{G}/\!\!/\pi\propto_{\mathcal{L}}\mathcal{G}$.*

Proof. The proof is given in [11] and is based on a sequence of min-max ineuqalities and the Courant–Fischer theorem (Theorem 2.4). In the perspective of this work, Theorem 2.6 can be seen as a specific case of Theorem 2.5 as follows: Let $\mathcal{G}/\!\!/\pi$ be an atom contraction with $C_{n-1}\left(\pi\right)=\{u,v\}$ and $\mathcal{N}_u\left(\mathcal{G}\right)\cap\{\mathcal{N}_v\left(\mathcal{G}\right)\cup v\}=\varnothing$. Without loss of generality we can label the vertices such that $C_{n-1}\left(\pi\right)=\{n-1,n\}$. Similar to Proposition 2.17 it can be shown that $R\left(\mathcal{L}\left(\mathcal{G}\right),p_{\mathcal{F}_\pi}\left(x\right)\right)\leq R\left(\mathcal{L}\left(\mathcal{G}/\!\!/\pi\right),x\right)$ and $R\left(\mathcal{L}\left(\mathcal{G}\right),p_{\tilde{\mathcal{F}}_\pi}\left(\tilde{x}\right)\right)\geq R\left(L\left(\mathcal{G}/\!\!/\pi\right),x\right)$, therefore, from Theorem 2.5 with $\mathcal{A}\equiv\mathcal{F}_\pi$ and $\mathcal{B}\equiv\tilde{\mathcal{F}}_\pi$ we then get that $\mathcal{G}/\!\!/\pi\propto_{\mathcal{L}}\mathcal{G}$. □

In this study, based on Theorem 2.5, we derive two interlacing theorems, Laplacian interlacing for node-removal equivalent edge-matching contractions (Theorem 2.7) and normalized Laplacian interlacing for cycle-invariant contractions (Theorem 2.6).

Theorem 2.7 (Laplacian interlacing node-removal equivalent contraction)**.** *Consider a graph $\mathcal{G}$ and an edge contraction set $\mathcal{E}_{cs}\in\Xi_{n-r}\left(\mathcal{G}\right)$ for $r<n$. If $\mathcal{G}/\!\!/\mathcal{E}_{cs}$ is edge-matching (Definition 2.11) and node-removal equivalent (Definition 2.4) then $\mathcal{G}/\!\!/\mathcal{E}_{cs}\propto_L\mathcal{G}$.*

Proof. The contraction $\mathcal{G}/\!\!/\mathcal{E}_{cs}$ is edge-matching and node-removal equivalent such that from Proposition 2.16 we have $R\left(L\left(\mathcal{G}\right),p_{\mathcal{F}_\pi}\left(x\right)\right)\leq R\left(L\left(\mathcal{G}/\!\!/\mathcal{E}_{cs}\right),x\right)$ and $R\left(L\left(\mathcal{G}\right),p_{\mathcal{F}_{\mathcal{V}_S}}\left(x\right)\right)\geq R\left(L\left(\mathcal{G}/\!\!/\mathcal{E}_{cs}\right),x\right)$. Therefore, from Theorem 2.5 with $\mathcal{A}\equiv\mathcal{F}_\pi$ and $\mathcal{B}\equiv\mathcal{F}_{\mathcal{V}}$ we then get that $\mathcal{G}/\!\!/\mathcal{E}_{cs}\propto_L\mathcal{G}$. □

Theorem 2.8 (normalized-Laplacian interlacing cycle-invariant contraction)**.** *Consider a graph $\mathcal{G}$ and an edge contraction set $\mathcal{E}_{cs} \in \Xi_{n-r}(\mathcal{G})$ for $r < n$. Then if $\mathcal{G} /\!\!/ \mathcal{E}_{cs}$ is cycle-invariant (Definition 2.4), $\mathcal{G} /\!\!/ \mathcal{E}_{cs} \propto_{\mathcal{L}} \mathcal{G}$.*

Proof. The graph contraction can be performed by a sequence of atom-contractions (Corollary 2.1), therefore, it is sufficient to show that the interlacing property holds for a single edge-contraction, i.e., $\mathcal{G} /\!\!/ \epsilon_{cs} \propto_{\mathcal{L}} \mathcal{G}$ where ϵ_{cs} is a single contracted edge. The interlacing of the sequence will then follow from Proposition 2.14. Let $\mathcal{G} /\!\!/ \varepsilon_{cs}$ be a cycle-invariant edge contraction with corresponding edge contraction partition $\pi \in \Pi_{n-1}(\mathcal{G})$. Without loss of generality we can label the vertices such that the contracted edge is $\varepsilon_{cs} = \{x_{n-1}, x_n\}$, and the anti-partition space is $\tilde{\mathcal{F}}_\pi(\tilde{x}) = \{x \in \mathbb{R}^n \,|x_{n-1} = -x_n\}$ (Eq. (2.90)). From Proposition 2.17 we have $R(\mathcal{L}(\mathcal{G}), p_{\mathcal{F}_\pi}(x)) \leq R(\mathcal{L}(\mathcal{G} /\!\!/ \epsilon_{cs}), x)$ and $R\left(\mathcal{L}(\mathcal{G}), p_{\tilde{\mathcal{F}}_\pi}(\tilde{x})\right) \geq R(L(\mathcal{G} /\!\!/ \varepsilon_{cs}), x)$, therefore, from Theorem 2.5 with $\mathcal{A} \equiv \mathcal{F}_\pi$ and $\mathcal{B} \equiv \tilde{\mathcal{F}}_\pi$ we then get that $\mathcal{G} /\!\!/ \epsilon_{cs} \propto_{\mathcal{L}} \mathcal{G}$. By performing the contraction sequence (Proposition 2.14) we get $\mathcal{G} /\!\!/ \mathcal{E}_{cs} \propto_{\mathcal{L}} \mathcal{G}$. □

Corollary 2.4. *Consider a tree $\mathcal{T} = (\mathcal{V}, \mathcal{E})$ of order n, and its contraction $\mathcal{T} /\!\!/ \mathcal{E}_{cs}$ for any $\mathcal{E}_{cs} \in \Xi_{n-r}(\mathcal{T})$. Then $\mathcal{T} /\!\!/ \mathcal{E}_{cs} \propto_{\mathcal{L}} \mathcal{T}$.*

Proof. The contraction $\mathcal{T} /\!\!/ \mathcal{E}_{cs}$ is cycle-invariant for any $\mathcal{E}_{cs} \in \Xi_{n-r}(\mathcal{T})$, therefore, from Theorem 2.8 we obtain that $\mathcal{T} /\!\!/ \mathcal{E}_{cs} \propto_{\mathcal{L}} \mathcal{T}$. □

Theorem 2.7 and Theorem 2.8 allow us to try and solve the interlacing graph contraction problem (Problem 2.2) for normalized Laplacian and Laplacian interlacing by finding a cycle-invariant contraction (Problem 2.3) or a node-removal equivalent and edge matching contraction (Problem 2.4) respectively.

Problem 2.3 (Cycle-invariant contraction)**.** *For a graph $\mathcal{G}$ and a given reduction order $r < n$, find $\mathcal{E}_{cs} \in \Xi_{n-r}(\mathcal{G})$ such that $\mathcal{G} /\!\!/ \mathcal{E}_{cs}$ is cycle-invariant (Definition 2.5).*

Problem 2.4 (Node-removal equivalent contraction)**.** *For a graph $\mathcal{G}$ and a given reduction order $r < n$, find $\mathcal{E}_{cs} \in \Xi_{n-r}(\mathcal{G})$ such that $\mathcal{G} /\!\!/ \mathcal{E}_{cs}$ is node-removal equivalent (Definition 2.4) and edge-matching (Definition 2.11).*

From Proposition 2.18, we can obtain a cycle-invariant contraction, if exists, from the zero rows of the Tucker representation.

Proposition 2.18. *Consider a graph $\mathcal{G}$ and an edge contraction set $\mathcal{E}_{cs} \in \Xi_{n-r}(\mathcal{G})$ for $r < n$, and let $\mathcal{T} \in \mathbb{T}(\mathcal{G})$. Then $\mathcal{G} /\!\!/ \mathcal{E}_{cs}$ is cycle-invariant (Definition 2.5) if and only if $\mathcal{E}_{cs} \subseteq \mathcal{E}(\mathcal{T})$ and the corresponding rows of $T_{(\mathcal{T},\mathcal{C})}$ are all zeros.*

Proof. If $\mathcal{G} /\!\!/ \mathcal{E}_{cs}$ is cycle-invariant then from Definition 2.5 the edges in $\mathcal{E}_{cs}$ are not part of any cycle of $\mathcal{G}$, therefore, $\mathcal{E}_{cs} \subseteq \mathcal{E}(\mathcal{T})$ for any $\mathcal{T} \in \mathbb{T}(\mathcal{G})$. If $\epsilon \in \mathcal{E}(\mathcal{T})$ is not part of any cycle in $\mathcal{G}$ then form the Tucker representation (Definition 2.20) we get that the corresponding row of $T_{(\mathcal{T},\mathcal{C})}$ is all zeros.

If $\mathcal{E}_{cs} \subseteq \mathcal{E}(\mathcal{T})$ and the corresponding rows of $T_{(\mathcal{T},\mathcal{C})}$ are all zeros, then the edges in $\mathcal{E}_{cs}$ are not part of any cycle in $\mathcal{G}$, such that the tree-based contraction (Definition 2.12) $\mathcal{G} /\!\!/ \mathcal{E}_{cs}$ is cycle-invariant. □

A Tucker representation $T_{(\mathcal{T},\mathcal{C})}$ can be calculated by finding a spanning tree $\mathcal{T} \in \mathbb{T}(\mathcal{G})$ and then finding the path in $\mathcal{T}$ between the end-nodes of each edge of $\mathcal{C}(\mathcal{T})$ as described in Algorithm 2.1. Each path finding operation, e.g., with a depth-first search, is of complexity $\mathcal{O}(n)$, and since $\mathcal{O}(|\mathcal{E}(\mathcal{C})|) = \mathcal{O}(|\mathcal{E}(\mathcal{G})|)$ the overall complexity of constructing $T_{(\mathcal{T},\mathcal{C})}$ is $\mathcal{O}(mn)$, where $m = |\mathcal{E}(\mathcal{G})|$. Therefore, the cycle-invariant contraction algorithm (Algorithm 2.1) is of complexity $\mathcal{O}(mn)$.

From Proposition 2.4, we can obtain a node-removal equivalent and edge matching contraction, if exists, by first finding for all vertices of $\mathcal{G}$ the connected components partition $\pi_{cc}(\mathcal{G}\backslash v)$ and then constructing $\mathcal{E}_{cs}$ by choosing from all partitions $\{\pi_{cc}(\mathcal{G}\backslash v)\}_{v=1}^{n}$ a subset of cells with a total number of $n-r$ unique nodes (Algorithm 2.2). Each connected component finding operation, e.g., with a depth-first search, is of complexity $\mathcal{O}(n+m)$, and repeated n times, the overall complexity of the algorithm is $\mathcal{O}\left(n^2+nm\right)$.

Algorithm 2.1 Cycle-invariant contraction algorithm

Input: graph $\mathcal{G}$ of order n**,** required reduction order r

1. **Find** a spanning tree $\mathcal{T} \in \mathbb{T}(\mathcal{G})$ and the co-tree $\mathcal{C}(\mathcal{T})$.
2. **Calculate** the tucker representation $T_{(\mathcal{T},\mathcal{C})}$ (Definition 2.20).
3. **Choose** $n-r$ cycle-invariant edges from the zero rows of $T_{(\mathcal{T},\mathcal{C})}$ and obtain $\mathcal{E}_{cs}$.

Output: $\mathcal{G}_r = \mathcal{G} /\!\!/ \mathcal{E}_{cs}$

Algorithm 2.2 Node-removal equivalent contraction algorithm

Input: graph $\mathcal{G}$ of order n**,** required reduction order r

1. **For** $v \in \mathcal{V}(\mathcal{G})$**: Calculate** $\pi_{cc}(\mathcal{G}\backslash v)$, the connected components partition of $\mathcal{G}\backslash v$.
2. **Choose** a subset of cells $\mathcal{S} \subseteq \{\pi_{cc}(\mathcal{G}\backslash v)\}_{v=1}^{n}$ with a total number of $n-r$ unique nodes**.**
3. **Construct** $\mathcal{E}_{cs} = \cup_{C_v \in \mathcal{S}} \mathcal{E}(\mathcal{G}[C_v \cup v])$.

Output: $\mathcal{G}_r = \mathcal{G} /\!\!/ \mathcal{E}_{cs}$

2.5 Case Studies

As a small-scale normalized Laplacian interlacing example, we consider a graph of order 6 presented in Figure 2.7, and we require the reduced graph to be of or-

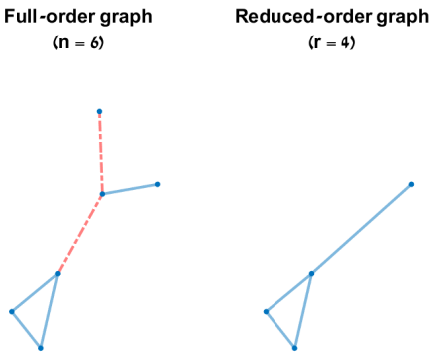

Figure 2.7: Small scale normalized-Laplacian interlacing graph contraction (contracted edges dashed-red).

der $r = 4$. A cycle-invariant graph contraction is then performed with two edges (Figure 2.7). The resulting reduced graph (Figure 2.7) has normalized-Laplacian spectra $\{\lambda_k(\mathcal{L}(\mathcal{G}_r))\}_{k=1}^{r}$ given in Figure 2.8 with the upper and lower interlacing bounds $\lambda_k(\mathcal{L}(\mathcal{G}))$ and $\lambda_{n-r+k}(\mathcal{L}(\mathcal{G}))$. Since $\mathcal{G} /\!\!/ \mathcal{E}_{cs}$ is cycle-invariant, then as according to Theorem 2.8, we get $\mathcal{G} /\!\!/ \mathcal{E}_{cs} \propto_{\mathcal{L}} \mathcal{G}$ and the reduced-order spectra is within the interlacing bounds (Figure 2.8).

As a small-scale Laplacian interlacing example, we consider a graph of order 6 presented in Figure 2.9 and require the reduction to be of order $r = 4$. For this case the only node-removal equivalent and edge-matching contraction is with the three edges shown in Figure 2.9. The resulting reduced graph (Figure 2.9) has Laplacian spectra given in Figure 2.10 with the interlacing bounds $\lambda_k(L(\mathcal{G}))$ and $\lambda_{n-r+k}(L(\mathcal{G}))$. Since $\mathcal{G} /\!\!/ \mathcal{E}_{cs}$ is node-removal equivalent and edge-matching, then as according to Theorem 2.7 we get $\mathcal{G} /\!\!/ \mathcal{E}_{cs} \propto_{L} \mathcal{G}$ and the reduced-order Laplacian spectra is within the interlacing bounds (Figure 2.10). Notice that for this case there is no cycle-invariant contraction, and for the same choice of $\mathcal{E}_{cs}$ (Figure 2.9) the reduced-order normalized-Laplacian does not interlace with the full-order normalized-Laplacian as $\lambda_4(\mathcal{L}(\mathcal{G}_r)) > \lambda_6(\mathcal{L}(\mathcal{G}))$ (Figure 2.11).

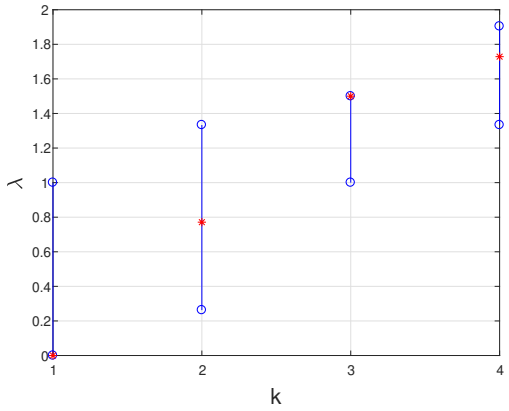

Figure 2.8: Reduced-order normalized-Laplacian spectra (stared-red) and interlacing bounds (circled-blue).

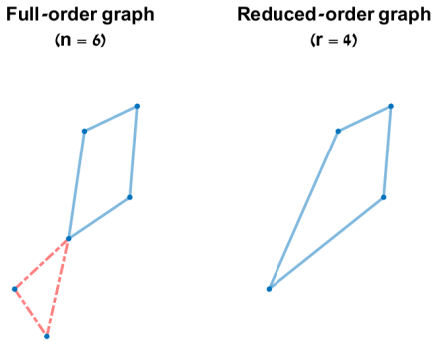

Figure 2.9: Small scale Laplacian interlacing graph contraction (contracted edges dashed-red).

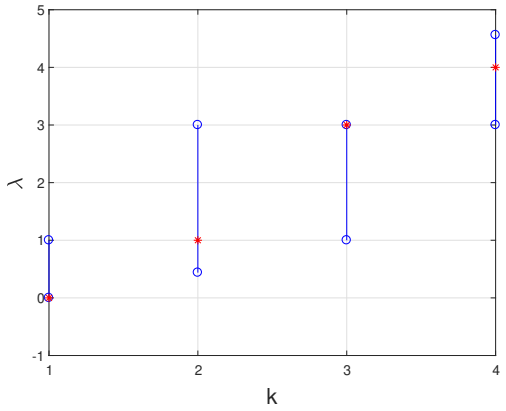

Figure 2.10: Reduced-order Laplacian spectra (stared-red) and interlacing bounds (circled-blue).

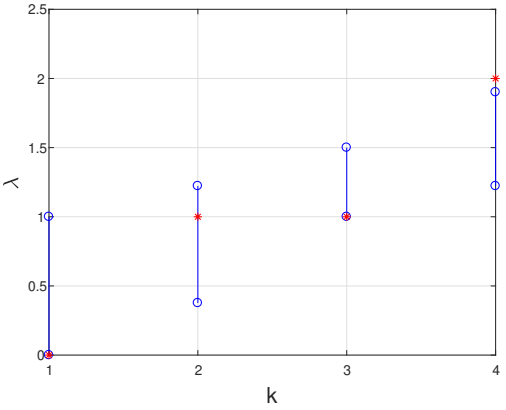

Figure 2.11: Reduced-order normalized-Laplacian spectra (stared-red) and interlacing bounds (circled-blue).

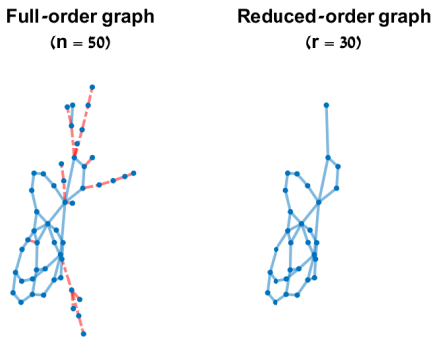

Figure 2.12: Large scale normalized-Laplacian interlacing graph contraction (contracted edges dashed-red).

As a larger and more complicated example, a random tree of order 50 is created and 10 cycle-completing edges are randomly added to it resulting in a graph of order 50 with 59 edges (Figure 2.12). The required reduction order is $r = 30$. Using the cycle-invariant contraction algorithm (Algorithm 2.1) an edge-contraction set $\mathcal{E}_{cs}$ with $n - r = 20$ edges is chosen from the edges of $\mathcal{G}$ (Figure 2.12), and the graph contraction is performed. As according to Theorem 2.8, the resulting reduced-order graph $\mathcal{G}_r = \mathcal{G} /\!\!/ \mathcal{E}_{cs}$ is normalized-Laplacian interlacing with $\mathcal{G}$ and the reduced spectra is within the interlacing bounds (Figure 2.13).

Using the node-removal equivalent contraction algorithm (Algorithm 2.2) a different edge-contraction set $\mathcal{E}_{cs}$ with $n-r = 20$ edges is chosen from the edges of $\mathcal{G}$ (Figure 2.14), and the graph contraction is performed. As according to Theorem 2.7, the resulting reduced order graph $\mathcal{G}_r = \mathcal{G} /\!\!/ \mathcal{E}_{cs}$ (Figure 2.14) is Laplacian interlacing with $\mathcal{G}$ and the reduced spectra is within the interlacing bounds (Figure 2.15).

2.6 Conclusions

The derived general reduced graph interlacing theorem (Theorem 2.5) extends the seminal min-max theorems and can be utilized as a spectral graph analysis tool. The found sub-classes of interlacing edge-matching contractions are a

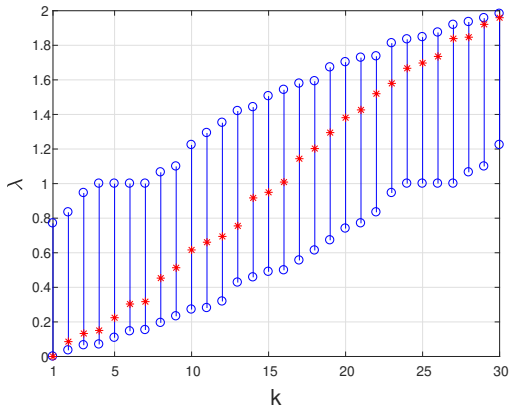

Figure 2.13: Reduced-order normalized-Laplacian spectra (stared-red) and interlacing bounds (circled-blue).

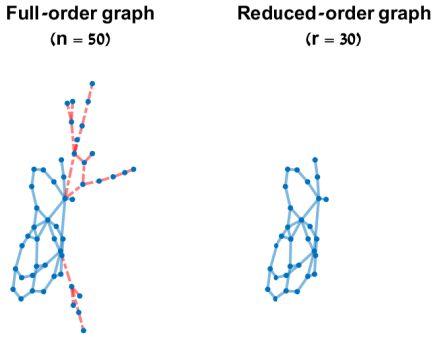

Figure 2.14: Large scale Laplacian interlacing graph contraction.

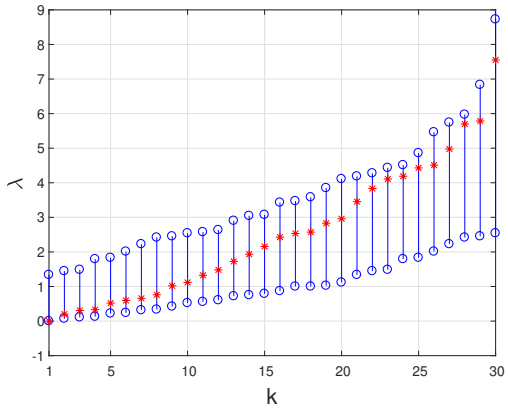

Figure 2.15: Reduced-order Laplacian spectra (stared-red) and interlacing bounds (circled-blue).

substantial contribution to the limited examples of interlacing graph contractions previously known. The feasibility of the cycle-invariant and node-removal equivalent problems requires further study. The edge-induced partitions and their usage for edge-based contractions will be found useful for the construction of an efficient graph-based model reduction method in the following chapters.

Chapter 3

Product Form of Projection-Based Model Reduction

Orthogonal projection-based reduced order models (PROM) are the output of widely-used model reduction methods. In this chapter, we reexamine the well known orthogonal PROMs and their realizations. A novel product form is derived for the reduction error system of these reduced models, and it is shown that any such PROM can be obtained from a sequence of 1-dimensional projection reductions. Investigating the error system product form, we then define interface-invariant PROMs, model order reductions with projection-invariant input and output matrices, and it is shown that for such PROMs the error product systems are strictly proper. Furthermore, exploiting this structure, an analytic $\mathcal{H}_\infty$ reduction error bound is obtained and an $\mathcal{H}_\infty$ bound optimization problem is defined.

3.1 Introduction

The error system of PROMs is naturally described with an augmented system realization, allowing the PROM reduction error to be evaluated with standard system performance metrics, such as the $\mathcal{H}_\infty$ and $\mathcal{H}_2$ norms. However, this error system realization usually does not provide any analytic insight, and various transformation techniques were derived to bring it to more useful forms. These include an upper triangular block structure [34], allowing derivation of analytical bounds. In this study we show that any orthogonal PROM error system can be presented as a product of three LTI systems, capturing the reduction effect of the input to state, state to output, and the internal dynamical structure. Investigating this error system product form, an analytic $\mathcal{H}_\infty$ reduction error bound is obtained and an $\mathcal{H}_\infty$ bound optimization problem is defined as a

relaxation of the optimal PROM problem. Furthermore, it is shown that any orthogonal PROM can be obtained from a sequence of singleton projections, projections from dimension n to $n-1$.

Of particular interest in this work are *interface invariant* PROMs (IIPROMs). These are reduced models that maintain the input-output structure of the full order model. It is shown that for IIPROMs the error product systems are strictly proper. IIPROMs are natural to multi-agent systems where a subset of agents serve as input and output ports of the network. These I/O ports may be interconnected with an external controller and it is required, therefore, that any reduced model preserves this interface structure. For this purpose, we propose an edge-based graph contraction method and utilize it in a tree-based greedy-edge heuristic to solve the PROM $\mathcal{H}_\infty$ bound optimization problem. We then apply an this graph contraction algorithm to obtain suboptimal $\mathcal{H}_\infty$ IIPROMs of Laplacian consensus systems.

The remaining sections of this chapter are as follows. In Section 3.2, we formulate the optimal orthogonal PROM and IIPROM problems. In Section 3.3.1, the product form of orthogonal PROMs is derived. In Section 3.3, the $\mathcal{H}_\infty$ error bound is derived for PROMs and PROM sequences. Section 4 presents model reduction of multi-agent systems by graph contractions and the greedy-edge optimization method, and Section 3.5 provides concluding remarks.

3.2 Problem Formulation

A widely used family of reduction methods are *projection-based reductions*. Given a system with realization $\Sigma := (A, B, C, D)$ of order n, a *projection-based reduced order model* (PROM) is a system $\Sigma_r := \left(P^\top AV, P^\top B, CV, D\right)$, for any two matrices $P, V \in \mathbb{R}^{n\times r}$ such that $P^\top V = I_r$ [24]. If in addition $P = V$, the PROM is termed *orthogonal*, i.e.,

$$\Sigma_r\left(\Sigma, P\right) := \left(P^\top AP, P^\top B, CP, D\right). \tag{3.1}$$

Hereafter, all PROMs referred to in this study are orthogonal.

In this work we will examine a special class of PROMs that we term *interface-invariant PROMs* . These are reduced models that maintain the input-output structure of the full order model under the projection operation. Such PROMs are required, for example, for the reduction of controlled MAS (4.2) where the interface agent structure is maintained in the reduced model. We will also show that IIPROMs arise naturally when examining the error system (1.8) of PROMs. We now define formally the notion of an interface-invariant PROM (IIPROM).

Definition 3.1 (IIPROM)**.** *Given a system with realization $\Sigma := (A, B, C, D)$, an IIPROM of Σ is any PROM $\Sigma_r\left(\Sigma, P\right) := \left(P^\top AP, P^\top B, CP, D\right)$ such that $C = CPP^\top$ and $B = PP^\top B$.*

With the above notions in place, we can now formally state the optimal IIPROM problem.

Problem 3.1 (optimal IIPROM)**.** *Consider a stable proper system of order n with realization $\Sigma := (A, B, C, D)$. Find $P \in \mathbb{R}^{n\times r}$ with $P^\top P = I_r$ such that the PROM $\Sigma_r\,(\Sigma, P)$ (3.1) minimizes the $\mathcal{H}_\infty$-norm of the reduction error system (1.8) and is interface-invariant, i.e.,*

$$\begin{aligned} \min_{P\in\mathbb{R}^{n\times r}} \|\Sigma_e\|_{\mathcal{H}_\infty} \\ s.t.\ P^\top P = I_r \\ C = CPP^\top \\ B = PP^\top B. \end{aligned} \tag{3.2}$$

The constraints $P^\top P = I_r$, $C = CPP^\top$ and $B = PP^\top B$ make Problem 3.1 non-convex, and there is, in general, no closed-form or computationally efficient solution. In the following section we investigate the error system structure of IIPROMs and derive an IIPROM $\mathcal{H}_\infty$ error upper bound. This bound will then be utilised for obtaining suboptimal solutions of Problem 3.1.

3.3 The PROM $\mathcal{H}_\infty$ Bound

The error system of PROMs can be described with the augmented system realization (1.8) of dimension $\dim(x) + \dim(x_r)$. In the following section we show that any orthogonal PROM error system can be presented as a product of three appropriately defined LTI systems, two of dimension $\dim(x_r)$ and the third of dimension $\dim(x)$. This product form is then applied for the derivation of a PROM $\mathcal{H}_\infty$ error bound.

3.3.1 The Product Form of Orthogonal PROMs

The following theorem presents a PROM error system product form, and this new error system structure will allow us to derive an $\mathcal{H}_\infty$ bound for the PROM error system.

Theorem 3.1 (PROM error system product form)**.** *Let $\Sigma := (A, B, C, D)$, and consider a PROM $\Sigma_r(\Sigma, P)$. Then the error reduction system $\Sigma_e(\Sigma, P) = \Sigma_r(\Sigma, P) - \Sigma$ has the TFM*

$$\hat{\Sigma}_e(\Sigma, P) = C\Phi^{-1}Q(Q^\top\Phi^{-1}Q)^{-1}Q^\top\Phi^{-1}B, \tag{3.3}$$

where $\Phi \triangleq sI_n - A$, and Q is any projection such that $Q^\top P = 0$ and $Q^\top Q = I_{n-r}$. Furthermore, Σ_e can be expressed as the product of three systems,

$$\Sigma_e(\Sigma, P) = \Theta(\Sigma, P)\Delta(\Sigma, P)\Gamma(\Sigma, P), \tag{3.4}$$

with realizations

$$\Theta(\Sigma, P) := (A_{PP}, A_{PQ}, CP, CQ), \tag{3.5}$$

$$\Gamma(\Sigma, P) := (A_{PP}, P^\top B, A_{QP}, Q^\top B), \tag{3.6}$$

$$\Delta(\Sigma, P) := (A, Q, Q^\top, 0_{p\times m}), \tag{3.7}$$

where $A_{PP} \triangleq P^\top AP$, $A_{PQ} \triangleq P^\top AQ$ *and* $A_{QP} \triangleq Q^\top AP$.

The proof of Theorem 3.1 is given in Section 3.4.

Investigating the error systems $\Theta(\Sigma, P)$ and $\Gamma(\Sigma, P)$ we observe that if the PROM is an IIPROM, then its realization is strictly-proper.

Corollary 3.1 (IIPROM error system)**.** *If* $\Sigma_r(\Sigma, P) := \left(P^\top AP, P^\top B, CP, D\right)$ *is an IIPROM, then* $\Theta(\Sigma, P)$ *in (3.5) and* $\Gamma(\Sigma, P)$ *in (3.6) are strictly-proper with realizations*

$$\Theta(\Sigma, P) := \left(A_{PP}, A_{PQ}, CP, 0_{p\times m}\right), \tag{3.8}$$

and

$$\Gamma(\Sigma, P) := \left(A_{PP}, P^\top B, A_{QP}, 0_{p\times m}\right). \tag{3.9}$$

Proof. Since $\Sigma_r(\Sigma, P)$ is an IIPROM, from Definition 3.1 we have $C = CPP^\top$ and $B = PP^\top B$. From $Q^\top P = 0$ and $Q^\top Q = I_{n-r}$ we get $PP^\top = I_n - Q^\top Q$ such that $C = C\left(I_n - QQ^\top\right)$ and $B = \left(I_n - QQ^\top\right)B$, therefore, $CQ = 0$ and $Q^\top B = 0$ obtaining our desired result. □

3.3.2 The PROM Error System Bound

The PROM error system is the product of three systems (3.4), and we will make use of this form to derive an $\mathcal{H}_\infty$ reduction error upper bound.

Proposition 3.1 (PROM error bound)**.** *Let* $\Sigma := (A, B, C, D)$ *with A Hurwitz, and consider a PROM* $\Sigma_r(\Sigma, P) := \left(P^\top AP, P^\top B, CP, D\right)$. *Then the* $\mathcal{H}_\infty$ *norm of the error reduction system (1.8) is bounded as*

$$\|\Sigma_e(\Sigma, P)\|_{\mathcal{H}_\infty} \le b(\Sigma, P),$$

where

$$b(\Sigma, P) = \|\Theta(\Sigma, P)\|_{\mathcal{H}_\infty}\|\Delta(\Sigma, P)\|_{\mathcal{H}_\infty}\|\Gamma(\Sigma, P)\|_{\mathcal{H}_\infty}. \tag{3.10}$$

Proof. The proof follows directly from the submultiplicative of the $\mathcal{H}_\infty$-norm applied to (3.4). □

For linear systems (1.1) with a symmetric matrix A, such as the controlled-consensus multi-agent systems studied in Section 4, we can simplify the calculation of the bound (3.10). The following Lemma, proven in [43, Appendix A] will be used for the derivation of Corollary 3.2, presenting this simplified bound.

Lemma 3.1 ([43])**.** *Let* A *be symmetric and Hurwitz. Then for any* B *of appropriate dimension,*

$$\|B^\top (sI - A)^{-1} B\|_{\mathcal{H}_\infty} = \|B^\top A^{-1} B\|_2. \tag{3.11}$$

Symmetric passive systems, as in Lemma 3.1, are a particular case of positive-real rational functions which have been extensively studied for model reduction [52, 60]. The following corollary provides a new bound for such systems.

Corollary 3.2. *Let $\Sigma := (A, B, C, D)$ with A symmetric and Hurwitz, and consider a PROM $\Sigma_r(\Sigma, P) := \left(P^\top AP, P^\top B, CP, D\right)$. Then the $\mathcal{H}_\infty$ norm of the error reduction system (1.8) is bounded as*

$$\|\Sigma_e(\Sigma, P)\|_{\mathcal{H}_\infty} \leq b(\Sigma, P),$$

where

$$b(\Sigma, P) = \|\Theta(\Sigma, P)\|_{\mathcal{H}_\infty} \|\Gamma(\Sigma, P)\|_{\mathcal{H}_\infty} \|Q^\top A^{-1} Q\|_2. \tag{3.12}$$

Proof. Applying Lemma 3.1, we get $\|\Delta(\Sigma, P)\|_{\mathcal{H}_\infty} = \|Q^\top A^{-1} Q\|_2$ and substituting it in (3.10) we obtain (3.12). □

The PROM error bound is the product of the $\mathcal{H}_\infty$-norms of the three LTI systems (3.5)-(3.7) constructing the error system. We observe that with the unitary transformation $\tilde{\Sigma} := \left(U^\top AU, U^\top B, CU, D\right)$ with $U = \begin{bmatrix} P & Q \end{bmatrix}$, the full-order system $\tilde{\Sigma}$ has a realization

$$\tilde{\Sigma} := \left(\left[\begin{array}{c|c} A_{PP} & A_{PQ} \\ \hline A_{QP} & A_{QQ} \end{array}\right], \left[\begin{array}{c} P^T B \\ \hline Q^T B \end{array}\right], \left[\begin{array}{c|c} CP & CQ \end{array}\right], D \right),$$

where the PROM is

$$\Sigma_r(\Sigma, P) := \left(A_{PP}, P^\top B, CP, D\right),$$

and the block-diagram of $\Sigma_r - \tilde{\Sigma}$ in additive form is shown in Figure 3.1a. If A_{PQ}, A_{QP}, A_{QQ}, CQ and $Q^T B$ are all zeros, then $\Sigma_r - \Sigma = 0$ (and in this case $\Sigma := (A, B, C, D)$ is not a minimal realization). If the reduction error is not zero, and each of the three product systems implicitly captures the contribution to the reduction error of these parts of $\tilde{\Sigma}$ left out in Σ_r. The map $\Theta(\Sigma, P)$ captures A_{PQ} and CQ, $\Gamma(\Sigma, P)$ captures A_{QP} and $Q^T B$ and $\Delta(\Sigma, P)$ captures A_{QQ} (Figure 3.1).

Since there are no closed-form solutions to the optimal IIPROM Problem 3.1, this structure suggests that minimizing the three reduction error contributions can provide good PROMs. As a first step in obtaining a suboptimal solution, we define the following suboptimal IIPROM problem that attempts to minimize the error reduction upper bound derived in Proposition 3.1.

Problem 3.2 (suboptimal IIPROM)**.** *Consider a stable proper system of order n with realization $\Sigma := (A, B, C, D)$. Find $P \in \mathbb{R}^{n \times r}$ with $P^\top P = I_r$ such that the PROM $\Sigma_r(\Sigma, P)$ (3.1) minimizes the reduction error bound (3.10) and is interface-invariant, i.e.,*

$$\begin{aligned} \min_{P \in \mathbb{R}^{n \times r}} \; & b(\Sigma, P) \\ s.t. \; & P^\top P = I_r \\ & C = CPP^\top \\ & B = PP^\top B. \end{aligned} \tag{3.13}$$

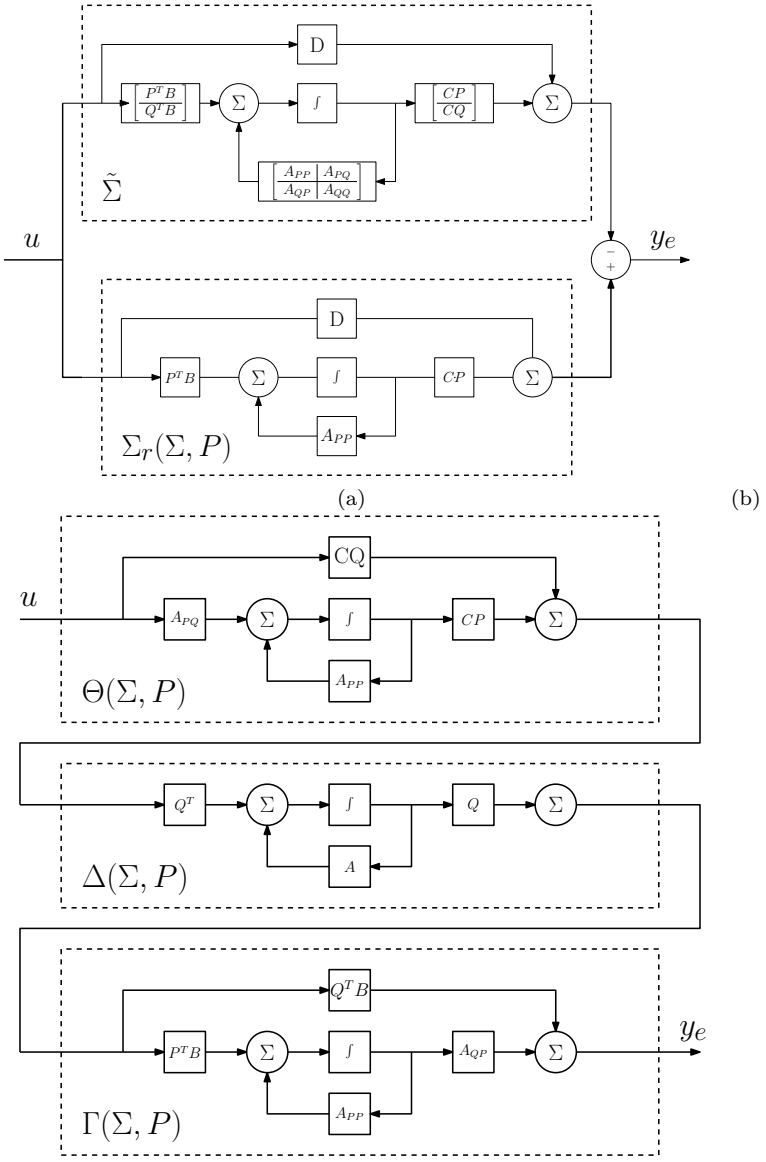

Figure 3.1: The PROM error system block diagram in (a) additive form and (b) product form (3.1).

The following simple example provides a comparison between the solutions for the optimal IIPROM Problem 3.1 and the optimal IIPROM bound Problem 3.2.

Example 3.1. *Consider the SISO system* $\Sigma := (A, B, C, D)$ *where*

$$A = \begin{bmatrix} -2 & 1 & 0 \\ 1 & -2 & 1 \\ 0 & 1 & -1 \end{bmatrix}, B = \begin{bmatrix} 1 \\ 0 \\ 0 \end{bmatrix}, C = \begin{bmatrix} 1 & 0 & 0 \end{bmatrix}, D = 0.$$

The corresponding TF is

$$\hat{\Sigma} = \frac{s^2 + 3s + 1}{s^3 + 5s^2 + 6s + 1}$$

and $\|\Sigma\|_{\mathcal{H}_\infty} = 1$. *We observe that all matrices* $P \in \mathbb{R}^{3\times 2}$ *complying with* $P^\top P = I_2$, $CPP^\top = C$ *and* $PP^\top B = B$, *can be parametrized by a scalar* $\alpha \in [-1, 1]$ *in the following form,*

$$P(\alpha) = \begin{bmatrix} 1 & 0 \\ 0 & \alpha \\ 0 & \beta(\alpha) \end{bmatrix},$$

where $\beta(\alpha) = \sqrt{1 - \alpha^2}$. *All matrices* $Q \in \mathbb{R}^{3\times 1}$ *such that* $P^\top Q = 0$ *are parametrized by*

$$Q(\alpha) = \begin{bmatrix} 0 & -\beta(\alpha) & \alpha \end{bmatrix}^\top.$$

All IIPROMs $\Sigma_r(\Sigma, P)$ *are then parameterized also by* α, *such that the matrices of the product form system realizations of Theorem 3.1 are*

$$A_{PP}(\alpha) = \begin{bmatrix} -2 & \alpha \\ \alpha & -\alpha^2 - (\beta(\alpha) - \alpha)^2 \end{bmatrix}$$

and

$$A_{PQ}(\alpha) = \begin{bmatrix} -\beta(\alpha) \\ 2\alpha^2 + \alpha\beta(\alpha) - 1 \end{bmatrix} = A_{QP}(\alpha)^\top.$$

The PROM TF is

$$\hat{\Sigma}_r = \frac{s + \gamma^2}{s^2 + (\gamma^2 + 2)s + 2\gamma^2 - \alpha^2},$$

and the product systems (3.5)-(3.7) TFs are

$$\hat{\Theta} = \hat{\Gamma} = \frac{-\beta s + \alpha^3 - \alpha^2\beta + \alpha\beta^2 - \beta^3}{s^2 + (\alpha^2 + \gamma^2 + 2)s + \alpha^2 + 2\gamma^2}$$

and

$$\hat{\Delta} = \frac{\left(\alpha^2 + \beta^2\right)s^2 + \left(2\gamma^2 + 2\alpha^2 + \beta^2\right)s + 2\gamma^2 + \alpha^2)}{s^3 + 5s^2 + 6s + 1},$$

where $\gamma \triangleq \sqrt{\alpha^2 + (\alpha - \beta)^2}$.

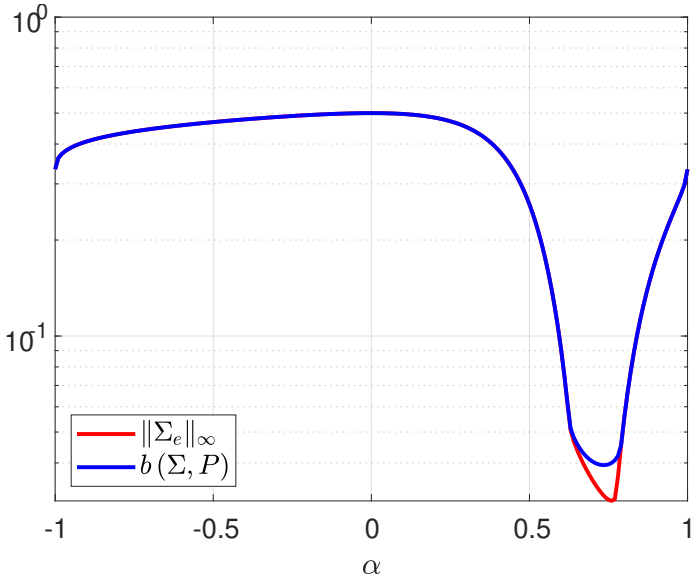

Figure 3.2: The IIPROM reduction error and bound of the second order system as a function of the projection parameter α.

The PROM reduction error and reduction error bound are plotted in Figure 3.2. It is observed that the solution of the optimal IIPROM problem (Problem 3.1) is $\min_\alpha \|\Sigma - \Sigma_r\|_\infty = 0.03$ *obtained for* $\alpha^* = 0.76$. *The solution of the optimal IIPROM bound problem (Problem 3.2) is* $\min_\alpha b(\Sigma, P) = 0.039$ *obtained for* $\alpha^{**} = 0.73$. *We observe that the optimal IIPROM error is close to the sub-optimal bound.*

3.3.3 The PROM Sequence Bound

In the following subsection we present a Lemma showing that any projection from $\mathbb{R}^n$ to $\mathbb{R}^r$ can be obtained from a sequence of $n-r$ projections, each reducing the dimension by one. We denote such projections as *singleton projections*. This sequential projection representation is then utilized to obtain a sequential PROM bound that is useful for obtaining sub-optimal solutions to Problem 3.2.

Lemma 3.2. *Let* $P \in \mathbb{R}^{n\times r}$ *with* $P^\top P = I_r$ *be a projection for* $r < n$. *Then there exists a sequence* $\left\{P_{(k)}\right\}_{k=1}^{n-r}$ *with* $P_{(k)} \in \mathbb{R}^{n-k+1\times n-k}$, $P_{(k)}^\top P_{(k)} = I_{n-k}$ *such that* $P = \Pi_{k=1}^{n-r} P_{(k)}$.

Proof. Let $P \in \mathbb{R}^{n\times r}$, $P^\top P = I_r$, then there exists $Q \in \mathbb{R}^{n\times n-r}$ with $Q^\top Q = I_{n-r}$ such that $P^\top Q = 0$. Construct $P_{(1)} = [P, q_1, q_2, \ldots, q_{n-r-1}]$, where q_i is the ith column of Q, and $P_{(k)} = [I_{n-k}, 0_{n-k\times 1}]^\top$ for $k \in [2, n-r]$. Since $P^\top P = I_r$ and $P^\top Q = 0$ we have $P_{(1)}^\top P_{(1)} = I_{n-1}$, and for $k \in [2, n-r]$ it is

trivial that $P_{(k)}^{\top}P_{(k)} = I_{n-k}$. From the construction we get

$$\begin{aligned}\left(\prod_{k=1}^{n-r} P_{(k)}\right) &= P_{(1)}\left(\prod_{i=1}^{n-r-1} P_{(1+i)}\right)\\ &= P_{(1)}\left(\prod_{i=1}^{n-r-1} \left[I_{n-i}, 0_{n-1\times 1}\right]^{\top}\right)\\ &= P.\end{aligned}$$

□

Note that infinite other sequences $P = \Pi_{k=1}^{n-r}\tilde{P}_{(k)}$ can be produced by the transformations $\tilde{P}_{(1)} = P_{(1)}U_{(1)}$, $\tilde{P}_{(k)} = U_{(k-1)}^{\top}P_{(k)}U_{(k)}$ for $k \in [2, n-r-1]$, and $\tilde{P}_{(n-r)} = U_{(n-r-1)}^{\top}P_{(n-r)}$, where $U_{(k)} \in \mathbb{R}^{n-k\times n-k}$ is an orthogonal matrix.

By expressing a PROM as a sequence of singleton projections, we obtain the following PROM sequence bound.

Proposition 3.2 (Singleton PROM sequence bound)**.** *Let Σ be an LTI system with realization (A, B, C, D) with A Hurwitz, and consider the PROM, $\Sigma_r := (P^{\top}AP, P^{\top}B, CP, D)$, and let $\left\{P_{(k)}\right\}_{k=1}^{n-r}$ be a sequence with $P_{(k)} \in \mathbb{R}^{n-k+1\times n-k}$, $P_{(k)}^{\top}P_{(k)} = I_{n-k}$ such that $P = \Pi_{k=1}^{n-r}P_{(k)}$. Then the $\mathcal{H}_\infty$ norm of the error reduction system Σ_e (1.8) is bounded by*

$$\|\Sigma_e\|_{\mathcal{H}_\infty} \leq \sum_{k=1}^{n-1} b\left(\Sigma_{(k-1)}, P_{(k)}\right), \tag{3.14}$$

with $b(\Sigma_{(k-1)}, P_{(k)})$ given in (3.10), and

$$\Sigma_{(k)} := \left(P_{(k)}^{\top}A_{(k-1)}P_{(k)}, P_{(k)}^{\top}B_{(k-1)}, C_{(k-1)}P_{(k)}, D\right) \tag{3.15}$$

with $\Sigma_{(0)} := (A, B, C, D)$.

Proof. We express $\Sigma_e(s) = \Sigma_r - \Sigma$ as the telescoping sum $\sum_{k=1}^{n-r}\left(\Sigma_{(k)} - \Sigma_{(k-1)}\right)$ with $\Sigma_{(0)} = \Sigma$ and $\Sigma_{(n-r)} = \Sigma_r$, such that

$$\begin{aligned}\|\Sigma_e(s)\|_{\mathcal{H}_\infty} &= \|\Sigma_r - \Sigma\|_{\mathcal{H}_\infty}\\ &= \|\sum_{k=1}^{n-r}\left(\Sigma_{(k)} - \Sigma_{(k-1)}\right)\|_{\mathcal{H}_\infty}\end{aligned}$$

and from the triangle inequality we get

$$\|\Sigma_e(s)\|_{\mathcal{H}_\infty} \leq \sum_{k=1}^{n-r}\|\Sigma_{(k)} - \Sigma_{(k-1)}\|_{\mathcal{H}_\infty}.$$

The system $\Sigma_{(k)}$ has realization

$$\begin{aligned}\Sigma_{(k)} &:= \left(A_{(k)}, B_{(k)}, C_{(k)}, D\right) \\ &= \left(P_{(k)}^{\top} A_{(k-1)} P_{(k)}, P_{(k)}^{\top} B_{(k-1)}, C_{(k-1)} P_{(k)}, D\right),\end{aligned}$$

which is an IIPROM of $\Sigma_{(k-1)}$, therefore, from Theorem 3.1,

$$\|\Sigma_{(k)} - \Sigma_{(k-1)}\|_{\mathcal{H}_\infty} \leq b\left(\Sigma_{(k-1)}, P_{(k)}\right),$$

and we obtain that

$$\|\Sigma_e(s)\|_{\mathcal{H}_\infty} \leq \sum_{k=1}^{n-r} b\left(\Sigma_{(k-1)}, P_{(k)}\right).$$

□

In the following section, we will utilize graph contractions for obtaining suboptimal solutions of Problem 3.2 for multi-agent systems, and therefore, also Problem 3.1.

3.4 Proof of the PROM Error System Product Form

In this section, we present the proof of Theorem 3.1. The proof is based on the matrix inverse lifting lemma along with a projection inversion corollary that we present here.

Definition 3.2 (Projected Schur complement)**.** *Let $M \in \mathbb{C}^{n\times n}$ and let P and Q be projections such that $P^{\top}P = I_r$, $Q^{\top}Q = I_{n-r}$ and $Q^{\top}P = 0$. Then for $P^{\top}MP$ invertible, we define the* projected Schur complement *of S by P as*

$$S(M, P) \triangleq M_{QQ} - M_{QP}M_{PP}^{-1}M_{PQ}, \tag{3.16}$$

and the projected Schur complement of S by Q as

$$S(M, Q) \triangleq M_{PP} - M_{PQ}M_{QQ}^{-1}M_{QP}, \tag{3.17}$$

where $M_{PP} \triangleq P^{\top}MP$, $M_{PQ} \triangleq P^{\top}MQ$, $M_{QP} \triangleq Q^{\top}MP$ and $M_{QQ} \triangleq Q^{\top}MQ$.

With the definition of the projected Schur complement we can derive the following corollary of the matrix inversion Lemma [7].

Lemma 3.3. *Let $M \in \mathbb{C}^{n\times n}$ and M^{-1} be a matrix and its inverse with corresponding block structures*

$$M = \begin{bmatrix} M_{11} & M_{12} \\ M_{21} & M_{22} \end{bmatrix} \qquad M^{-1} = \begin{bmatrix} W & X \\ Y & Z \end{bmatrix},$$

then

$$W = (M_{11} - M_{12}M_{22}^{-1}M_{21})^{-1}, \tag{3.18}$$

and

$$X = -M_{11}^{-1}M_{12}Z. \tag{3.19}$$

Corollary 3.3. *Consider a matrix $M \in \mathbb{C}^{n\times n}$, and let P and Q be matrices such that $P^\top P = I_r$, $Q^\top Q = I_{n-r}$ and $Q^\top P = 0$. Then*

$$P^\top M^{-1} P = S^{-1}(M, Q), \tag{3.20}$$

and

$$P^\top M^{-1} Q = -M_{PP}^{-1} M_{PQ} \left(Q^\top M^{-1} Q\right). \tag{3.21}$$

Proof. Apply the matrix inversion Lemma to the matrix $\tilde{M} = [PQ]^\top M [PQ]$ and obtain $P^\top M^{-1} P = S^{-1}(M, Q)$ and $P^\top M^{-1} Q = -M_{PP}^{-1} M_{PQ} \left(Q^\top M^{-1} Q\right)$. □

We denote a *matrix lifting* $f_P : \mathbb{R}^{r\times r} \to \mathbb{R}^{n\times n}$ as the function $f_P(M) \triangleq PMP^\top$. The following lemma extends the matrix inversion lemma to the matrix lifting of $\left(P^\top MP\right)^{-1}$.

Lemma 3.4 (Matrix Inverse Lifting)**.** *Consider a matrix $M \in \mathbb{C}^{n\times n}$ and let P and Q be matrices such that $P^\top P = I_r$, $Q^\top Q = I_{n-r}$ and $Q^\top P = 0$. Then*

$$P\left(P^\top MP\right)^{-1} P^\top = \Upsilon(M, Q), \tag{3.22}$$

where we define $\Upsilon(M, Q)$ as,

$$\Upsilon(M, Q) \triangleq M^{-1} - M^{-1}Q\left(Q^\top M^{-1} Q\right)^{-1} Q^\top M^{-1}.$$

Proof. We have $I_n = PP^\top + QQ^\top$ such that

$$\begin{aligned}\Upsilon(M, Q) &= \left(PP^\top + QQ^\top\right)\Upsilon(M, Q)\left(PP^\top + QQ^\top\right)\\ &= PP^\top\Upsilon(M, Q)PP^\top + PP^\top\Upsilon(M, Q)QQ^\top\\ &\quad + QQ^\top\Upsilon(M, Q)PP^\top + QQ^\top\Upsilon(M, Q)QQ^\top.\end{aligned}$$

Evaluating the four expressions in the sum we get

$$\begin{aligned}P^\top\Upsilon(M, Q)Q &= P^\top M^{-1}Q - P^\top M^{-1}Q\left(Q^\top M^{-1}Q\right)^{-1}Q^\top M^{-1}Q = 0,\\ Q^\top\Upsilon(M, Q)P &= Q^\top M^{-1}P - Q^\top M^{-1}Q\left(Q^\top M^{-1}Q\right)^{-1}Q^\top M^{-1}P = 0,\\ Q^\top\Upsilon(M, Q)Q &= Q^\top M^{-1}Q - Q^\top M^{-1}Q\left(Q^\top M^{-1}Q\right)^{-1}Q^\top M^{-1}Q = 0,\\ P^\top\Upsilon(M, Q)P &= P^\top M^{-1}P - P^\top M^{-1}Q\left(Q^\top M^{-1}Q\right)^{-1}Q^\top M^{-1}P.\end{aligned}$$

We observe that the last term $P^\top \Upsilon\left(M,Q\right)P$ is the projected Schur complement $S\left(M^{-1},Q\right)$ (Def. 3.2). From the projection inversion corollary (Corollary 3.3) we then obtain

$$P^\top \Upsilon\left(M,Q\right)P = \left(P^\top MP\right)^{-1},$$

and therefore

$$\Upsilon\left(M,Q\right) = P\left(P^\top MP\right)^{-1}P^\top.$$

□

We are now prepared to proceed with the proof of Theorem 3.1.

Proof. We begin by proving the first part of the theorem, i.e.,

$$\hat{\Sigma}_e(\Sigma,P) = C\Phi^{-1}Q(Q^\top\Phi^{-1}Q)^{-1}Q^\top\Phi^{-1}B. \tag{3.23}$$

The error system TFM is

$$\begin{aligned}\hat{\Sigma}_e &= \hat{\Sigma}_r - \hat{\Sigma}\\ &= CP\left(sI_r - P^\top AP\right)^{-1}P^\top B - C\Phi^{-1}B\\ &= CP\left(P^\top\Phi P\right)^{-1}P^\top B - C\Phi^{-1}B\\ &= C\left(P\left(P^\top\Phi P\right)^{-1}P^\top - \Phi^{-1}\right)B.\end{aligned}$$

We now employ the matrix inverse lifting lemma (Lemma 3.4),

$$P(P^\top\Phi P)^{-1}P^\top - \Phi^{-1} = \Phi^{-1}Q(Q^\top\Phi^{-1}Q)^{-1}Q^\top\Phi^{-1},$$

thus leading to the expression (3.23). Next, we prove the second part of the theorem, i.e.,

$$\Sigma_e(\Sigma,P) = \Theta(\Sigma,P)\Delta(\Sigma,P)\Gamma(\Sigma,P), \tag{3.24}$$

with the three realizations

$$\begin{aligned}\Theta(\Sigma,P) &:= (A_{PP}, A_{PQ}, CP, CQ)\\ \Gamma(\Sigma,P) &:= (A_{PP}, P^\top B, A_{QP}, Q^\top B)\\ \Delta(\Sigma,P) &:= (A, Q, Q^\top, 0_{p\times m}).\end{aligned}$$

With $I = \left(Q^\top\Phi^{-1}Q\right)\left(Q^\top\Phi^{-1}Q\right)^{-1}$ we get

$$C\Phi^{-1}Q\Xi(\Phi,Q)Q^\top\Phi^{-1}B = \hat{\Theta}\left(\Sigma,P\right)\hat{\Delta}\left(\Sigma,P\right)\hat{\Gamma}\left(\Sigma,P\right),$$

where $\Xi(\Phi,Q) \triangleq \left(Q^\top\Phi^{-1}Q\right)^{-1}$ and

$$\begin{aligned}\hat{\Theta}\left(\Sigma,P\right) &\triangleq C\Phi^{-1}Q\Xi(\Phi,Q),\\ \hat{\Delta}\left(\Sigma,P\right) &\triangleq Q^\top\Phi^{-1}Q,\\ \hat{\Gamma}\left(\Sigma,P\right) &\triangleq \Xi(\Phi,Q)Q^\top\Phi^{-1}B.\end{aligned}$$

We have $I = PP^\top + QQ^\top$ such that

$$\begin{aligned}\Phi^{-1}Q\left(Q^\top\Phi^{-1}Q\right)^{-1} &= \left(PP^\top + QQ^\top\right)\Phi^{-1}Q\Xi(\Phi,Q)\\ &= Q + P\left(P^\top\Phi^{-1}Q\right)\Xi(\Phi,Q).\end{aligned}$$

From the projection inversion corollary (Corollary 3.3), we have

$$\begin{aligned}P^\top\Phi^{-1}Q &= -\Phi_{PP}^{-1}\Phi_{PQ}\left(Q^\top\Phi^{-1}Q\right)\\ &= \left(sI_r - P^\top AP\right)^{-1}P^\top AQ\left(Q^\top\Phi^{-1}Q\right)\end{aligned}$$

and

$$\Phi^{-1}Q\Xi(\Phi,Q) = Q + P\left(sI_r - P^\top AP\right)^{-1}P^\top AQ, \tag{3.25}$$

such that

$$\hat{\Theta}(\Sigma,P) = CP\left(sI_r - P^\top AP\right)^{-1}P^\top AQ + CQ,$$

which is the TFM with realization $\Theta(\Sigma,P) := (A_{PP}, A_{PQ}, CP, CQ)$. Similarly we get

$$\begin{aligned}\hat{\Gamma}(\Sigma,P) &= \left[Q^\top\Phi^{-1}Q\right]^{-1}Q^\top\Phi^{-1}B\\ &= Q^\top AP\left(sI_r - P^\top AP\right)^{-1}P^\top B + Q^\top B,\end{aligned}$$

and the realization $\Gamma(\Sigma,P) := \left(A_{PP}, P^\top B, A_{QP}, Q^\top B\right)$. Finally $\hat{\Delta}(\Sigma,P) = Q\Phi^{-1}Q$ has realization $\Delta(\Sigma,P) := \left(A, Q, Q^\top, 0_{p\times m}\right)$. □

3.5 Conclusions

In this chapter we have derived a unique product form of the error system of orthogonal projection-based reduced models from which the notion of interface-invariant PROMs has emerged. The proof of this theorem was based on a matrix-inverse lifting lemma, an extension of the matrix inversion lemma. The derived product form was then used to construct an $\mathcal{H}_\infty$ error bound for the PROM error system and a corresponding bound optimization PROM problem, which will be applied for the reduction of MAS in the following chapter.

Chapter 4

Model Reduction of Multi-Agent Systems by Graph Contractions

Interface-invariant reduced models are natural to graph-based model reduction of multi-agent systems where subsets of agents function as the input and output of the system. In this chapter, graph contractions are used as a constructive solution approach to the $\mathcal{H}_\infty$ bound optimization problem for MAS. Edge-based contractions are then utilized in a greedy-edge reduction algorithm, and these results are demonstrated with some numerical examples of model reduction of a first-order Laplacian controlled consensus protocol.

4.1 Introduction

Multi-agent systems may be of extremely large scale, and designing and implementing full order controllers for such systems is not feasible without applying model reduction on the design model or the full-order controller. Several recent studies were performed in order to derive PROM producing methods for the reduction of MAS that utilize the underlying network structure of MAS. In [47], a projection reduction of the controlled consensus protocol is performed based on partitioning of the graph vertices. The resulting reduced order projected system is then interpreted as an input-output consensus system over a directed graph, and it is shown that the reduction error is $\mathcal{H}_2$-optimal for a special class of partitions. In [34], a similar partition-based projection method is used for reduction of a single input networked dynamic system, resulting in a reduced networked system over a non-simple graph with $\mathcal{H}_\infty$ reduction error bounds. It has been observed in these previous studies that partition-based PROMs maintain an MAS structure, i.e., the PROM is an MAS (4.2) defined over a reduced order graph.

These methods, while contributing analytical results such as error bounds, did not provide efficient algorithms for optimal, or suboptimal model reduction of MAS. In that direction, in this work we investigate PROMs based of vertex partitions. We are able to utilize the edge-induced partitions introduced in Chapter 2, together with the PROM bound derived in Chapter 3, to construct a suboptimal efficient model reduction method for MAS.

In this work we introduce the notion of edge-induced PROMs. These are PROMs which are constructed over edge-induced partitions of the graph. This graph-based model reduction method allows us to derive sub-optimal but efficient IIPROMs of MAS.

We first provide the system theoretic basis of MAS. We consider a *multi-agent system* as a set of n agents connected over a network described by a graph $\mathcal{G} = (\mathcal{V}, \mathcal{E}, \mathcal{W})$. Each agent has LTI dynamics, which depend on their internal dynamics and a response to their local neighborhood $\mathcal{N}_i \subseteq \mathcal{V}$. The state space realization of each agent system is then

$$\begin{cases} \dot{x}_i(t) &= A_i x_i(t) + \sum_{j \in \mathcal{N}_i} A_{ij} x_j(t) + B_i u_i(t) \\ y_i(t) &= C_i x_i(t) + D_i u_i(t) \end{cases} \tag{4.1}$$

where $x_i \in \mathbb{R}^{d_x}$ is the i'th agent state vector, A_i, A_{ij}, B_i, C_i, C_{ij} and D_i are realization parameters, and $u_i \in \mathbb{R}^{d_u}$ is an external input signal. We assume further that in such a network, a subset of the agents may be subject to external control inputs, and a subset may be accessed for measurements. Formally, we denote the *input nodes* by the set $\mathcal{U} \subseteq \mathcal{V}(\mathcal{G})$, and the set of *output nodes* by the set $\mathcal{Y} \subseteq \mathcal{V}(\mathcal{G})$. In the case of linear MAS, we then have the realization

$$\Sigma(\mathcal{G}, \mathcal{U}, \mathcal{Y}) := (A(\mathcal{G}), B(\mathcal{G}, \mathcal{U}), C(\mathcal{G}, \mathcal{Y}), D(\mathcal{U}, \mathcal{Y})), \tag{4.2}$$

where the matrices $A(\mathcal{G}) \in \mathbb{R}^{n_x \times n_x}$, $B(\mathcal{G}, \mathcal{U}) \in \mathbb{R}^{n_x \times n_u}$, $C(\mathcal{G}, \mathcal{Y}) \in \mathbb{R}^{n_y \times n_x}$ and $D(\mathcal{U}, \mathcal{Y}) \in \mathbb{R}^{n_y \times n_u}$ are the system matrices as a function of the underlying graph structure, with $n_x = d_x \times n$, $n_u = d_u \times |\mathcal{U}|$ and $n_y = d_y \times |\mathcal{Y}|$. Here, d_x, d_u, and d_y represent the dimension of the state, input, and output of each agent in the network. The TFM representation of (4.2) is,

$$\Sigma_{\mathcal{M}}(s) = C(\mathcal{G}, \mathcal{Y})(sI - A(\mathcal{G}))^{-1} B(\mathcal{G}, \mathcal{U}). \tag{4.3}$$

This system is visualized in Figure 4.1. Note that MAS models of this form include classical setups such as diffusively coupled networks [10] and Laplacian dynamics [45].

If $\mathcal{Y} = \mathcal{U}$ we define $\Sigma(\mathcal{G}, \mathcal{U}, \mathcal{Y})$ as an *interface system*, a multi-agent system where a subset of agents are the interface of the system with an external observer-controller. If $C(\mathcal{G}, \mathcal{U}) = B^T(\mathcal{G}, \mathcal{U})$ and $A(\mathcal{G})$ is symmetric then $\Sigma(\mathcal{G}, \mathcal{U}, \mathcal{Y})$ is a *balanced interface system*.

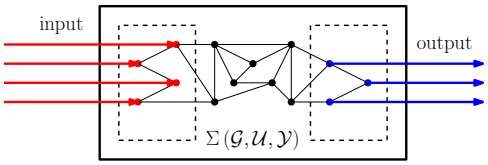

Figure 4.1: A controlled MAS with interface agents, red nodes identify the set $\mathcal{U}$, blue nodes the set $\mathcal{Y}$.

The Laplacian matrix plays a key role in networked an multi-agent systems. For a multi-graph, i.e., a graph that may include duplicate edges and self loops, the Laplacian matrix $L(\mathcal{G}) \in \mathbb{R}^{|\mathcal{V}|\times|\mathcal{V}|}$ is defined as [25]

$$[L(\mathcal{G})]_{uv} = \begin{cases} \sum_{v\in\{\mathcal{N}_u\cup u\}} w(\{u,v\}) & u = v \\ -w(\{u,v\}) & u \sim v \\ 0 & o.w. \end{cases}, \tag{4.4}$$

where $w(\{u,v\})$ denotes the weight of the edge $\{u,v\}$.

As a test case model of an interface MAS of the form (4.2), we consider the *Laplacian controlled consensus model (LCC)* (4.5), a generalisation of the Laplacian Consensus protocol $\dot{x} = -L(\mathcal{G})\,x$, a benchmark model of an uncontrolled multi-agent system [45],. The LCC has a realization

$$\begin{cases} \dot{x} &= -L(\mathcal{G})\,x + B(\mathcal{U})\,P \\ y &= C(\mathcal{Y})\,x + D(\mathcal{U},\mathcal{Y})\,u \end{cases}, \tag{4.5}$$

where $B(\mathcal{U}) \in \mathbb{R}^{|\mathcal{V}|\times|\mathcal{U}|}$ maps each of the inputs to the corresponding node in the network, i.e., $[B(\mathcal{U})]_{ij} = 1$ if i is the j'th input node and 0 otherwise, and similarly $C(\mathcal{U}) \in \mathbb{R}^{|\mathcal{Y}|\times|\mathcal{V}|}$ maps each of the outputs to the corresponding node in the network, i.e., $[C(\mathcal{U})]_{ji} = 1$ if i is the j'th output node and 0 otherwise.

4.2 Graph-Based Model Reduction

Based on the networked structure of linear MAS, we define its graph-based model reduction:

Definition 4.1 (Graph-based model reduction)**.** *Consider an MAS consisting of n agents with realization*

$$\Sigma(\mathcal{G},\mathcal{U},\mathcal{Y}) := (A(\mathcal{G}), B(\mathcal{G},\mathcal{U}), C(\mathcal{G},\mathcal{Y}), D(\mathcal{U},\mathcal{Y})),$$

then we define a graph-based model reduction of Σ as an MAS consisting of $r < n$ agents with realization

$$\Sigma(\mathcal{G}_r,\mathcal{U},\mathcal{Y}) := (A(\mathcal{G}_r), B(\mathcal{G}_r,\mathcal{U}), C(\mathcal{G}_r,\mathcal{Y}), D(\mathcal{U},\mathcal{Y})),$$

where $\mathcal{G}_r$ is any graph of order r.

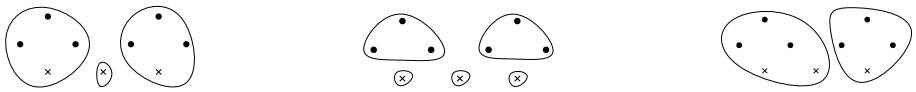

Figure 4.2: A set of 9 nodes, with subset $\mathcal{I}$ of three nodes (marked with x), (a) is an $\mathcal{I}$-invariant 3-partition, (b) is a strongly $\mathcal{I}$-invariant 5-partition, and (c) is a 2-partition which is not $\mathcal{I}$-invariant.

Problem 4.1 (Graph-based model reduction problem)**.** *Consider an MAS* $\Sigma(\mathcal{G},\mathcal{U},\mathcal{Y})$ *of order* n*. Find a graph* $\mathcal{G}_r$ *of a given order* $r < n$ *such that the reduced system* $\Sigma_r = \Sigma(\mathcal{G}_r,\mathcal{U},\mathcal{Y})$ *minimizes the* $\mathcal{H}_\infty$ *reduction error* $\|\Sigma_e(\Sigma,\Sigma_r)\|_{\mathcal{H}_\infty}$.

Finding a solution to Problem 4.1 may be numerically intractable for a moderate number of nodes, e.g., the number of simple connected graphs of order r increases exponentially and for $r = 1,\ldots,6$, it is 1, 1, 4, 38, 728, 26704 [64, p.87].

The general statement of Problem 4.1 does not suggest any constructive way to find the optimal reduced MAS. However, it is expected that an optimal solution will have some functional dependency on the MAS structure. Vertex partitions have been widely used in graph theory, e.g., for graph clustering [55] and in the study of network communities [49]. Vertex partitions have been also used for constructing projection-based model reductions of multi-agent systems as the consensus protocol [47] and bidirectional networks [34].

We recall some definitions of partitions and graph contractions discussed in Chapter 2. An *r-partition*, π, of a vertex set $\mathcal{V}$ is the partition $\{C_i\}_{i=1}^r$ of $\mathcal{V}$ to r cells such that $\cup_{i=1}^r C_i = \mathcal{V}$ and $|C_i \cap C_j| = 0$ for $i \neq j$. An r-partition $\pi = \{C_i\}_{i=1}^r$ is $\mathcal{I}$-invariant for $\mathcal{I} \subseteq \mathcal{V}$ if $\forall i \in [1,r]$, one has $|C_i \cap \mathcal{I}| \leq 1$, i.e., no partition cell contains more than one node in $\mathcal{I}$. The r-partition is *strongly* $\mathcal{I}$-invariant if all partition cells containing nodes in $\mathcal{I}$ are singletons, i.e., $|C_i| = 1$ whenever $C_i \subset \mathcal{I}$. We denote the set of all strongly $\mathcal{I}$-invariant r-partitions as $S_r(\mathcal{V})$. Figure 4.2 illustrates these definitions.

We recall from Chapter 2 Definition 2.9 that given a graph $\mathcal{G} = (\mathcal{V},\mathcal{E})$, and an $n-r$ edge subset $\mathcal{E}_S \subseteq \mathcal{E}$, an *edge-induced partition* $\pi(\mathcal{E}_S)$ is an r-partition of $\mathcal{V}$ constructed as follows: (i) A graph $\mathcal{G}(\mathcal{V},\mathcal{E}_S)$ is created from the vertices of $\mathcal{G}$ and the edge-subset $\mathcal{E}_S$, (ii) the connected components of $\mathcal{G}(\mathcal{V},\mathcal{E}_S)$ are found, (iii) the vertices of each component is registered as a partition cell, and the set of all components cells constitutes the partition $\pi(\mathcal{E}_S)$ of $\mathcal{V}$ (Figure 4.3).

In the following section, we will utilize the edge-induced partitions to construct partition-based PROMs in a model reduction method suboptimal in the $\mathcal{H}_\infty$ IIPROM reduction error bound (Eq. (3.1)) derived in Chapter 3.

4.3 $\mathcal{H}_\infty$ - Suboptimal PROMs of Controlled MAS

In this section, graph contractions are used as a constructive solution approach to the $\mathcal{H}_\infty$ bound optimization problem for multi-agent systems. Edge-induced partitions are then utilized in a greedy-edge reduction algorithm and are demonstrated for the model reduction of a first-order Laplacian controlled consensus protocol.

We first construct the optimal partition PROM problem that we are aiming to solve.

Problem 4.2 (Optimal partition PROM)**.** *Consider a stable MAS $\Sigma(\mathcal{G},\mathcal{U},\mathcal{Y})$ with n agents, each with local state of dimension d_x. Find an r-partition π such that the PROM $\Sigma_r(\Sigma, P(\pi))$ minimizes the $\mathcal{H}_\infty$ reduction error, where $P(\pi)$ is the PPM (Definition 2.13).*

Interface systems are natural to MAS where a subset of agents interact with an external controller. Therefore, we restrict the PROM to be an IIPROM (Definition 3.1) by requiring the partition to be $\mathcal{I}$-invariant. Additionally, we replace the PROM error with the IIPROM bound derived in Chapter 3, which has lower computational complexity. The resulting partition IIPROM bound problem is then introduced:

Problem 4.3 (Optimal partition IIPROM bound)**.** *Consider a stable MAS $\Sigma(\mathcal{G},\mathcal{U},\mathcal{Y})$ with n agents, each with local state of dimension d_x, and an interface set $\mathcal{I} = \mathcal{U} \cup \mathcal{Y}$. Find an $\mathcal{I}$-invariant r-partition π such that the PROM $\Sigma_r(\Sigma, P(\pi))$ minimizes the reduction error bound $b(\Sigma(\mathcal{G},\mathcal{U},\mathcal{Y}), I_{d_x} \otimes P(\pi))$ given in (3.12).*

Similar to the interlacing graph reduction problem (Problem 2.1) of Chapter 2, finding a solution to Problem 3.2 may be numerically intractable for a moderate number of nodes, and we seek for an efficient suboptimal solution.

Given a subset of edges $\mathcal{E}_c \subseteq \mathcal{E}$, an *edge-induced partition* $\pi(\mathcal{E}_c)$ can be constructed as described above. Here we utilize the edge-induced partition to

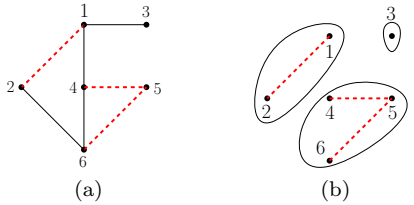

Figure 4.3: An edge-induced partition of a graph of order r, (a) a graph $\mathcal{G} = (\mathcal{V}, \mathcal{E})$ with a selected edge subset $\mathcal{E}_\mathcal{S} = \{\{1,2\},\{4,5\},\{5,6\}\}$ (dashed red), (b) the graph $\mathcal{G}(\mathcal{V}, \mathcal{E}_S)$ and its connected components inducing the partition $\pi(\mathcal{E}_S) = \{\{1,2\},\{3\},\{4,5,6\}\}$ on $\mathcal{V}(\mathcal{G})$.

derive a greedy-edge IIPROM bound (GEIB) algorithm (Algorithm 4.1). The input to the algorithm is an MAS $\Sigma(\mathcal{G},\mathcal{U},\mathcal{Y})$ (4.2), the required reduction order r and a subset of candidate edges $\mathcal{E}_c \subseteq \mathcal{E}$ (assuming there are more than $n-r$ edges in $\mathcal{E}_c$). The first step of the algorithm is to check if each of the edges is strongly $\mathcal{I}$-invariant by examining if both end nodes of an edge are not in $\mathcal{I}$. If an edge is found to be strongly $\mathcal{I}$-invariant, a PPM in constructed with its induced edge partition and the PROM error bound (3.1) is calculated. The PPM of the induced-edge partition of the $n-r$ edges with lowest bound is then used to obtain a PROM and serves as a suboptimal solution to Problem 4.3.

Algorithm 4.1 Greedy-edge IIPROM bound Algorithm

Input: An MAS $\Sigma(\mathcal{G},\mathcal{U},\mathcal{Y})$ of order n with realization $\Sigma := (A(\mathcal{G}), B(\mathcal{G},\mathcal{U}), C(\mathcal{G},\mathcal{Y}), D(\mathcal{U},\mathcal{Y}))$, interface set $\mathcal{I} = \mathcal{U} \cup \mathcal{Y}$, edge subset $\mathcal{E}_c \subseteq \mathcal{E}$, reduction order r.

1. **For** each $\{u,v\} \in \mathcal{E}_c$
   - **if** $u \in \mathcal{I}$ or $v \in \mathcal{I}$, skip to next edge,
   - **else** construct the edge-induced partition $\pi(\{u,v\})$ and its PPM $P(\pi)$, and calculate $b(\Sigma, P(\pi))$.
2. **Find** $n-r$ edges $\mathcal{E}^* \subseteq \mathcal{E}_c$ with the lowest bound values.
3. **Construct** the edge-induced r-partition $\pi(\mathcal{E}^*)$.

Output: $\Sigma_r(\Sigma, P(\pi(\mathcal{E}^*)))$ (3.1)
Notation: $\Sigma_r = GEIB(\Sigma(\mathcal{G},\mathcal{U},\mathcal{Y}), \mathcal{E}_c, r)$

The greedy-edge IIPROM bound algorithm does not specify the method to choose the edge subset $\mathcal{E}_c$. Trees are the building blocks of any connected graph. A basic graph-theoretic principle is that a spanning tree of a connected graph $\mathcal{G} = (\mathcal{V},\mathcal{E})$ of order n is a subgraph with a minimal set of $n-1$ edges connecting all vertices. Furthermore, trees and cycle-completing edges are strongly related to the performance of networked systems [69]. With this intuition, we derive the tree-based IIPROM bound (TBIB) algorithm (Algorithm 4.2), where given an MAS $\Sigma(\mathcal{G},\mathcal{U},\mathcal{Y})$ (4.2), a spanning-tree is found. The edges of the tree are then used as the subset $\mathcal{E}_c$ when applying the GEIB algorithm.

We have derived the TBIB algorithm utilizing the PROM error bound as a general framework for model reduction of MAS. In the following case study section, we examine the performance of the algorithm, and it will be shown to provide excellent results for the reduction of large-scale MAS.

4.4 Case Studies

In this section we present some numerical examples illustrating the results of this work. In the following subsections we will demonstrate the effectiveness

Algorithm 4.2 Tree-based IIPROM bound Algorithm

Input: An MAS $\Sigma(\mathcal{G},\mathcal{U},\mathcal{Y})$ of order n with realization $\Sigma := (A(\mathcal{G}), B(\mathcal{G},\mathcal{U}), C(\mathcal{G},\mathcal{Y}), D(\mathcal{U},\mathcal{Y}))$, interface set $\mathcal{I} = \mathcal{U} \cup \mathcal{Y}$, reduction order r.

1. **Find** a spanning tree $\mathcal{T}$ of $\mathcal{G}$.
2. **Perform** greedy edge algorithm

$$\Sigma_r = GEIB(\Sigma(\mathcal{G},\mathcal{U},\mathcal{Y}), \mathcal{E}(\mathcal{T}), r).$$

Output: Σ_r
Notation: $\Sigma_r = TBIB(\Sigma(\mathcal{G},\mathcal{U},\mathcal{Y}), r)$

of the graph-based model reduction Algorithms derived in Section 4 for the reduction of small and large-scale LCC models.

Example 4.1. *As a first case study we consider the reduction of an LCC model (4.5) associated to a small-scale graph $\mathcal{G}$ with 20 nodes and 23 edges with 2 interface nodes (Figure 4.4a). We perform an edge-based IIPROM for each of the $\mathcal{I}$-invariant singleton partitions induced by the edges of $\mathcal{G}$. In this case, only the partitions induced by edge 1 are not $\mathcal{I}$-invariant since both its end nodes are interface nodes. For each of these IIPROMs, the $\mathcal{H}_\infty$-norm of the error system (3.1) and the $\mathcal{H}_\infty$ error bound (3.1) are calculated and normalized by $\|\Sigma\|_{\mathcal{H}_\infty}$ (Figure 4.4b). We observe that the choice of edge has a great effect on the reduction error magnitude, some edges produce reduction errors smaller than 1% of $\|\Sigma\|_{\mathcal{H}_\infty}$, while other edges induce IIPROM errors that are 10% of $\|\Sigma\|_{\mathcal{H}_\infty}$. It is also observed that the error bound is relatively tight for small reduction errors, while for larger errors the bound may differ more than an order of magnitude from the error.*

We then demonstrate the tree-based IIPROM bound algorithm (Algorithm 4.2) on the LCC. The spanning tree edges are found and Algorithm 4.2 is then performed for $r \in [10, 19]$. Figure 4.4c plots the reduction error $\|\Sigma_e\|_{\mathcal{H}_\infty}$, and the error bound $b_r(\mathcal{G}, U_r)$ (3.10), as a function of the normalized reduction depth $\frac{n-r}{n}$. We observe that the log reduction error has a quasi-linear trend as a function of $\frac{n-r}{n}$, and that the bound is tight for low reduction depths and differs as the reduction increases; however, the bound follows the same trend as the error, therefore, minimizing the bound is consistent with minimizing the error in this case.

Example 4.2. *As a large-scale case study, a small-world graph is created with the Watts-Strogatz random rewiring procedure with $k = 5$ and $\beta = 0.15$ [63] starting from a 5-regular graph of order 100 with 5 interface nodes $\mathcal{U} = \mathcal{Y} = \{1, \ldots, 5\}$ (Figure 4.5).*

An LCC is constructed over this graph and the tree-based IIPROM bound algorithm (Algorithm 4.2) is then performed. Figure 4.6 plots the reduction error $\|\Sigma_e\|_{\mathcal{H}_\infty}$, and the error bound $b_r(\mathcal{G}, U_r)$ (3.10) (normalized by $\|\Sigma\|_{\mathcal{H}_\infty}$), as a

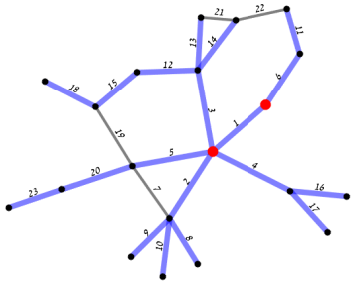

(a)

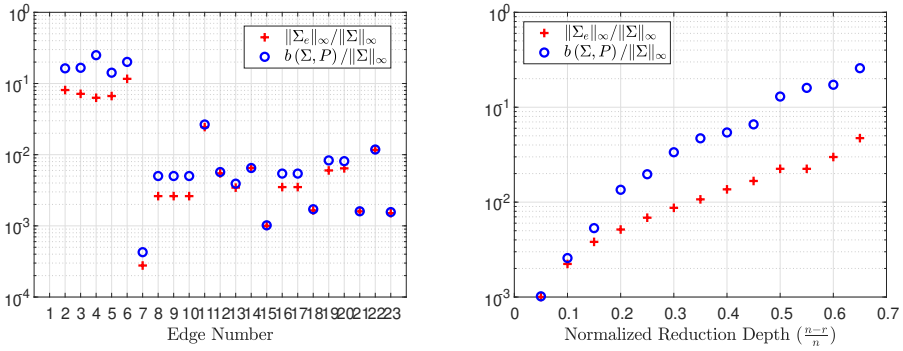

(b) (c)

Figure 4.4: A small-scale edge-based IIPROM case study (a) The graph associated to the Laplacian consensus in this example, interface nodes marked red, labels on edges indicate the edge numbers, a spanning tree is highlighted in blue and (b) The reduction error and reduction error bound of each edge-based IIPROM of the Laplacian consensus associated to the graph in Figure 4.4a. Notice that no values are assigned to edge 1 since it does not induce an interface invariant PROM. (c) The reduction error and reduction error bound resulting from applying the tree-based IIPROM bound algorithm to the the Laplacian consensus associated to the graph.

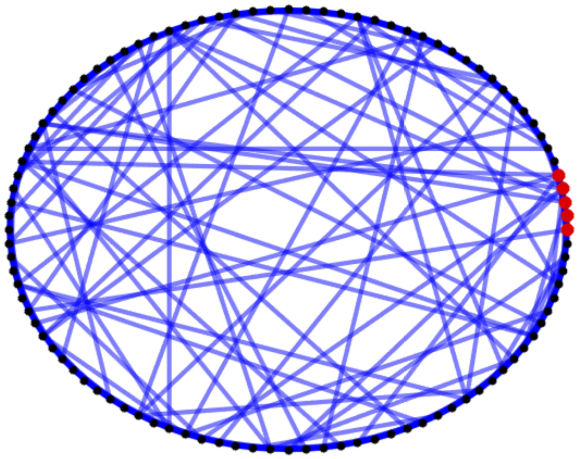

Figure 4.5: The Laplacian consensus in this example is associated to a small-world graph with 5 interface nodes (marked red).

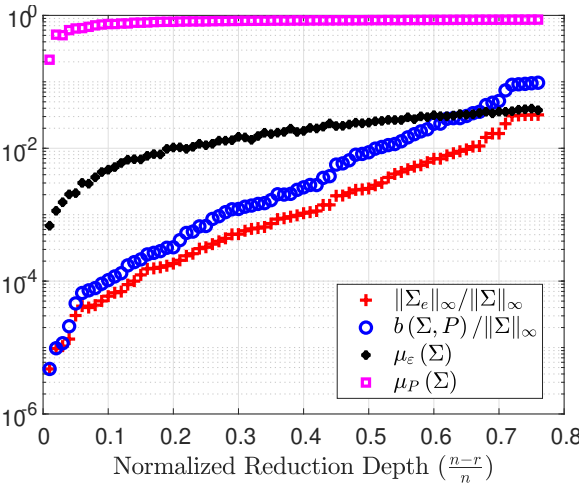

Figure 4.6: The reduction error and reduction error bound of the Laplacian consensus associated to the graph in Figure 4.5.

function of the normalized reduction depth $\frac{n-r}{n}$*. As a comparison to the reduction error and bound results, we calculate the empirical mean-IIPROM* $\mu_P(\Sigma)$*, the mean reduction error* $\|\Sigma_e\|_{\mathcal{H}_\infty}$ *of* $N = 50$ *randomly selected IIPROMs, and the empirical mean edge-based IIPROM* $\mu_\varepsilon(\Sigma)$*, the mean reduction error* $\|\Sigma_e\|_{\mathcal{H}_\infty}$ *of* $N = 50$ *randomly selected edge-based PPM IIPROMs.*

We observe that bound is tight for the entire reduction depth range. Furthermore, the reduction with the proposed tree-based method is several orders of magnitude lower than the empirical mean-IIPROM, and for lower reduction depth is significantly better than the empirical mean edge-based IIPROM. As expected, for high reduction depth, the tree-based method converges to the empirical mean edge-based IIPROM.

4.5 Conclusions

A suboptimal bound optimization solution for MAS is obtained with a graph-based spanning tree algorithm. Applying this algorithm on a Laplacian consensus model constructed with a large-scale small-world network, demonstrates the utility of the method to large scale multi-agent systems. In the examined case studies, the bound obtained with the tree-base algorithm is tight, therefore, the optimal PROM bound for those cases is close to the optimal reduction error PROM. The same technique presented can be applied to various multi-agent systems other than the consensus models.

Chapter 5

Summary

In this chapter, we conclude the research presented in this thesis. We begin with a brief summary of the contributions, followed by suggestions for future research paths.

5.1 Conclusions

This research thesis aimed to provide efficient graph-based model reduction methods for multi-agent systems, a crucial tool for implementing controllers for the emerging field of large scale multi-agent systems. Although an efficient optimal solution to the graph-based model reduction problem has yet to be found, the endeavour has resulted in significant contributions, including combinatorial, algebraic and spectral graph theorems, a system-theoretic model reduction theorem and a framework for suboptimal model reduction of MAS preserving their networked structure.

The graph theoretic part of the work was performed in Chapter 2. It provided a comprehensive study of vertex partitions and graph contractions, and introduced edge-induced partitions (Definition 2.9) and edge-based graph contractions (Definition 2.10), combinatorial graph reduction operations that, later in the thesis, were found to be highly useful for deriving efficient reduction methods. We also explore for the first time, the algebraic representations of graph contractions including the algebraic representation of the incidence matrix (Proposition 2.9), three type of Laplacian matrices (Theorem 2.1), and the Tucker representation (Theorem 2.2).

An important spectral graph theory finding is the graph reduction interlacing theorem (Theorem 2.1) that provides a set-theoretic extension of the min-max theorem for interlacing graph matrices. Additionally, we define two classes of edge-matching graph contractions, node-removal equivalent contractions (Definition 2.4) and cycle-invariant contractions (Definition 2.5). It was proven how these two classes provide Laplacian interlacing (Theorem 2.7) and normalized-Laplacian interlacing (Theorem 2.8), and two efficient algorithms

were constructed for finding such contractions in a graph (Algorithm 2.2&2.1).

In Chapter 3 of the thesis, the well known orthogonal PROM is studied. A novel product form is derived for the PROM reduction error system in Theorem 3.1 based on an extension of the matrix inversion lemma we denoted as the matrix lifting lemma (Lemma 3.4). Investigating the PROM error system product form, we define interface-invariant PROMs, PROMs with projection-invariant input and output matrices (Definition 3.1), and it is proven that for such PROMs the error product systems are strictly proper (Proposition 3.1). Furthermore, exploiting this structure, an analytic $\mathcal{H}_\infty$ reduction error bound is obtained and shown to be tight for a toy model (Example (3.1). We then present a suboptimal greedy-edge efficient algorithm for $\mathcal{H}_\infty$ graph-based model reduction of multi-agent systems utilizing the derived edge-matching graph contractions and the analytic $\mathcal{H}_\infty$ reduction error bound.

Combining results from Chapters 2 and 3, in Chapter 4, a suboptimal solution is derived for the graph-based model reduction problem of MAS. The solution is based on a greedy-edge spanning tree algorithm (Algorithm 4.2) optimizing the $\mathcal{H}_\infty$ PROM error bound (3.1). The utility of the method to large scale multi-agent systems is then demonstrates for a Laplacian consensus model constructed with a large-scale small-world network. The reduction error obtained with the suboptimal tree-base algorithm provides promising results, scale of magnitude smaller than the average random PROM.

5.2 Outlook

The closing of the thesis is an outlook into possible extensions of the the main three categories of research conducted in this work.

Graph contractions Several attempts have been performed during this research to combine combinatorial operations related to graph contractions to system theoretic metrics of reduced models. These included the work initiating this research that established the framework for the graph-based model reduction of the controlled consensus protocol [40]; however, with no concrete analytic results. A major effort was then performed to link spectral graph theorems such as interlacing graph matrices and a model reduction bound for MAS, utilizing mathematical tools such as spectral majorization theorems, again with no worthy results. These attempts emphasized the inherent complexity of model reduction both from the system theoretical approach and the graph theoretical perspective.

The natural extension of this work will be to successfully connect graph contractions and model reduction error bounds, e.g., via interlacing of graph matrices. Such results, if found, will provide a deeper understanding of the effect of graph theoretical properties to system performance, and may lead to improved model reduction methods of MAS.

The significant contributions of this work in the graph theoretical study of graph contractions suggest further research. The same spectral inter-

lacing theorem (Theorem 2.5) can be applied for finding other classes of graph contractions providing interlacing graph matrices. The proposed algorithms for finding classes of interlacing contractions will benefit from the addition of a prior feasibility step determining if there are no cycle-invariant or node-removal equivalent contractions in a graph.

Finally, the algebraic representations of graph contractions may be used for the development of various other graph-based model reduction methods of MAS.

Model reduction The established PROM error system product form (3.1) can be useful for the derivation of model reduction optimization methods, such as convex relaxations. Furthermore, if one restricts the projections to be orthogonal, as in this thesis, it appears that the orthogonal matrices may be parametrized through Givens or Householder rotations, which constitute a convex set.

The realizations of the product form systems opens new possibilities in the analysis of PROMs, and further research is required to explain the tightness of the PROM error bound, as seen in the case study (Figure 3.2). The notion of interface-invariant PROMs (Definition 3.1), natural to graph-based model reduction of MAS, and the derived $\mathcal{H}_\infty$ bound (Theorem 3.1), may be applicable to model reduction problems from various other domains.

Application to MAS The same graph-based model reduction framework used in Chapter 4 can be applied to the reduction of generally any controlled MAS of the form (4.2). Various other suboptimal structure reduction methods can be derived for such problems, with other reduction error metrics.

Bibliography

[1] S. N. Afriat. Orthogonal and oblique projectors and the characteristics of pairs of vector spaces. In *Mathematical Proceedings of the Cambridge Philosophical Society*, volume 53, pages 800–816. Cambridge University Press, 1957. 1.1, 1.2.2

[2] C. O. Aguilar and B. Gharesifard. Graph controllability classes for the laplacian leader-follower dynamics. *IEEE transactions on automatic control*, 60(6):1611–1623, 2014. 1.1

[3] A. C. Antoulas. *Approximation of large-scale dynamical systems*. Siam, 2009. 1.1

[4] A. C. Antoulas, D. C. Sorensen, and S. Gugercin. A survey of model reduction methods for large-scale systems. *Contemporary Mathematics*, 280:193–219, 2001. 1.1

[5] R. Bellman. *Introduction to matrix analysis*, volume 19. Siam, 1997. 2.4

[6] P. Benner and E. S. Quintana-Ortí. *Model reduction based on spectral projection methods*. Springer, 2005. 1.1, 1.2.1

[7] D. S. Bernstein. *Matrix mathematics: theory, facts, and formulas*. Princeton university press, 2009. 3.4

[8] G. Birkhoff and G. Grätzer. Lattice theory. *Bull. Amer. Math. Soc*, 79:35–39, 1973. 2.2.1

[9] V. D. Blondel and J. N. Tsitsiklis. A survey of computational complexity results in systems and control. *Automatica*, 36(9):1249–1274, 2000. 1.1

[10] M. Bürger, D. Zelazo, and F. Allgöwer. Duality and network theory in passivity-based cooperative control. *Automatica*, 50(8):2051–2061, 2014. 4.1

[11] G. Chen, G. Davis, F. Hall, Z. Li, K. Patel, and M. Stewart. An interlacing result on normalized laplacians. *SIAM Journal on Discrete Mathematics*, 18(2):353–361, 2004. 2.1, 2.4, 2.4, 2.4, 2.4

[12] X. Cheng, Y. Kawano, and J. M. Scherpen. Reduction of second-order network systems with structure preservation. *IEEE Transactions on Automatic Control*, 62(10):5026–5038, 2017. 1.1

[13] K. W. Chong and T. W. Lam. Finding connected components in o (log n log log n) time on the erew pram. *Journal of Algorithms*, 18(3):378–402, 1995. 2.2

[14] F. R. Chung and F. C. Graham. *Spectral graph theory*. Number 92. American Mathematical Soc., 1997. 2.4

[15] B. De Schutter. Minimal state-space realization in linear system theory: an overview. *Journal of computational and applied mathematics*, 121(1-2):331–354, 2000. 1.2.1

[16] N. Deo. *Graph theory with applications to engineering and computer science*. Courier Dover Publications, 2017. 2.3

[17] J. C. Doyle, K. Glover, P. P. Khargonekar, and B. A. Francis. State-space solutions to standard h_2 and h_∞ control problems. *IEEE Transactions on Automatic control*, 34(8):831–847, 1989. 1.2.1

[18] J. C. Doyle and G. Stein. Multivariable feedback design: Concepts for a classical/modern synthesis. In *IEEE Trans. on Auto. Control*. Citeseer, 1981. 1.2.1

[19] G. E. Dullerud and F. Paganini. *A Course in Robust Control Theory: A Convex Approach*. Springer New York, 2000. 1.1

[20] D. F. Enns. Model reduction with balanced realizations: An error bound and a frequency weighted generalization. In *The 23rd IEEE conference on decision and control*, pages 127–132. IEEE, 1984. 1.2.2

[21] M. Fiedler. A property of eigenvectors of nonnegative symmetric matrices and its application to graph theory. *Czechoslovak Mathematical Journal*, 25(4):619–633, 1975. 2.1

[22] B. A. Francis and W. M. Wonham. The internal model principle of control theory. *Automatica*, 12(5):457–465, 1976. 1.1

[23] M. Fu and Z.-Q. Luo. Computational complexity of a problem arising in fixed order output feedback design. *Systems & Control Letters*, 30(5):209–215, 1997. 1.1

[24] K. Gallivan, A. Vandendorpe, and P. Van Dooren. Sylvester equations and projection-based model reduction. *Journal of Computational and Applied Mathematics*, 162(1):213–229, 2004. 1.1, 1.2.2, 3.2

[25] C. Godsil and G. Royle. *Algebraic Graph Theory*. Springer, 2001. 1.3, 1.2.3, 1.2.3, 2.3.3, 4.1

[26] C. D. Godsil. Compact graphs and equitable partitions. *Linear Algebra and its Applications*, 255(1-3):259–266, 1997. 2.4

[27] M. Green and D. J. Limebeer. *Linear robust control*. Courier Corporation, 2012. 1.1

[28] K. M. Grigoriadis and R. E. Skelton. Low-order control design for lmi problems using alternating projection methods. *Automatica*, 32(8):1117–1125, 1996. 1.1

[29] W. H. Haemers. Interlacing eigenvalues and graphs. *Linear Algebra and its applications*, 226:593–616, 1995. 2.1, 2.4

[30] R. A. Horn and C. R. Johnson. *Topics in Matrix Analysis*. Cambridge University Press, New York, NY, 1991 (1st edition 1985, (expanded) 2nd edition 2013). 1.1

[31] X. Huang, F. Arvin, C. West, S. Watson, and B. Lennox. Exploration in extreme environments with swarm robotic system. In *2019 IEEE International Conference on Mechatronics (ICM)*, volume 1, pages 193–198, 2019. 1.1

[32] D. Hyland and D. Bernstein. The optimal projection equations for fixed-order dynamic compensation. *IEEE Transactions on Automatic Control*, 29(11):1034–1037, 1984. 1.1

[33] Y. Ikebe, T. Inagaki, and S. Miyamoto. The monotonicity theorem, cauchy's interlace theorem, and the courant-fischer theorem. *The American Mathematical Monthly*, 94(4):352–354, 1987. 2.4

[34] T. Ishizaki, K. Kashima, J.-i. Imura, and K. Aihara. Model reduction and clusterization of large-scale bidirectional networks. *IEEE Transactions on Automatic Control*, 59(1):48–63, 2014. 1.1, 3.1, 4.1, 4.2

[35] I. M. Jaimoukha and E. M. Kasenally. Implicitly restarted krylov subspace methods for stable partial realizations. *SIAM Journal on Matrix Analysis and Applications*, 18(3):633–652, 1997. 1.1

[36] H. Jongsma, H. Trentelman, and M. Camlibel. Model reduction of consensus networks by graph simplification. In *2015 54th IEEE Conference on Decision and Control (CDC)*, pages 5340–5345, 2015. 1.1

[37] S. Kamboj, W. Kempton, and K. S. Decker. Deploying power grid-integrated electric vehicles as a multi-agent system. In *The 10th International Conference on Autonomous Agents and Multiagent Systems-Volume 1*, pages 13–20, 2011. 1.1

[38] I. Khalil, J. Doyle, and K. Glover. *Robust and optimal control*. prentice hall, new jersey, 1996. 1.1

[39] N. Leiter and D. K. Geller. Optimal reduced-order LQG synthesis: Non-separable control and estimation design. *Optimal Control Applications and Methods*, 40(5):961–977, 2019. 1.1

[40] N. Leiter and D. Zelazo. Graph-based model reduction of the controlled consensus protocol. volume 50, pages 9456–9461, 2017. 20th IFAC World Congress. 1.1, 5.2

[41] F. L. Lewis, H. Zhang, K. Hengster-Movric, and A. Das. Introduction to synchronization in nature and physics and cooperative control for multi-agent systems on graphs. In *Cooperative Control of Multi-Agent Systems*, pages 1–21. Springer, 2014. 1.1

[42] L. Li and F. Paganini. Structured coprime factor model reduction based on lmis. *Automatica*, 41(1):145–151, 2005. 1.1

[43] W. Liu, V. Sreeram, and K. L. Teo. Model reduction for state-space symmetric systems. *Systems & Control Letters*, 34(4):209–215, 1998. 3.3.2, 3.1

[44] A. J. Majda, C. Franzke, and D. Crommelin. Normal forms for reduced stochastic climate models. *Proceedings of the National Academy of Sciences*, 106(10):3649–3653, 2009. 1.1

[45] M. Mesbahi and M. Egerstedt. *Graph theoretic methods in multiagent networks*. Princeton University Press, 2010. 1.1, 4.1, 4.1

[46] G. Minty. A simple algorithm for listing all the trees of a graph. *IEEE Transactions on circuit theory*, 12(1):120–120, 1965. 2.2

[47] N. Monshizadeh, H. L. Trentelman, and M. K. Camlibel. Projection-based model reduction of multi-agent systems using graph partitions. *IEEE Transactions on Control of Network Systems*, 1(2):145–154, 2014. 1.1, 4.1, 4.2

[48] B. Moore. Principal component analysis in linear systems: Controllability, observability, and model reduction. *IEEE transactions on automatic control*, 26(1):17–32, 1981. 1.1, 1.2.1, 1.2.2, 1.2.2

[49] M. E. Newman and M. Girvan. Finding and evaluating community structure in networks. *Physical review E*, 69(2):026113, 2004. 1.1, 2.1, 4.2

[50] A. Y. Ng, M. I. Jordan, and Y. Weiss. On spectral clustering: Analysis and an algorithm. In *Advances in neural information processing systems*, pages 849–856, 2002. 2.1

[51] R. Olfati-Saber, J. A. Fax, and R. M. Murray. Consensus and cooperation in networked multi-agent systems. *Proceedings of the IEEE*, 95(1):215–233, 2007. 1.1

[52] J. R. Phillips, L. Daniel, and L. M. Silveira. Guaranteed passive balancing transformations for model order reduction. *IEEE Transactions on Computer-Aided Design of Integrated Circuits and Systems*, 22(8):1027–1041, 2003. 3.3.2

[53] R. T. Rockafellar. *Network flows and monotropic optimization*. Number 1-237. Wiley-Interscience, 1984. 2.3.3

[54] H. Sandberg. An extension to balanced truncation with application to structured model reduction. *IEEE Transactions on Automatic Control*, 55(4):1038–1043, 2010. 1.1

[55] S. E. Schaeffer. Graph clustering. *Computer science review*, 1(1):27–64, 2007. 1.1, 2.1, 4.2

[56] M. Sharf and D. Zelazo. Analysis and synthesis of mimo multi-agent systems using network optimization. *IEEE Transactions on Automatic Control*, 64(11):4512–4524, 2019. 1.1

[57] M. Siami and N. Motee. Systemic measures for performance and robustness of large-scale interconnected dynamical networks. In *53rd IEEE Conference on Decision and Control*, pages 5119–5124. IEEE, 2014. 1.1

[58] D. A. Spielman and S.-H. Teng. A local clustering algorithm for massive graphs and its application to nearly linear time graph partitioning. *SIAM Journal on computing*, 42(1):1–26, 2013. 1.1

[59] C. Sturk, L. Vanfretti, F. Milano, and H. Sandberg. Structured model reduction of power systems. In *2012 American Control Conference (ACC)*, pages 2276–2282. IEEE, 2012. 1.1

[60] H. L. Trentelman. Bounded real and positive real balanced truncation using σ-normalised coprime factors. *Systems & control letters*, 58(12):871–879, 2009. 3.3.2

[61] A. E. Turgut, H. Çelikkanat, F. Gökçe, and E. Şahin. Self-organized flocking in mobile robot swarms. *Swarm Intelligence*, 2(2):97–120, 2008. 1.1

[62] M. Vasile and P. De Pascale. Preliminary design of multiple gravity-assist trajectories. *Journal of Spacecraft and Rockets*, 43(4):794–805, 2006. 1.1

[63] D. J. Watts and S. H. Strogatz. Collective dynamics of âsmall-worldânetworks. *nature*, 393(6684):440–442, 1998. 4.2

[64] H. Wilf. *Generatingfunctionology*. Academic Press Inc - New York, 1994. 2.4, 2.4, 4.2

[65] P. Winter. An algorithm for the enumeration of spanning trees. *BIT Numerical Mathematics*, 26(1):44–62, 1986. 2.2

[66] B.-F. Wu, J.-Y. Shao, and Y. Liu. Interlacing eigenvalues on some operations of graphs. *Linear Algebra and its Applications*, 430(4):1140–1150, 2009. 2.1

[67] L. Yu, X. Cheng, J. Scherpen, and J. Xiong. H_2 model reduction for diffusively coupled second-order networks by convex-optimization. *arXiv preprint arXiv:2104.04321*, 2021. 1.1

[68] D. Zelazo, A. Rahmani, and M. Mesbahi. Agreement via the edge laplacian. In *2007 46th IEEE Conference on Decision and Control*, pages 2309–2314. IEEE, 2007. 2.16

[69] D. Zelazo, S. Schuler, and F. Allgöwer. Performance and design of cycles in consensus networks. *Systems & Control Letters*, 62(1):85–96, jan 2013. 1.1, 2.10, 4.3

גרפים, ומפתחים את התיאור האלגברי של מטריצות המייצגות גרפים מכווצים. תרומה חשובה נוספת היא הצגת משפט ספקטרלי כללי לשזירות מטריצות של גרפים מסדר מופחת. אלגוריתמים יעילים חדשים מסופקים למציאת שני סוגים של התכווציות גרפים המבטיחים שזירות של מטריצות לפלס.

בפרק השלישי של התזה אנו בוחנים מחדש את המבנה של הפחתת סדר מבוססת השלכה. אנו מפתחים מבנה מכפלה חדשני של מערכת השגיאה הנובעת מהפחתת סדר מבוססת השלכה. על בסיס מבנה מכפלה זה מפותח חסם אנליטי של שגיאת הפחתת הסדר, ומוגדרת בעיית אופטימיזציה של החסם.

הפרק הרביעי של התזה עוסק ביישום תוצאות משני הפרקים הקודמים לצורך פיתוח שיטות הפחתת סדר מבוססת גרפים למערכות מרובות סוכנים. כצעד ראשון, אנו מנסחים את בעית הפחתת הסדר כאופטימיזציה של הפחתת סדר בתורת הגרפים. עם זאת, נמצא כי בעיה זו היא קשה חישובית, ועל מנת להפיק פתרונות לא אופטימליים יעילים של בעיית האופטימיזציה של הפחתת סדר הגרפים, אנו מפתחים אלגוריתם יעיל להפחתת סדר המבוסס על איגוד קודקודים וקשתות בגרף, ועושים שימוש בחסם השגיאה של שיטת ההשלכה. השיטה מודגמת על מערכת קונסנזוס בקנה מידה גדול.

הפרק החמישי והאחרון של התזה מסכם אותה ומציג כיווני מחקר לעתיד.

תקציר עברי

יש כיום גידול ניכר בשימוש במערכות מרובות סוכנים בטכנולוגיות מודרניות רבות, כגון נחילים רובוטיים ולהקות רחפנים, המאפשרים פעולות אוטונומיות מורכבות בסביבות הקשות ביותר. יישומים אחרים של מערכות מרובות סוכנים כוללים רשתות חשמל מבוזרות, ומודלים בתחומי מדע רבים לרבות פיזיקה, כלכלה וסוציולוגיה.

גרפים מאפיינים את המבנה של מערכות מרובות סוכנים, כאשר כל סוכן מיוצג על ידי צומת בגרף וקשתות מייצגות את האינטראקציות המקומיות בין סוכנים סמוכים, למשל, מדידות יחסיות או תקשורת נתונים. סוכן בהקשר זה הוא כל מערכת דינמית הפועלת בצימוד למערכות אחרות ובמחקר זה נעסוק במערכות הומוגניות בהן לכל הסוכנים יש את אותו מודל דינמי. דוגמא בולטת למערכת מסוג זה הוא מודל הקונצנזוס שפותח על ידי אולפטי (Olfati) ואחרים. במודל זה כל הסוכנים שואפים להגיע למצב זהה לזה של הסוכנים הסמוכים להם ברשת באמצעות חוק בקרה מקומי. כפי שמראה מסבחי (Mesbahi), תחת כמה תנאים, ובהתאם למודל הספציפי, המערכת כולה מתכנסת לאותו המצב ומתקבלת הסכמה.

הפחתת סדר היא ענף פעיל של תורת המערכות הלינאריות עם חשיבות גוברת, שכן יישומים מודרניים כגון מערכות מרובות סוכנים, עשויים להיות בקנה מידה גדול במיוחד. מודלים מופחתי־סדר של מערכות אלו נדרשים בכל פעם שזה בלתי אפשרי מבחינה חישובית ליישם, לנתח או לדמות את מערכת המלאה, ולצורך תכנון ומימוש בקרים. מודלים מופחתי־סדר מבוססי השלכה אורתוגונלית (PROM) הם הנפוצים ביותר, ומודלים מסוג זה מאפשרים לשמור על יציבות ולהבטיח מינימליות של המערכת מופחתת הסדר, ולספק גבולות של שגיאת הפחתת הסדר. עם זאת, שיטות אלה עשויות להיות בלתי ניתנות לביצוע עבור מערכות בקנה מידה גדול מאוד בשל המורכבות החישובית שלהם, ובעיות בקרה מופחתות־סדר של מערכות לינאריות מציגות אתגר חישובי מורכב. כתוצאה מכך, עבודות רבות שמטרתן למצוא פתרונות יעילים לא אופטימליים, למשל על ידי שיטות השלכה מתחלפות, או טכניקות קרילוב שהן יעילות חישוביות ומתאימות למערכות בקנה מידה גדול במיוחד. עם זאת, שיטות אלו לא מבטיחות יציבות ומינימליות.

אתגר גדול בחקר מערכות מרובות סוכנים הוא למצוא שיטות יעילות להפחתת סדר המבטיחות יציבות ומינימליות. שיטות הפחתת סדר המשמרות מבנה פותחו עבור מערכות המורכבות ממספר קטן של תת־מערכות בקנה מידה גדול המחוברות זו לזו, ויושמו להפחתת סדר של רשתות חשמל . שיטות כאלה, עם זאת, אינן ישימות עבור מערכות מרובות סוכנים המורכבות ממספר רב של סוכנים מסדר נמוך. עבור מערכות מרובות סוכניסת המאופיינות במבנה המרושת שלהן, המאפיינים של הגרף המתאר את המערכת יכולים להיות קשורים במקרים מסוימים ליציבות המערכת, וכפי שהראה אגוילאר (Aguilar) גם לבקירות ולצפיות של המערכת. לכן, רצוי שימצאו שיטות להפחתת סדר המשמרות את המבנה הרשתי של המערכת. אנו מגדירים שיטות הפחתת סדר כאלו כסוג חדש של שיטת הפחתת סדר הנקראת `הפחתת סדר מבוססת גרפים`, ובהקשר זה בוצעו כמה מחקרים עדכניים.

מונשיזאדה (Monshizadeh) ואישיזאקי (Ishizaki), חקרו שיטות הפחתת סדר המבוססות השלכה המתארת את איגוד הקודקודים בגרף, ופיתחו חסמי שגיאה עבור מודל הקונסנזוס מסדר ראשון. הפחתת סדר של מערכות מסדר שני עם שימור מבנה באמצעות שימוש באשכולות היררכיים הודגמה על ידי צ'נג (Cheng). שיטה להפחתת סדר אופטימלית מבוססת הרפיה קונווקצית המשמרת את המבנה הרשתי במערכות מרובות סוכנים מסדר שני, הוצגה לאחרונה על ידי יו (Yu). שיטות אלו מוגבלות למערכות מרובות סוכנים מסדר ראשון או שני, והמטרה של מחקר זה היא לפתח שיטות יעיל להפחתת סדר מבוססות גרפים עבור מערכות מרובות סוכנים מסדר כללי.

פרק המבוא של התזה כולל סקר של הרקע הנדרש בתורת המערכות הלינאריות והפחתת סדר שלהן, ומושגים מרכזיים בתורת הגרפים. פרק זה כולל גם תמצית של הממצאים בכל אחד מפרקי התזה.

הפרק השני של התזה מהווה מחקר יסודי בתורת הגרפים של גרפים מכווצים, גרפים בסדר מופחת המבוססים על איגוד קודקודים. אנו מזהים תתי־מחלקות יחודיים של איגוד קודקודים, מנסחים גישה מבוססת קשתות לכיווץ

המחקר בוצע בהנחיית פרופ דניאל זלזו

בפקולטה להנדסת אווירונוטיקה וחלל

אני מודה לקרן הלאומית למדע
ולקרן המדע הדו־לאומית של ארצות הברית־ישראל

על התמיכה הכספית הנדיבה בהשתלמותי

שיטות מבוססות־גרפים להפחתת סדר של מערכות מרובות סוכנים

חיבור על מחקר לשם מילוי חלקי של הדרישות
לקבלת התואר דוקטור לפילוסופיה

נעם לייטר

הוגש לסנט הטכניון - מכון טכנולוגי לישראל

אייר התשפ`ב חיפה מאי **2022**